

Metabolic pathways of aggregate-associated microbes along estuarine gradients

New insights into estuarine particle dynamics, properties, and processing
from microscopy, particle combustion, and sequencing approaches

Dissertation

with the aim of achieving a doctoral degree at the Faculty
of Mathematics, Informatics, and Natural Sciences in the
Department of Biology, University of Hamburg

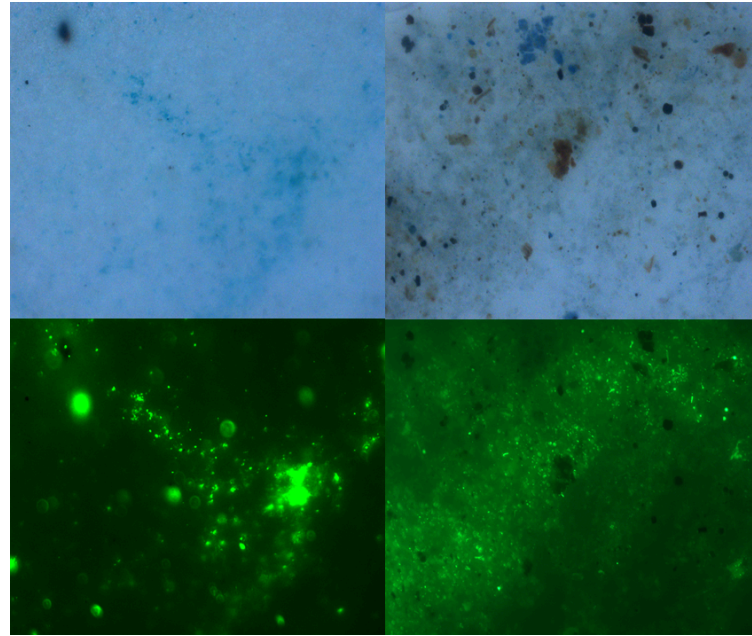
Submitted by:

Sven Patrik Tobias-Hünefeldt

Hamburg

2025

PhD candidate, reviewers, and examination members



PhD candidate: Sven Patrik Tobias-Hünefeldt

First supervisor and Examination Commission Deputy Chair: Prof. Dr. Wolfgang R. Streit
Co-supervisor and Examination Commission member: Prof. Dr. Hans-Peter Grossart

Examination Commission Chair: Prof. Dr. C. Elisa Schaum

Examination Commission member: Prof. Dr. Paul del Giorgio
Examination Commission member: Dr. Andrej Fabrizius

Day of Disputation:
21-07-2025

Publications

Chapter 2 consists of a modified manuscript version that was published as: Tobias-Hünefeldt, S.P., van Beusekom, J.E.E., Russnak, V., Dähnke, K., Streit, W.R., Grossart, H.-P., 2024. Seasonality, rather than estuarine gradient or particle suspension/sinking dynamics, determines estuarine carbon distributions. *Science of The Total Environment* 926, 171962. <https://doi.org/10.1016/j.scitotenv.2024.171962>

Chapter 3 consists of the manuscript currently under review as: Tobias-Hünefeldt, S.P., Woodhouse, J.N., Ruscheweyh, H.-J., Sunagawa, S., Russnak, V., Streit, W.R., Grossart, H.-P., Microbial organic carbon processing along the Elbe Estuary is driven by salinity and salinity sensitive organisms. *In Review*

Manuscript modifications were limited to the figure and section numbers required to integrate the publications into the thesis.

As the first author of both publications, I carried out literature research to identify knowledge gaps, developed the study design, carried out all sample collection and preparation (e.g. microscopy, particle weighing and combustion, and DNA/RNA extractions), quantified sample properties (e.g. excitation and emission matrices, microscope image capture and analysis, and particle weighing), and carried out all data analysis via data visualisation and statistical tests. I also wrote the first drafts and revised the manuscripts based on co-author and peer-review feedback.

Neustrelitz, 21-05-2025

Sven Patrik Tobias-Hünefeldt
(PhD Candidate)

21. Mai 2025

Prof. Dr. Wolfgang R. Streit
(PhD Supervisor)

22. Mai 2025

Prof. Dr. Hans-Peter Grossart
(PhD Co-Supervisor)

Abstract

Estuarine systems are essential for global carbon cycling; mediating exchanges between aquatic, atmospheric, and terrestrial systems. Estuaries are important blue carbon storage and greenhouse gas processing centres. In estuaries particles undergo microbial transformation and vertical/horizontal transport, shaping organic matter. Yet, connections between estuarine dissolved and particulate organic matter, and their relationship to microbiome composition and functions, remain poorly explored.

I investigate organic matter and microbiome dynamics across the Elbe Estuary's highly dynamic and turbid gradients, using a multifaceted approach. Particles were fractionated into suspended and sinking fractions, using microscopy to determine carbon characteristics (SYBR Green I for bacterial colonisation and Alcian Blue and Coomassie Brilliant Blue for exopolymers), elemental analysis (C/H/N), and dry weight analysis to identify compositional differences. Dissolved parameters included nutrient and carbon abundance, and spectrofluorometric evaluations to characterise physicochemical concentrations and dissolved organic matter properties. Finally, samples underwent shotgun metagenome, and metatranscriptome sequencing to determine microbiome composition, functional potential, and transcription profiles.

The initial focus was to determine whether particulate and dissolved organic carbon dynamics were shaped by spatiotemporal gradients, including seasonality (e.g. phytoplankton blooms) and salinity (e.g. freshwater inflow). No consistent salinity-driven carbon patterns were revealed, likely due to strong mixing forces and high particle heterogeneity. However, suspended organic carbon could be linked to terrestrial-like signatures, while sinking organic matter was linked to marine-like dissolved organic matter. Across the estuary, bacterial colonisation decreased with increasing salinity, indicative of microbial community composition and functional shifts. The integration of microbiome data agrees, linking colonisation across the salinity gradient to the presence of osmoregulation genes.

Microbiome integration built on the descriptive assessment of carbon dynamics in the Elbe Estuary, linking relevant variables to the microbiome composition and functionality. In agreement with current knowledge, free-living and particle-associated microbiomes showed significant differences, although the separation of suspended and sinking fractions in such a highly turbid environment represents novel investigations. One of which shows sinking particle-associated microbiomes preferentially expressing coenzyme M biosynthesis, a methanogenesis cofactor, while suspended particle-associated transcripts favour energy acquisition and growth.

Findings show how environmental changes such as dredging, projected sea-level rise, and decreased freshwater inflow may drive microbial shifts and methane oxidation, with higher suspended-sinking particle ratios potentially reducing methane concentrations. My work highlights how multifaceted approaches provide deeper analyses, studying organic carbon dynamics and microbial processes in a highly turbid estuary, offering ecological context and informing climate-resilient management.

Lay summary

Estuaries, lower river areas that merge into oceans, play a big role in Earth's carbon cycle. They help store carbon and manage greenhouse gases, and exchange carbon between land, water, and the air. In estuaries one of the big ways carbon behaviour is controlled is with particles and the microbes living on them. However, it's still not fully understood how carbon dissolved into water and as particles relate to each other, or how they connect to the microbes in the water and on the particles.

My research looks at how carbon and microbes interact across different parts of the Elbe Estuary in Germany. The Elbe is known for its highly turbid waters and how much it changes over time. Using a range of techniques, such as separating floating and sinking particles, measurements of carbon and nitrogen, and DNA sequencing we sought to understand how microorganisms interact with and transform carbon in the Elbe estuary. The study first looked at how carbon changes with the season (like during algae blooms) and with freshwater inflow from the river. We found a connection between soil carbon and floating particles, while ocean-like carbon signatures were linked to sinking particle carbon concentrations. However, against what we expected, salt did not have a clear effect on carbon dynamics, most likely because the water is very mixed and particles can be very different even in the same litre of water. As salt levels increased closer to the ocean, fewer bacteria were found on particles, suggesting changes in what microbes can be found and what they do. Genetic analyses agree, with microbes adapting to higher salt concentrations with genes that regulate how salt is handled and help them cope.

By combining all the different approaches, we could show strong links between carbon and microbial communities, with microbes on sinking particles associated with the production of methane, while those on floating particles are more focused on growing and getting enough energy. Findings lead us to the conclusion that human activities, like dredging, sea-level rise associated with climate change, and drought brought reduced river inflow, would change microbial, and subsequently carbon behaviour. For example, how much methane is removed from the estuary, where more floating particles vs. sinking particles could help reduce how much methane is released into the atmosphere. Overall, my thesis offers useful knowledge for managing cloudy estuaries, like the Elbe Estuary, in the face of climate change.

Zusammenfassung

Ästuare, als Flussgebiete, die in die Ozeane münden, spielen eine wichtige Rolle im globalen Kohlenstoffkreislauf. Sie speichern Kohlenstoff ‚Blue Carbon‘ und sind somit ein Reservoir für den Austausch von CO₂. Sie tragen zum Austausch von Treibhausgasen und Kohlenstoff zwischen Land, Wasser und Luft aus, und haben einen wichtigen Einfluss auf das globale Klima.

In Flussmündungen wird die Verwertung des Kohlenstoffs unter anderem durch Partikel und die auf ihnen lebenden Mikroben beeinflusst. Aufgrund der relativ hohen Anzahl an Partikeln, ist der Einfluss beachtlich. Es gibt jedoch große Wissenslücken, wie der Wasser gelöste Kohlenstoff mit den umliegenden Partikeln und deren assoziiertem Mikrobiota, interagiert und welche Rolle die Mikrobiota für CO₂-fixierende oder CO₂-Freisetzungsprozesse sind.

Im Rahmen der vorliegenden Dissertation habe ich die qualitative und quantitative Veränderung des gelösten Kohlenstoffs (C_{org/anorg}) analysiert und dabei insbesondere die Veränderungen in der Mikrobiota in der Wassersäule der Elbe untersucht. Das Elbe Ästuar, einer der größten und wirtschaftlich wichtigsten Ästuars Deutschlands, ist bekannt für erhöhte Dynamiken in der Wassertrübe und Kohlenstoffanteile. Ich habe unterschiedliche Methoden und Techniken angewandt, um z. B. schwimmende und sinkende Partikel zu trennen, den Kohlenstoff/Stickstoff Gehalt, sowie bakterielle Zellzahlen und Mikrobiota zu bestimmen. Anhand analytischer Methoden konnten gelöste Konzentrationen, sowie Eigenschaften von Nährstoffen (z. B. Ammonium und Sauerstoff) und Kohlenstoffmengen und deren Dynamiken bestimmt werden. Schließlich wurde das genetische Potential der Mikrobiota der Wassersäule sowie die exprimierten Gene unter verschiedenen räumlichen und zeitlichen Bedingungen mithilfe von Next-Gen Sequenzierung bestimmt. Mit Hilfe dieser tiefen Datensätze konnten erste Rückschlüsse auf das genetische Potential der Mikrobiota und deren Genexpressionsmuster erstellt werden.

Ein wesentlicher Bestandteil meiner Dissertation war dabei den Kohlenstofffluss im Verlaufe des Jahres und mit einem sich verändernden Anteil von C und auch im Hinblick auf die ständig veränderte Salinität zu erfassen, und den Einfluss auf die Mikrobiota zu analysieren. Dabei konnte ich zeigen, dass es einen direkten Zusammenhang zwischen terrestrisch-ähnlichen Kohlenstoff und der Quantität von partikulären Schwebstoffen in der Wassersäule gibt. Darüber hinaus konnte ich zeigen, dass die bakterielle Kolonisation von Partikeln und auch die Diversität durch die Salinität stark beeinflusst ist.

Dabei wurde auch deutlich, dass es sowohl in der Geneausstattung als auch im Expressionsprofil signifikante Unterschiede gibt mit Hinblick auf die freien und Partikel-assoziierten Mikroorganismen. Mikroorganismen auf sinkenden Partikeln waren oft mit der Methanproduktion assoziiert, während die Mikroorganismen in der Schwebstoff-Fraktion eher auf Wachstum und aerobe Energiegewinnung ausgerichtet waren. Dabei wurde insbesondere die Expression des Co-Faktors CoM, ein zentraler Kofaktor der Methanogenese, als Indikator für die Methanogenese genutzt.

Meine Ergebnisse deuten darauf, dass anthropogene Aktivitäten wie Baggerarbeiten, der mit dem Klimawandel verbundene Anstieg des Meeresspiegels und extreme Dürreperioden (die Zufluss vom Fluss verringern oder verhindern) das Verhalten der Mikroben und damit auch das des Kohlenstoffs verändern würden. Insgesamt bietet meine Arbeit nützliche Erkenntnisse für die Bewirtschaftung von trüben Ästuaren wie der Elbe, angesichts von dynamischen Umweltbedingungen und des Klimawandels.

Eidesstattliche Erklärung / Statement under Oath

Hiermit erkläre ich an Eides statt, dass ich die vorliegende Dissertation selbst verfasst und keine anderen als die angegebenen Quellen und Hilfsmittel benutzt habe.

I hereby declare under oath that I have written the present dissertation independently and have not used further resources and aids than those stated in the dissertation.

Neustrelitz, 21-05-2025



Sven Patrik Tobias-Hünefeldt

Erklärung Exemplare / Declaration on Copies

Ich versichere, dass dieses gebundene Exemplar der Dissertation und das in elektronischer Form eingereichte Dissertationsexemplar (über den Docata-Upload) und das bei der Fakultät (zuständiges Studienbüro bzw. Promotionsbüro Physik) zur Archivierung eingereichte gedruckte gebundene Exemplar der Dissertationsschrift identisch sind.

I, the undersigned, declare that this bound copy of the dissertation and the dissertation submitted in electronic form (via the Docata upload) and the printed bound copy of the dissertation submitted to the faculty (responsible Academic Office or the Doctoral Office Physics) for archiving are identical.

Neustrelitz, 21-05-2025



Sven Patrik Tobias-Hünefeldt

Eidesstattliche Versicherung

Hiermit versichere ich an Eides statt, die vorliegende Dissertationsschrift selbst verfasst und keine anderen als die angegebenen Hilfsmittel und Quellen benutzt zu haben.

Sofern im Zuge der Erstellung der vorliegenden Dissertationsschrift generative Künstliche Intelligenz (gKI) basierte elektronische Hilfsmittel verwendet wurden, versichere ich, dass meine eigene Leistung im Vordergrund stand und dass eine vollständige Dokumentation aller verwendeten Hilfsmittel gemäß der Guten wissenschaftlichen Praxis vorliegt. Ich trage die Verantwortung für eventuell durch die gKI generierte fehlerhafte oder verzerrte Inhalte, fehlerhafte Referenzen, Verstöße gegen das Datenschutz- und Urheberrecht oder Plagiate.

Neustrelitz, 21-05-2025



Sven Patrik Tobias-Hünefeldt

Affidavit

I hereby declare and affirm that this doctoral dissertation is my own work and that I have not used any aids and sources other than those indicated.

If electronic resources based on generative artificial intelligence (gAI) were used in the course of writing this dissertation, I confirm that my own work was the main and value-adding contribution and that complete documentation of all resources used is available in accordance with good scientific practice. I am responsible for any erroneous or distorted content, incorrect references, violations of data protection and copyright law or plagiarism that may have been generated by the gAI.

Neustrelitz, 21-05-2025



Sven Patrik Tobias-Hünefeldt

Acknowledgements

I want to thank my Supervisors Hans-Peter Grossart and Wolfgang Streit for guiding me through my PhD journey, it wasn't always easy and straightforward but they supported and encouraged me the entire time. I'm also grateful to my Panel Chair C.-Elisa Schaum, and colleague Jason N. Woodhouse who were always ready to share an opinion.

I wanted to thank my Research Training Group (BiCEst) for the supportive environment they cultivated, especially so Kai Jensen and Susanne Stirn. Also thank you to the people who were always in a good mood and enthusiastic discussion participants, including Raphael Koll and Vanessa Russnak, and those without who the science would have been 100 times harder, Solvig Pinnow, the crew of the Ludwig Prandtl, Monika Degebrodt, and Uta Mallok.

Finally, I want to thank my family for their unwavering support to me on the other side of the planet and across continents. Although we may not always make the group chats, we always know that if we really need it, we're always just a phone call away.

Table of Contents

Publications	iii
Abstract.....	iv
Lay summary	v
Zusammenfassung	vi
Eidesstattliche Erklärung / Statement under oath.....	viii
Erklärung Exemplare / Declaration on Copies.....	viii
Eidesstattliche Versicherung.....	ix
Affidavit.....	ix
Acknowledgements.....	x
Table of Contents.....	1
List of Figures	4
List of abbreviations	7
Chapter 1: General Introduction	9
1.1 The importance of estuaries for carbon cycling.....	9
1.2 Effects of changing estuary conditions.....	9
1.3 Primary DOM control mechanisms	10
1.4 Particle characteristics can drive carbon cycling in aquatic ecosystems	10
1.5 Linking particles, DOM, and microbial carbon cycling in estuaries	12
1.6 Previous Elbe Estuary carbon processing.....	13
1.7 Study project and graduate school: RTG2530 (BiCEst)	14
1.8 Objectives:.....	15
1.9 Thesis outline	18
Chapter 2: Seasonality, rather than estuarine gradient or particle suspension/sinking dynamics, determines estuarine carbon distributions.	19
2.1 Abstract	19
2.2 Introduction.....	19
2.3 Materials and Methods	22
2.3.1 Sampling	22
2.3.2 Particle sampling.....	23
2.3.3 Physicochemical parameters	23
2.3.4 Microscopic image analysis.....	24
2.3.5 Dissolved organic matter (DOM) analysis.....	25

2.3.6 Statistical analysis	26
2.4 Results	26
2.4.1 Minimal salinity gradient effects on carbon abundance and characteristics	26
2.4.2 Differences in bacterial particle colonisation along the Elbe estuary.....	28
2.4.3 Strong seasonality effects on carbon dynamics.....	29
2.4.4 DOM interactions with particle characteristics	31
2.4.5 Few differences between suspended and sinking particles in highly mixed environments	31
2.5 Discussion	33
2.5.1 Only weak interactions occur between carbon distribution and within the Elbe estuary's salinity gradient	33
2.5.2 DOM aromaticity does not vary with salinity	36
2.5.3 DOM properties are affected by seasonality	36
2.5.4 Seasonality drives particle differences, with no phytoplankton bloom link	37
2.5.5 Density determines suspended and sinking particle differences, with DOM compound links	38
2.5.6 Bacterial particle colonisation significantly differs in response to the estuarine gradient.....	39
2.6 Conclusion.....	40
Chapter 3: Suspended and sinking particle-associated microbiomes exhibit distinct lifestyles	42
3.1 Abstract	42
3.2 Introduction.....	42
3.3 Materials and Methods	44
3.3.1 Sampling	44
3.3.2 DNA extraction and sequencing	45
3.3.3 Physicochemical parameters	46
3.3.4 Statistical analysis	47
3.4 Results and Discussion	47
3.4.1 Salinity and osmoregulation genes drive dissolved CO ₂ and CH ₄ processing gene profiles	48
3.4.2 Exopolymer TEP correlated taxa are salinity specific, unlike CSP	54
3.4.3 Particle-associated activity is split into growth vs. methanogenesis focuses.....	54
3.5 Conclusion.....	56
Chapter 4: General Discussion	57
4.1 Key Findings.....	58
4.1.1 Spatiotemporal carbon and microbiome dynamics	58

4.1.2 Carbon and microbiome dependent fraction differences.....	61
4.1.3 How does particle colonisation change across Estuarine gradients?.....	62
4.3 Challenges and limitations	62
4.4 Conclusions and Outlook	64
Bibliography	65
Appendices	107
Appendix A: Chapter 2	107
Appendix B: Chapter 3	112

List of Figures

Figure 1.1. Elbe Estuary map. The map depicts the Elbe estuary, from Hamburg Harbour to Cuxhaven, with marks of the Elbe length (in kilometre) shown. Sample stations are shown as stars. Adapted from Tobias-Hünefeldt et al. (2024).

Figure 1.2: A conceptual diagram of carbon transfers in estuaries. The focus of each thesis chapter has been marked with either a hollow (chapter 2) or filled (chapter 3) circle. All plots and images were created/taken by Sven P. Tobias-Hünefeldt.

Figure 2.1. Elbe estuary map. The map depicts the outline of the Elbe, from Hamburg Harbour to Cuxhaven, with marks of the Elbe length (in kilometre) shown as circles, and sample sites indicated as red stars.

Figure 2.2. Exopolymer area and particle contribution in the Elbe estuary. Exopolymers TEP and CSP concentrations (left axis) are shown here as area per Litre (bars), and the percentage that the exopolymer area (right axis) contributed to the overall particle (unstained/TEP/CSP) area in the sample (lines). Error bars represent the standard deviation of duplicate samples. The average of parallel measurements is displayed for exopolymer concentrations.

Figure 2.3. Dry-weight and particle area over the Elbe. Bars represent particulate dry-weight (mg L^{-1}), while the lines represent particle area ($\mu\text{m}^2\text{L}^{-1}$). The average of parallel measurements is displayed.

Figure 2.4. Elbe salinity and turbidity. Lines represent the measured salinity (A) and turbidity (B) of the Elbe estuary across the sample points. Colours represent the dates of sampling.

Figure 2.5. Particulate and dissolved organic carbon concentrations over the Elbe estuary. Shapes differentiate dissolved (triangles) and particulate (squares) carbon concentrations. The average of parallel measurements is displayed.

Figure 2.6. PCA biplot of DOM characteristics in the Elbe estuary. Shapes represent sample times, while the colour gradient represents sample location (in kilometre) along the Elbe estuary. The top 5 contributors are depicted to show their relation to sample distribution/dissimilarity. Coble peak A represents a humic-like signature, absorbance at 254 and 300 represent the aromatic DOM content and photooxidation, respectively, the 350/400 slope is indicative of molecular weight and aromaticity, just as MW/aromaticity does.

Figure 2.7. PARAFAC component contribution to total fluorescence is depicted over the Elbe estuary. Component percentage is based on component contribution to total fluorescence of the sample. Colours represent individual PARAFAC components; C1: marine humic-like, C2: terrestrial humic-like, C3: protein (tryptophan) like, and C4: protein (tyrosine) like and petroleum derived. The average of parallel measurements is displayed.

Figure 2.8. Direct correlation plots between particle characteristics. Correlations between TEP (A,B,D), CSP (A,C,E) and unstained (D,E,F) particle concentrations, and SYBR Green stained particle associated bacteria concentrations (B,C,F). Particle associated organisms are associated specifically with TEP/CSP/unstained areas. The shaded area

corresponds to the 95% confidence interval, and displayed p and rho values represent a spearman correlation between the axes.

Figure 3.1. Elbe Estuary map. The map (**A**) depicts the outline of the Elbe Estuary, from Hamburg Harbour to Cuxhaven, with marks of the Elbe Estuary length (in kilometre) shown as black circles. Sample stations are depicted as red shapes, used throughout the manuscript, with pictures depicting the horizontal sampler, suspended/sinking particle separation and filtration results. The sequencing workflow (**B**) with the total and average number of raw, quality checked, and merged reads, assemblies, MAGs, and genes per sample. The PCA (**C**) depicts environmental changes across the study period during sample acquisition, only 2022 samples are shown due to their complete physicochemical profiles. The top 5 contributors to sample dissimilarity are shown. Adapted from Tobias-Hünefeldt et al. (2024).

Figure 3.2. Microbiome aspects in the ecosystem. Pairwise correlations between the microbial community composition, functional potential, and transcription profiles (**A**) using Mantel tests. Colours represent the pairwise correlation, and alpha the Mantels R value. Non-significant interactions (corrected $p > 0.05$) are not shown. DIST = Elbe Estuary kms, PSU = Salinity (practical salinity units), TEMP = temperature ($^{\circ}$ Celsius), NTU = Turbidity (Nephelometric Turbidity Units), DW = Particulate Dry Weight (mg L^{-1}), PA = Particle Area ($\mu\text{m}^2 \text{L}^{-1}$), DENS = particle density, PTC = Particulate Total Carbon (mg L^{-1}), POC = Particulate Organic Carbon (mg L^{-1}), DOC = Dissolved Organic Carbon (mg L^{-1}), DIC = Dissolved Inorganic Carbon (mg L^{-1}), dCO₂ = Dissolved CO₂ concentration (μM), dCH₄ = Dissolved CH₄ concentration (μM), dO₂ = Dissolved Oxygen concentration (μM), PTN = Particulate Total Nitrogen (mg L^{-1}), DTN = Dissolved Total Nitrogen (mg L^{-1}), NH₄ = Dissolved Ammonium (mg L^{-1}), NO₃ = Dissolved Nitrate (mg L^{-1}), NO₂ = Dissolved Nitrite (mg L^{-1}), TDP = Total Dissolved Phosphate (mg L^{-1}), SRP = Soluble Reactive Phosphate (mg L^{-1}), Si = Dissolved Silicate (mg L^{-1}), TEP = Transparent Exopolymer Particles ($\mu\text{m}^2 \text{L}^{-1}$), CSP = Coomassie Stainable Protein ($\mu\text{m}^2 \text{L}^{-1}$). (**B**) NMDs plots of microbiome mOTUs, functional potential, and transcripts per gene, with free-living (FL) and particle-associated (PA) samples separated. Colours represent sample dates, and shape sample stations along the Elbe Estuary. Outliers have been removed.

Figure 3.3. WGCNA mOTU module abundance in relation to salinity. Total module mOTU (**A, C**) and genes per genome (**B, D**) abundance is shown in relation to Elbe km (**A, B**) and sample dates (**C, D**). Additionally, Total mOTU module abundance is shown against salinity, binned every 3 PSU, with an adjusted R^2 value.

Figure 3.4. Particulate methane monooxygenase subunit A (*pmoA*) abundance in the Elbe Estuary for functional potential per genome and transcription per gene. The mean of two samples *pmoA* (**A, B**) functional potential and (**C, D**) transcripts per gene are shown across the Elbe Estuary. *pmoA* abundance has been taxonomically corrected against *amoA*. Colours depict sample dates and standard errors are shown as error bars and free-living (**A, C**) and particle-associated (**B, D**) abundances have been divided.

Figure 3.5. Lifestyle differences between suspended vs. sinking particle-associated functional potential and transcripts per gene. Significantly different functional potential genes (**A**) and transcripts per gene (**B**) are depicted, based on Wilcoxon tests. Colour denotes the Mantel p-value, with the y-axis representing the Wilcoxon R value, and x-axis the ratio between suspended to sinking abundance.

Figure 4.1. Overview of key findings. Processes localised to freshwater areas are surrounded by light-blue boxes. Source contributions of suspended and sinking particles are shown in orange and brown, representing terrestrial wash-in and resuspended sediments. Sun and snowflakes represent the predominantly temporal influence on carbon, while a salt shaker represents the primarily salinity dependent microbiome functionality. Black triangles show how the spatially dependent salinity drives associated osmoregulation genes and functionality, while TEP and its associated phytoplankton/prokaryote distributions are shown to localise to their area of influence (i.e. freshwater areas). Please note that findings are highly simplified for clarity.

List of abbreviations

C	Carbon
CH ₄	Methane
CO ₂	Carbon dioxide
CSP	Coomassie stainable particles
dCH ₄	Dissolved methane
dCO ₂	Dissolved carbon dioxide
dO ₂	Dissolved oxygen
DIC	Dissolved inorganic carbon
DOC	Dissolved organic carbon
DOM	Dissolved organic matter
DP	Dissolved phosphate
LISST	Laser <i>in-situ</i> scattering and transmissometry
mOTUs	Marker-gene based operational taxonomic units
MAGs	Metagenome assembled genomes
N	Nitrogen
NH ₄ ⁺	Ammonia
NO ₂ ⁻	Nitrite
NO ₃ ⁻	Nitrate
O ₂	Oxygen
POC	Particulate organic carbon
PTC	Particulate total carbon
Si	Silicate
SPM	Suspended particulate matter
SRP	Soluble reactive phosphate
TCA cycle	Tricarboxylic acid cycle
TDP	Total dissolved phosphate
TEP	Transparent exopolymer particles

WGCNA

Weighted gene co-expression network analysis

Chapter 1: General Introduction

Aquatic environments are vital CO₂ reservoirs and processing centres (Liu et al., 2022). Accurate global carbon models require production, utilisation, and storage estimates when faced with global climate and human induced changes. Estuaries are particularly vulnerable, with flooding and droughts affecting aquatic flow-rates leading to marine intrusion and eutrophication. Future considerations should include the genes and processes that drive current CO₂ and CH₄ production and utilisation for better estimates. My thesis assesses estuarine characteristics and carbon dynamics with a multifaceted approach; including microscopy, shotgun metagenomics, and metatranscriptomics to assess particle exopolymer concentrations, particle colonisation, and particle and free-living associated microbiome carbon cycling processes.

1.1 The importance of estuaries for carbon cycling

Estuaries are critical contributors to global carbon cycling (Borges & Abril, 2011; Ciais et al., 2013; Murray et al., 2015), linking terrestrial, freshwater, and pelagic ecosystems (Levin et al., 2001). Estuarine conditions promote high respiration and carbon sequestration rates, contributing to a notably large annual carbon footprint (Cole et al., 2007; Tranvik et al., 2009). Despite only representing 0.14-0.2% of the global surface area, dependent on definition, (Dürr et al., 2011; Laruelle et al., 2023) estuaries account for 0.5% and 2.5% of global CH₄ and CO₂ emissions (Borges & Abril, 2011; Ciais et al., 2013; Murray et al., 2015). However, net carbon production vs. storage is dependent on environmental conditions, including the characteristic salinity gradient and to predict future scenarios it is important to understand how estuaries function in detail now.

Estuaries form where freshwater inflows and tidal cycles mix river and marine waters. Tidal fluctuations can create dynamics whereby dense marine waters overlay otherwise less dense freshwater flows. As the marine waters sink, they create turbulent mixing which results in resuspension of inorganic and organic matter from sediments. (Savenije, 2005). Marine-freshwater interactions are highly dynamic on spatiotemporal scales. For example, warmer months, with reduced freshwater flows, are typically associated with carbon storage, while cooler temperatures increase CO₂ and CH₄ release (Zimmermann-Timm, 2002). Due to their dependence on freshwater inflows and tidal cycles, estuaries are sensitive to climate and anthropogenic influences (Kennish, 2005; O'Connor et al., 2022), affecting coastal ecosystem health (Statham, 2012).

1.2 Effects of changing estuary conditions

Estuarine biogeochemical shifts alter atmospheric and marine carbon exchanges, affecting the CO₂/CH₄ flux and greenhouse gas emissions. Under the current climate change model, extreme-weather events (e.g. droughts and floods; Christensen & Christensen, 2004; S. Huang et al., 2015) are expected to increase. Droughts deepen marine intrusions, while floods boost freshwater flows, both disrupt the hydrodynamic equilibrium (Barendrecht et al., 2024) and established patterns of biodiversity, microbial metabolism rate, food-web efficiency, and seawards nutrient/carbon transport, often leading to eutrophication (Chilton et al., 2021; Giblin et al., 2010; Gillanders & Kingsford, 2002; Santoro, 2010). However, the mechanism of these shifts is yet to be completely understood.

Salinity represents an important estuarine driving force, gradients often serving as barriers. Salinity concentrates nutrients and pollutants in deeper freshwater pockets (Iglesias et al., 2020), separates freshwater and marine organisms, and shifts brackish species ranges. Salinity increases, especially marine intrusions, reduce phytoplankton primary production rates (Sá et al., 2023; Xiong & Liu, 2018), expanding hypoxic zone sizes and frequency (Sanders et al., 2023). While present in estuaries across the globe, suboxic zones are expanding in size, frequency, and duration due to anthropogenic and climate change effects (Hinson et al., 2024). Suboxic zones damage ecosystem health by creating hostile conditions, killing or isolating endemic species, and shifting ecosystem conditions and affecting carbon cycling. For example, oxygen decreases paired with pH increases enhances mineralisation (Amann, Weiss, and Hartmann 2012a) and atmospheric CO₂ releases. Suboxic conditions also promote denitrification, further elevating greenhouse gas emissions (Balch & Mitchell, 2023; Y. Huang & An, 2022; van Hoek et al., 2021). However, more work must be done to understand how these zones form and what processes they disrupt.

1.3 Primary DOM control mechanisms

Most aquatic carbon is in an inorganic, dissolved form (CO₂, HCO₃⁻, and CO₃²⁻), with dissolved organic carbon (DOC) second in abundance (Balch & Mitchell, 2023; Cole & Prairie, 2014; van Hoek et al., 2021). While dissolved inorganic carbon (DIC) is easily quantified and characterised, DOC is composed of diverse compounds collectively known as dissolved organic matter (DOM) whose relative abundance is challenging to determine. Estuarine carbon concentrations are dependent on many factors, such as land use, nutrient loading, and water residence time (García-Martín et al., 2021). Aquatic flow rates determine water retention times, with slow flows leading to higher water retention and phytoplankton growth (Reynolds & Descy, 1996). Flow rate changes mean that labile carbon is usually accumulating labile material, high discharge areas and times contain more recalcitrant material (Lian et al., 2018). But the primary driver with 1-2 orders of magnitude concentration differences is dependent on spatiotemporal variations (García-Martín et al., 2021; Sanyal et al., 2020). This is exemplified with DOC in the Elbe Estuary 10-fold more degradable upstream compared to downstream. The majority of these spatiotemporal differences are driven by autochthonous plankton inputs (Zander et al., 2020) that generate labile carbon. This is particularly relevant as the ratio of recalcitrant:labile carbon helps predict CO₂ emissions. Here high labile freshwater DOC concentrations fuel recalcitrant DOM degradation (Neubauer et al. 2021) and increase CO₂ emissions (Amann et al., 2012; LaBrie et al., 2020). Autochthonous plankton therefore represent one of the primary control mechanisms of CO₂ emissions in estuaries, together with salinity driven primary productivity decreases (Sugie et al., 2020). The degree of recalcitrance can be estimated with the relative abundance of aromatic and humic material (Tanaka et al., 2014) using techniques like excitation and emission matrices (EEM). EEMs let us assess specific, previously identified, wavelengths to determine DOM pool characteristics (Murphy et al., 2013), such as the relative abundance of protein-like and humic-like DOM.

1.4 Particle characteristics can drive carbon cycling in aquatic ecosystems

Particulate carbon, although less abundant than dissolved, is crucial for carbon transfers and storage, linking pelagic, benthic, aquatic, and terrestrial ecosystems. Particles are highly heterogeneous (Bižić-Ionescu et al., 2018) and include non-living geogenic materials (e.g. clay

minerals), anthropogenic compounds (e.g. fly ash), non-living biogenic materials (e.g. biogenic calcite, TEP [transparent exopolymer particles], CSP [Coomassie stainable particles]), attached microorganisms (e.g. phytoplankton, bacteria, fungi), detritus (e.g. dead zooplankton, macrophytes), and faecal pellets (Zimmermann-Timm, 2002). Exact particle composition is dependent on many factors including physical, (e.g. current/tidal interactions, shear-stress, sediment resuspension; Fugate & Friedrichs, 2003; Ransom et al., 1998; Zimmermann-Timm, 2002), chemical (salinity and nutrients; Zimmermann-Timm, 2002), biotic interactions (e.g. planktonic algae), and somatic aggregation dynamics. These variable compositions result in equally variable characteristics and particle fate (Baumann et al., 2023; Cael et al., 2021; Grossart, 1999; Grossart et al., 2006) such as sequestration, resuspension, transportation, and/or microbial degradation (Dähnke et al., 2022).

Carbon fate is heavily dependent on sinking velocity, with fast-sinking particles more likely to be sequestered, while slow-sinking/suspended particles favour transportation into oceanic or terrestrial environments, or are degraded en route (Casas-Ruiz et al., 2023; Grossart, Hietanen, et al., 2003). Therefore, factors that modify sinking velocity play a large role in carbon cycles. Exopolymers, such as TEP and CSP, modify sinking velocity as they are ‘sticky’ and buoyant, enhancing aggregation and/or increasing particle degradation at the surface (Cisternas-Novoa et al., 2015; Mari et al., 2017; Passow, 2002; Simon et al., 2002; Thornton, 2018). However, it is challenging to disentangle their net role, as aggregation usually increases sinking velocity, while buoyancy decreases sinking velocities. However, bigger does not always mean faster due to porosity which slows sinking-velocity of even large particles (Baumann et al., 2023). A closer examination in a highly turbid estuary is required to determine which of their properties takes precedence.

TEP is produced by both phytoplankton and bacteria (Alldredge et al., 1993; Decho, 1990; Logan et al., 1994; Simon et al., 2002), with salinity enhancing TEP production and stickiness (Decho, 1990). Additionally, new TEP represents bioavailable carbon to eutrophic ecosystems (Bar-Zeev & Rahav, 2015), although bacteria may modify TEP without affecting concentrations (Stoderegger & Herndl, 1998). Meanwhile, bacteria are the primary protein-containing CSP producers (de Moreno et al., 1986; Thornton, 2018), although algal lysis also contributes (Bratbak et al., 1993; Møller et al., 2003; Møller, 2007; Yamada et al., 2018). Although CSP’s ecological role remains largely unclear, it is thought to play an important role in carbon remineralisation and microbial colonisation (Busch et al., 2017; Long & Azam, 1996).

Although models incorporate physical traits, they often oversimplify chemical and biotic interactions due to a lack of previous research – such as exopolymer-driven aggregation or the effects of salinity – leading to poor predictions (Burd & Jackson, 2009; Jackson & Burd, 2015). High-turbidity, fast flowing estuaries like the Elbe Estuary with high small particle abundances and shear stress (Boller & Blaser, 1998), are especially challenging, especially when the role of buoyant exopolymers and microbiome metabolic activities remains understudied. Yet, many studies still focus on large, easy to assess, particles when small particles are important biogeochemical contributors (Cael et al., 2021). This is an important knowledge gap that requires addressing. The best method includes *in situ* studies, as laboratory-generated (*ex situ*) particles lack the natural particle heterogeneity of *in situ* particles, resulting in oversimplification (Williams & Giering, 2022). For example, phytoplankton produced labile carbon in spring and summer increases particle degradability, including recalcitrant matter (Hansell & Carlson, 2014). However, even this is dependent on phytoplankton species (Becker et al., 2014) and life-stage (Olofsson et al., 2022). I set out to

help address the role of exopolymers as a particle characteristic, connecting these findings with chemical factors and biotic factors, such as nutrient and salinity gradients, and microbiome composition and transcription patterns.

1.5 Linking particles, DOM, and microbial carbon cycling in estuaries

Particles and DOM interconvert through physical, chemical, and biological processes (Lee et al., 2021). These processes include shear-stress, photodegradation, consumption, and microbial degradation, but are themselves dependent on physicochemical conditions including phytoplankton blooms and flow rates (Hillebrand et al., 2018; Reynolds & Descy, 1996; Zimmermann, 1997). Shear-stress physically separates larger/fragile particles with little-to-no DOM generation (Zhang et al., 2020). Photodegradation chemically degrades particulate matter to a dissolved form, simultaneously releasing CO₂ and CH₄ (Li et al., 2020; Xie & Zafiriou, 2009). Consumption by higher trophic-levels leads to respiration and/or food-web integration via higher level predation (Alfonso et al., 2023; Zimmermann-Timm, 2002). Microbial degradation is a hotspot of microbial activity (Grossart et al., 2007; Lyons & Dobbs, 2012; Nguyen et al., 2022; Wang et al., 2024) and carbon recycling and remineralisation (Simon et al., 2002). Microbial particle degradation therefore represents a major CO₂ source (Cai, 2011; Simon et al., 2002) that can drive biogeochemical cycles (Jiao et al., 2010; Longhurst & Glen Harrison, 1989).

Microbial particle degradation first requires colonisation. Colonisation is usually a stochastic process with some deterministic influence (e.g. chemotaxis; Grossart et al., 2003; Tobias-Hünefeldt et al., 2020) to the nutrient-rich environment (Grossart et al., 1998; Wörner et al., 2002). Following colonisation, particles are extensively modified (Baumas et al., 2021; Bižic-Ionescu et al., 2018) as the microbiome matures. Previous studies have extensively characterised microbial community composition and colonisation in response to estuarine physicochemical gradients and particle properties (Jürgens et al., 1997; Lin et al., 2024; Wörner et al., 2002). However, microbial functionality represents an important and often neglected microbiome aspect. Links between particle organisms and their metabolic potential/activity must be established to understand how carbon is transferred through the system (Liu et al., 2020; Trevathan-Tackett et al., 2019; Urvoy et al., 2022; Zoccarato & Grossart, 2019). Including processes inside of particle microenvironments such as methanogenesis (Bianchi et al., 2018). To better predict how future anthropogenic and climate changes may affect carbon cycling we must establish microbiome functionality, particle characteristics, and estuarine gradients interact.

Carbon dioxide (CO₂) and methane (CH₄) production and utilisation represent important connections between microbial particle degradation and carbon cycling (Macreadie et al. 2019). However, CO₂ production and utilisation are complex affairs, with many different pathways and associated genes, encompassing 585 KEGG (Kyoto Encyclopedia of Genes and Genomes) terms. There are 7 classified autotrophic carbon fixation pathways; the Calvin Cycle, the Reverse Krebs Cycle, the reductive acetyl-CoA, the 3-HP bicycle, the 3-HP/4-HB cycle, the DC/4-HB cycles, and the reductive glycine pathway (Santos Correa et al., 2022). However, even these 7 pathways do not capture the full extent of CO₂ fixation, with diverse heterotrophic and chemolithotrophic pathways playing significant roles (Braun et al., 2021; Zhao et al., 2020). Complications also include the reversibility of pathways, dependent on environmental conditions. Carbon dioxide utilisation is equally complex, ranging from central carbon pathways to secondary metabolisms such as antibiotic biosynthesis (e.g. *bacA*;

Mahlstedt & Walsh, 2010). Therefore, many different genes and pathways must be assessed to identify ecologically relevant patterns and reach valid conclusions.

Studies usually assess methane processing using marker genes for methanogenesis (*mcrA*: *methyl-coenzyme-M reductase*) and methanotrophy (*pmoA*: *particulate methane monooxygenase*; Liu et al., 2024). The focus on these two genes disregards non-canonical methane processing pathways. Non-canonical methanogenesis pathways, such as methylphosphonate degradation, represent a significant portion of aerobically produced methane in marine environments (Karl et al., 2008; Teikari et al., 2018). Estuaries, however, are usually dominated by hydrogenic methanogenesis, although it remains a minor CH₄ source (Feldewert et al., 2020; Li et al., 2023). Especially as sediments generally produce more methane than the water column through the *mcrA* gene (Bogard et al., 2014; Li et al., 2022). As a result, my thesis utilises the widely accepted marker genes to quantify methanogenesis vs. methanotrophy in the Elbe Estuary.

1.6 Previous Elbe Estuary carbon processing

The Elbe Estuary is one of Europe's largest and of vital commercial importance. The Elbe Estuary supports diverse habitats and species from Geesthacht to the North Sea. It is a well-mixed mesotidal estuary characterised by high turbidity, strong currents, and substantial nutrient loads partially exported to the North Sea (Bergemann and Gaumert, 2010). Recent dredging and deepening, alongside climate-driven hydrological shifts have altered its physicochemical profile (Kerner, 2007; Sanders et al., 2023). The Elbe Estuary represents a good model system to assess biogeochemical carbon cycling in an estuary strongly impacted by anthropogenic (industrial activities and urbanisation) and climate (marine intrusion and freshwater inflow) changes.

Carbon research in estuaries predominantly focuses on freshwater regions, overlooking brackish and marine zones (Amann et al., 2012, 2015; Cisternas-Novoa et al., 2015; Jürgens et al., 1997; Matoušů et al., 2018; Zimmermann-Timm, 2002). To address this gap, my sampling scheme includes freshwater, brackish, and mesohaline sites (Figure 1.1). Thereby I can assess the role of microbial degradation and associated genes across the salinity gradient and in the context of heterotrophic activities and community diversity, which represents another knowledge gap.

Previous particle studies in the Elbe Estuary often neglect small particles and overestimate size due to their chosen methods. Therefore, their findings must be interpreted with caution. Previous methods included manually selecting an insufficient number of larger particles (>20 fields of view or 350 events are required; Muthukrishnan et al., 2017) and determining size under 10x magnification (Zimmermann, 1997). Since then Laser *In-Situ* Scattering and Transmissometry (LISST) particle analysers have been deployed 5m below the surface (Papenmeier et al., 2014). The deeper deployment means particles are under lower disaggregation forces, reducing wind-forcing, and may even represent different particle characteristics from surface particles due to weak seasonal stratification (Pein et al., 2021). Additionally, high-turbidity environments cause multi-scattering in LISST systems, leading to particle size distribution degradation, especially of small particles.



Figure 1.1. Elbe Estuary map. The map depicts the Elbe estuary, from Hamburg Harbour to Cuxhaven, with marks of the Elbe length (in kilometre) shown. Sample stations are shown as stars. Originates from Tobias-Hünefeldt et al. (2024).

Upper freshwater particles are dominated by plankton and catchment area derived organic carbon, with ~90% bacterioplankton on particles (Zimmermann, 1997). During downstream transport carbon is continuously degraded (Zimmermann-Timm et al., 2002) resulting in mineral-rich particles whose OC originates from the North Sea during tidal cycles and marine intrusions (Zander et al., 2020, 2023) and aromatic and humic-like material (Crump & Baross, 1996; Jürgens et al., 1997). Leading to only ~40% of bacterioplankton in the water column located on the particles (Zimmermann, 1997). Particles between these areas also differ significantly in size (Mari et al., 2012; Wörner et al., 2002; Zimmermann-Timm, 2002) due to flow-rate differences (Eisma, 1993), with organic matter content (e.g. TEP/CSP) also important (Zimmermann & Kausch, 1996). Salinity is a major driver behind these differences, affecting carbon quality and particle composition (Fast & Kies, 1990; O'Boyle & Silke, 2010; Sugie et al., 2020), decreasing primary production from $260 \mu\text{g C L}^{-1} \text{ h}^{-1}$ to $50 \mu\text{g C L}^{-1} \text{ h}^{-1}$ (Fast & Kies, 1990; Sugie et al., 2020), reducing bacterioplankton particle colonisation (Jürgens et al., 1997; Wörner et al., 2002) and particle-associated microbial activity (Fast & Kies, 1990), and reducing dissolved CH_4 concentrations (median 416 vs 40 nmol L^{-1}) and oxidation rates (median 161 vs $10 \text{ nm L}^{-1} \text{ day}^{-1}$) in brackish conditions (Matoušů et al., 2018). Seasonal hypoxia also plays a significant role in the Elbe Estuary's carbon cycle with the turbidity maximum zone (TMZ) traditionally removing up to 50% of the incoming POC (Amann et al., 2012, 2015). However, pH and hypoxia increases in the oxygen minimum zone (OMZ) could lead to increased CO_2 emissions as a result of increased mineralisation efficiencies (Sanders et al., 2023). Therefore, the exploration of the estuarine salinity gradient is of great interest, especially when linked to microbial carbon processing, seaward carbon transport, and dissolved CO_2/CH_4 ($\text{dCO}_2/\text{dCH}_4$) concentrations (Macreadie et al., 2019).

1.7 Study project and graduate school: RTG2530 (BiCEst)

My thesis (Project B2) is part of the DFG-funded graduate school 'Biota-mediated effects on carbon cycles in Estuaries (BiCEst)', investigating how physicochemical gradients in an

estuarine system, both aquatic and terrestrial, affect organisms across multiple trophic levels, and their interactions across environments. The research training group answers research gaps in the role of estuaries as carbon sinks and sources, identifying conditions that drive carbon processing as many biological estuarine carbon cycling processes remain underexplored (Ren et al., 2022). The work revisits previous Elbe research carried out decades ago (Bernát et al., 1994; Eisma, 1993; Kies et al., 1996) which classified the Elbe as a CO₂ source based on DIC dynamics (Amann et al., 2015). Yet, details were lacking, specifically which biological processes affect estuarine carbon cycling, now or under future climate scenarios. The research program is approaching the research question from multiple angles and at multiple scales in both terrestrial and aquatic ecosystems. Eventually linking both environments and identifying carbon exchanges. Approaches include creating and refining hydrodynamic and gas flux models, characterising fish, zooplankton, and phytoplankton distributions, the food-web they are associated with, and their stress responses across spatiotemporally diverse estuarine gradients. The in-depth analysis requires a wide range of techniques and methods such as stable isotope analysis, DNA/RNA extractions, modelling, and laboratory based mesocosm experiments.

My project (B2) focuses on the microscale, assessing aquatic particle and dissolved organic matter characteristics, and particle- and free-living-associated microbiome composition. My project represents an important component, assessing one of the lowest food-web components and CO₂ and CH₄ measurements (important greenhouse gases) and *in situ* microbial processing. Specifically, the project concerns itself with how changes across a spatiotemporally dynamic estuarine gradient affects carbon cycling in the context of microbial processing, captured via metabolic potential and transcription profiles. Measurements include nutrient and relevant physicochemical parameter concentrations (such as dCO₂ and dCH₄, DOC, silicate, total dissolved phosphate, nitrate, temperature, and oxygen, to name just a few). Microscopy is used to determine particle and exopolymer abundance patterns, bacterial particle and exopolymer colonisation. Excitation and emission spectra are measured to determine DOM characteristics. Next-Gen sequencing of DNA and RNA allows us to assess the microbiome composition, functional potential, and transcription profiles. Samples are taken from the surface (~1m) due to their relevance as sites of CO₂/CH₄ production and storage, and atmospheric exchange. Many of these measures are additionally used by other projects in the graduate school to refine models, and inform on ecological reasons behind their own area of interest. One example, the determination of brackish vs. freshwater areas and how connected terrestrial and aquatic ecosystems differ along the estuarine gradient.

1.8 Objectives:

The many techniques used during my thesis' completion allows for deeper insights into knowledge gaps (Figure 1.2) pertaining to particulate-dissolved carbon dynamics, the potential role and impact of exopolymers, and how the microbiome interacts with both in a gene specific manner. These gaps are of particular interest as physicochemical conditions are expected to shift under future climate change scenarios, and it is vital we understand the results of these changes and interactions to accurately predict follow-up effects and how we may alleviate them. Thereby informing future policy decisions.

The first manuscript focuses on particulate and dissolved carbon dynamics in the Elbe estuary in changing physicochemical gradients over a spatiotemporal framework to give a comprehensive overview. I explore particle characteristics in the face of seasonal differences

and the expected phytoplankton blooms, freshwater-brackish water DOM recalcitrance and links to particle characteristics, and particle colonisation difference due to the salinity gradient and suspended vs. sinking particle characteristics.

- 1) The first objective determines how particle and dissolved organic matter characteristics respond to physicochemical gradients across a high-turbidity and velocity estuary using microscopy to determine exopolymer concentrations, combustion techniques to assess particle carbon compositions, and excitation and emission matrices to determine DOM properties. **Hypothesis 1:** Seasonality and freshwater vs. brackish differences lead to significant spatiotemporal differences in accordance with phytoplankton distributions.
- 2) The second objective examines the relationship between particle and dissolved carbon, due to the intrinsic link between photosynthesis and microbial degradation. Combining the previously established characteristics from objective one and identifying interactive trends between particulate and dissolved organic matter characteristics. **Hypothesis 2:** Suspended and sinking particle characteristics represent distinct carbon sources, with resuspended sediment playing a major role in sinking particles and linked to more recalcitrant DOM. Suspended particles, meanwhile, are made up of more labile carbon originating from an autochthonous DOM pool.
- 3) The third objective assesses particle colonisation across the salinity gradient and between suspended and sinking particles. Microscopy utilised with stains to identify exopolymers and bacterial abundances. **Hypothesis 3:** lability increases lead to increased microbial colonisation, with freshwater particles increasingly colonised over brackish particles, and suspended particles more colonised by bacteria than sinking particles due to higher exopolymer concentrations acting as buoyancy agents.

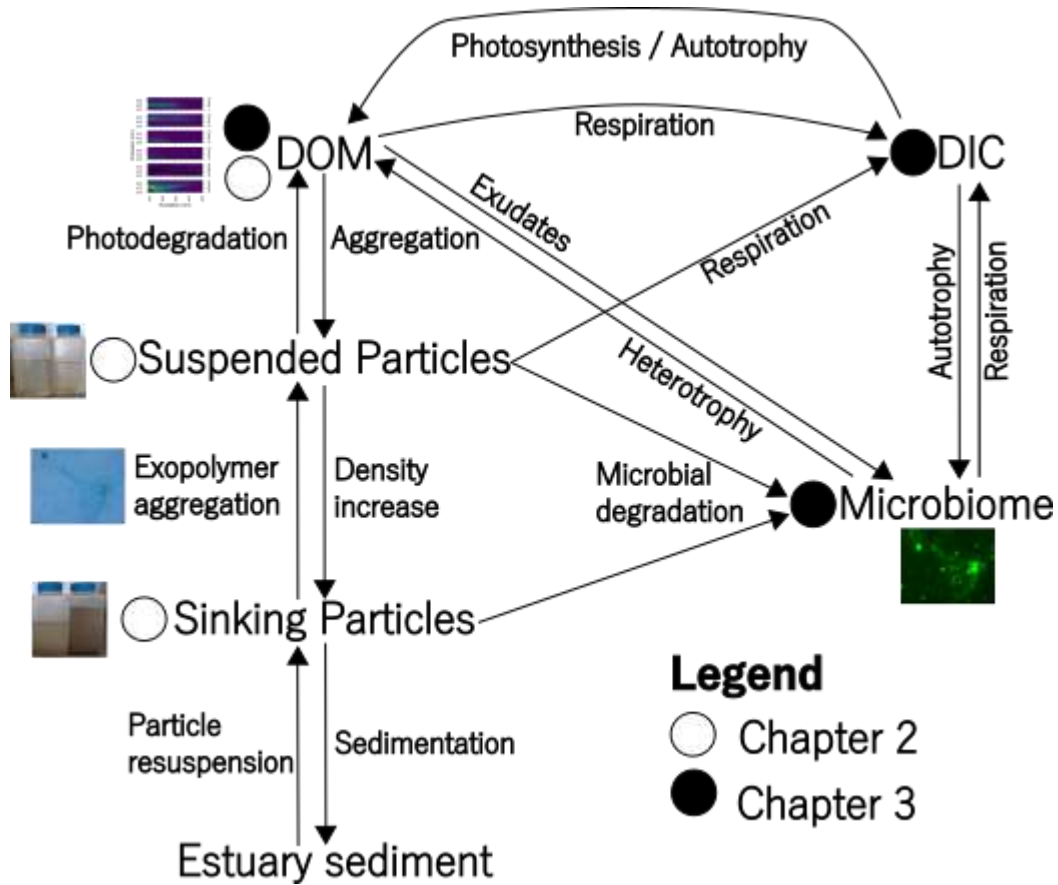


Figure 1.2: A conceptual diagram of carbon transfers in estuaries. The focus of each thesis chapter has been marked with either a hollow (chapter 2) or filled (chapter 3) circle. All plots and images were created/taken by Sven P. Tobias-Hünefeldt.

The second manuscript focuses on microbiome interactions and relates the previously established carbon dynamics to microbiome profiles across the estuary. We explore the particle-water column characteristics in more depth by focusing on carbon relevant variables, microbiome composition, functional potential, and transcriptional profile differences between suspended and sinking particles. Finally, spatiotemporal contributions to microbiome composition and carbon processing are evaluated.

- 1) The first objective contextualises microbiome composition, functional potential, and transcription profiles in the context of carbon processing across spatiotemporal gradients by associating microbiome patterns with physicochemical measurements. **Hypothesis 3:** We hypothesise that osmotic pressure spatially constrains taxa, driving shifts in microbiome composition and functionality.
- 2) The second objective assesses dCO₂ and dCH₄ profiles during the study period, relating them to microbiome composition and functionality. **Hypothesis 1:** Salinity and phytoplankton blooms result in carbon process localisation driving primary production, heterotrophy, methanogenesis, and methanotrophy.

- 3) The third objective concerns itself with identifying significant carbon processing differences between free-living and particle associated microbiomes, independent of spatiotemporal gradient. **Hypothesis 2:** Particle-associated microorganisms play a large role in complex polymer degradation, unlike free-living microbes. Additionally, suspended-particle microbes are associated terrestrial processes, while sinking particles instead show increased transcription of methanogenesis-associated genes.

1.9 Thesis outline

This thesis is structured as a cumulative thesis, each manuscript represents the two main chapters. A general introduction to the topic is followed by chapters 2 and 3 that represent original research articles corresponding to the main objectives of my PhD thesis. All manuscripts have either been published or are currently undergoing peer-review in scientific journals, their status is detailed in Table 1.1. Finally, Chapter 4 is a general discussion that summarises the overall findings and expands on future perspectives. Cited references from all chapters are listed after the Chapter 4: General Discussion, after which the appendix contains supporting information for all manuscripts and chapters. Tables and figures in each chapter have been renumbered to fit the thesis structure.

Table 1.1. Overview and publication status of thesis manuscripts.

Manuscript I	Seasonality, rather than estuarine gradient or particle suspension/sinking dynamics, determines estuarine carbon distributions
Authors	Sven P. Tobias-Hünefeldt, Justus E.E. van Beusekom, Vanessa Russnak, Kirstin Dähnke, Wolfgang R. Streit, Hans-Peter Grossart
Status	Published in <i>Science of The Total Environment</i> 2024, Volume 926, 171962
Manuscript II	Suspended and sinking particle-associated microbiomes exhibit distinct lifestyles
Authors	Sven P. Tobias-Hünefeldt, Jason N. Woodhouse, Hans Joachim Ruscheweyh, Shinichi Sunagawa, Vanessa Russnak, Wolfgang R. Streit, Hans-Peter Grossart
Status	Submitted 4.05.2024

Chapter 2: Seasonality, rather than estuarine gradient or particle suspension/sinking dynamics, determines estuarine carbon distributions.

This chapter's figure and section numbers have been modified to integrate the publication into the thesis and was published as: Tobias-Hünefeldt, S.P., van Beusekom, J.E.E., Russnak, V., Dähnke, K., Streit, W.R., Grossart, H.-P., 2024. Seasonality, rather than estuarine gradient or particle suspension/sinking dynamics, determines estuarine carbon distributions. *Science of The Total Environment* 926, 171962. <https://doi.org/10.1016/j.scitotenv.2024.171962>

2.1 Abstract

Estuaries are important components of the global carbon cycle; exchanging carbon between aquatic, atmospheric, and terrestrial environments, representing important loci for blue carbon storage and greenhouse gas emissions. However, how estuarine gradients affect sinking/suspended particles, and dissolved organic matter dynamic interactions remains unexplored. We fractionated suspended/sinking particles to assess and characterise carbon fate differences. We investigated bacterial colonisation (SYBR Green I) and exopolymer concentrations (TEP/CSP) with microscopy staining techniques. C/H/N and dry weight analysis identified particle composition differences. Meanwhile, nutrient and carbon analysis, and excitation and emission matrix evaluations with a subsequent parallel factor (PARAFAC) analysis characterised dissolved organic matter.

The lack of clear salinity driven patterns in our study are presumably due to strong mixing forces and high particle heterogeneity along the estuary, with only density differences between suspended and sinking particles. Elbe estuary particles' organic portion is made up of marine-like (sinking) and terrestrial-like (suspended) signatures. Salinity did not have a significant role in microbial degradation and carbon composition, although brackish estuary portions were more biologically active. Indicative of increased degradation rates, leading to decreased greenhouse gas emissions, which are especially relevant for estuaries, with their disproportionate greenhouse gas emissions. Bacterial colonisation decreased seawards, indicative of decreased degradation, and shifts in microbial community composition and functions.

Our findings span diverse strands of research, concerning steady carbon contributions from both marine and terrestrial sources, carbon aromaticity, humification index, and bioavailability. Their integration highlights the importance of the Elbe estuary as a model system, providing robust information for future policy decisions affecting dissolved and particulate matter dynamics within the Elbe Estuary.

2.2 Introduction

The carbon cycle is a vital biogeochemical component in aquatic environments and encompasses both organic and inorganic states. In particular, estuaries are characterised by large carbon footprints and transportation mechanisms (Khatiwala et al., 2013; Rackley, 2010), modulating greenhouse gas emissions and thus climate change feedback. Therefore, it is crucial to understand how carbon is transferred throughout these aquatic systems.

Estuarine conditions result in high respiration and carbon sequestration rates (Cole et al., 2007; Tranvik et al., 2009) and thus a disproportionately high global carbon cycle proportion. Even though they only make up 0.14–0.2 % of the global surface area (Dürr et al., 2011; Laruelle et al., 2023), they contribute 0.5 % and 2.5 % of global methane and CO₂ production (Borges & Abril, 2011; Ciais et al., 2013; Murray et al., 2015). Estuaries can act as carbon sinks during productive seasons (i.e. spring and summer), but high CO₂ production in the freshwater section results in annual net CO₂ production (Zimmermann-Timm, 2002).

Particles are major components of any aquatic ecosystem, and play a central role in estuarine carbon cycles, influencing the fate of organic materials by connecting pelagic, benthic, and aquatic environments. Particles can undergo sequestration in estuarine and marsh sediments, resuspension under high discharge conditions, as well as microbial degradation, and consumption (Simon et al., 2002; Zimmermann-Timm, 2002). Particulate matter can be washed onto terrestrial systems such as marshland and sequestered into the marsh sediments (Yuan et al., 2022) and resuspended and washed in from terrestrial sources, be that surrounding farmland, marshlands, or beaches (Yuan et al., 2022). Evidence has shown that estuarine biogeochemistry is governed by the settlement, resuspension, and remineralisation of particulate matter (Dähnke et al., 2022).

Buoyancy is an important aspect of particulate matter and carbon fate, be it carbon degradation and release into the atmosphere or sequestration into long term carbon storage within the riverbed. Transparent exopolymer particles (TEP) and Coomassie sustainable particles (CSP) have been identified to play a key role in buoyancy (Mari et al., 2017). These sticky exopolymer compounds are characterised by their stainable properties and composition, that affect physical and chemical properties, and ultimately their environmental fate. TEP is produced by both phytoplankton (Alldredge et al., 1993; Decho, 1990; Logan et al., 1994) and bacteria (Simon et al., 2002) and plays a key role in the formation of marine snow, an important ocean carbon sequestration mechanism (Passow, 2002). TEP also acts as a metabolic surrogate in eutrophic ecosystems, adding fresh bioavailable carbon through tight bacterial associations (Bar-Zeev & Rahav, 2015). It has been shown that bacteria can also cause modification to exopolymers without affecting concentrations, however the exact mechanisms and changes have yet to be understood (Stoderegger & Herndl, 1998). Meanwhile, CSP production and its ecological role are not neatly defined, although microorganisms are a significant CSP source (Long & Azam, 1996; Thornton, 2018). CSP primarily consists of proteins, and has been shown to stain tyrosine and tryptophan containing compounds (de Moreno et al., 1986), and is thought to be an important site of microbial colonisation and carbon remineralisation (Busch et al., 2017). The relative composition of TEP and CSP has implications for carbon cycling by affecting sinking velocities and aggregation dynamics (Cisternas-Novoa et al., 2015; Passow, 2002; Thornton, 2018). Higher TEP and CSP concentrations cause aggregation via particulate matter recruitment and keep carbon near the surface, increasing surface carbon recycling and remineralisation, while also decreasing the biological carbon pump effectiveness (Mari et al., 2017; Passow, 2002).

Efforts have been made to differentiate particles according to their settling properties (Lunau et al., 2004). In the Wadden Sea, of which the Elbe estuary is a tributary, a large tidal influence on various fraction features was identified based on sinking velocity, specifically POC:SPM, size, and bacterial colonisation (Lunau et al., 2006). Seasonality was another driver, with decreased particle abundance and increased size during the growing season (Spring-Summer). This study concluded that aggregation and sedimentation dynamics were

predominantly driven by microbial processes during the growing season, but physical forcing in fall and winter. Therefore, phytoplankton blooms represent additional, seasonal, carbon influxes above the normal, year-round, additions. This would also affect particle characteristics, due to phytoplankton providing labile carbon, and even increase the degradation of recalcitrant organic matter due to the priming effect (Hansell & Carlson, 2014), resulting in changes to the dissolved organic matter pool.

Dissolved organic matter can be studied with excitation and emission matrices, identifying distinct sources of fluorescent dissolved organic matter, and their characteristics, such as protein (e.g. tyrosine and tryptophan) or humic-like (Murphy et al., 2013). It has been shown that residence time (age of material) is a large factor due to continuous breakdown of organic carbon compounds via microbial- and photochemical degradation (Painter et al., 2018), affecting DOC characteristics and spectral signatures. Recalcitrance and lability are not only linked to the age of POC, but also spatially distinct. Zander et al., (2020) identified a 10-fold increase in organic matter degradability upstream compared to downstream areas; attributed to increased organic matter and DNA concentrations from the increased catchment effects, and that upstream areas contained more autochthonous plankton-derived (degradable) organic matter. However, indirect salinity effects could also play a role due to primary productivity decreases in response to salinity, dependent on phytoplankton community morphological and functional changes (Sugie et al., 2020).

The Elbe estuary is an important system for studying the dynamics of particles and dissolved organic matter in estuarine environments. It is one of the largest estuaries in Europe, and supports a wide range of habitats and species, and is of great commercial importance. However, the last few decades have seen large changes in its water characteristics, both due to climate change and warming conditions, and continuous dredging and water channel deepening events (Kerner, 2007). The Elbe shows large differences between its upper (freshwater) and lower (brackish and marine influenced) estuary areas. Freshwater particles are smaller (Mari et al., 2012; Wörner et al., 2002; Zimmermann-Timm et al., 2002), as seaward estuary portions tend to have lower flow rates (Eisma, 1993) with links between particle size and the organic matter content (Zimmermann & Kausch, 1996), possibly due to TEP and CSP. Carbon quality and particulate composition differences have been indirectly attributed to the salinity gradient (Fast & Kies, 1990; O'Boyle & Silke, 2010; Sugie et al., 2020) and potentially lead to qualitative carbon differences, such as the labile to recalcitrant carbon ratio, over an estuary's salinity gradient. High salinity estuary particles primarily consist of more aromatic and humic-like material (Crump & Baross, 1996; Jürgens et al., 1997) due to continuous particle degradation during seaward particle transport (Zimmermann-Timm, 2002). In fact, the organic matter near the Elbe's mouth was found to be dominated by mineral bound organic matter, rather than fresher, non-mineral bound organic matter (Zander et al., 2023). Particulate degradation occurs for the large part near Hamburg Harbour, as evidenced by low oxygen concentrations, and a seasonal oxygen 'hole' (Sanders et al., 2023), just as increased oxygen values downstream near Cuxhaven are indicative of increased primary phytoplankton production. However, while the Elbe's upper estuary organic matter was composed primarily of organic material from the Elbe's catchment and of autochthonous origin (i.e. plankton remnants), downstream regions received organic matter from the North Sea through tidal movements, which was primarily allochthonous (e.g. plant litter and eroded soils; Zander et al., 2020).

Elbe particles showed an unusually high level of colonisation from 0.3×10^6 to 25×10^6 bacteria per particle (Zimmermann-Timm et al., 2002) to 0.3×10^6 to 25×10^6 bacteria L⁻¹ (Zimmermann, 1997). While 85 % of particles were colonised by bacteria, downstream particles, dominated by mineral particles, were not as densely colonised as upstream (Zimmermann, 1997).

We assessed three primary hypotheses.

- Seasonality leads to significant differences in particle characteristics, with increased organic carbon concentrations in spring and summer due to phytoplankton blooms.
- Downstream areas contain more recalcitrant DOM compounds compared to upstream areas, with seasonal exacerbation.
- Freshwater particles are more heavily colonised than downstream. With suspended particles less colonised than sinking particles.

The Elbe is a well-studied system in terms of particle dynamics. However, this study represents a step forward as it characterises the connection between particulate and dissolved matter, specifically POC and DOC within the aquatic water-column, identifying interactions between them with both spatial and seasonal considerations. In this article, we assess carbon cycling within the Elbe Estuary, with a focus on salinity gradient based changes, the differences between suspended and sinking particles, and POC/DOC interactions. We will also discuss the relative contribution of DOC and POC to the River Elbe carbon cycle. By synthesising these diverse strands of research, we provide a comprehensive overview of the importance of particles in estuarine systems, and highlight the importance of the Elbe estuary as a model system for studying these processes, providing robust information for future policy decisions.

2.3 Materials and Methods

2.3.1 Sampling

Samples were taken from the River Elbe estuary in the main channel, Germany, in Jul-21, Feb-22, May-22, Jun-22, and Nov-22 at 5 stations (Mühlenberger Loch [53.54907, 9.82338], Twielenfleth [53.60921, 9.56536], Schwarztonnensand [53.71442, 9.46976], Brunsbüttel [53.88742, 9.19429], and Medemgrund [53.8363, 8.88777]; Figure 2.1). Cruises were timed for consistent high-tide slack-water at the center station, Schwarztonnensand; flooding at Mühlenberger Loch and Twielenfleth, and ebbing at Brunsbüttel and Medemgrund. Samples were taken with a horizontal sampler (Lunau et al., 2004) at a depth of 1 m, due to very high Elbe turbidity which rapidly decreases primary production over depth. Suspended and sinking particles were allowed to vertically separate for 30 min, and downstream particle analyses were carried out on each separate fraction. All samples were collected in duplicate, unless otherwise stated.



Figure 2.1. Elbe estuary map. The map depicts the outline of the Elbe, from Hamburg Harbour to Cuxhaven, with marks of the Elbe length (in kilometre) shown as circles, and sample sites indicated as red stars.

2.3.2 Particle sampling

Particle fractions (suspended/sinking) were filtered through pre-weighed and rinsed GF75 filters, followed by another rinsing to remove salts, to determine their particulate matter dry weight and particulate total and organic carbon contents. Before use, filters were pre-combusted for 5 h at 400 °C to avoid residual organic carbon.

Microscopic analyses used fractionated particles filtered onto three 25 mm 5 µm polycarbonate filters. All filters were stained with SYBR Green I solution (Molecular Probes). One filter was stained with Alcian Blue to identify Transparent Exopolymer Particles (TEP), one with Coomassie Brilliant Blue G-250 to identify Coomassie Stainable Particles (CSP; Klawonn et al., 2023), and one remained unstained as a negative control. Free-living organisms were identified by filtering bulk water onto a 25 mm 0.22 µm polycarbonate filter, and stained with SYBR Green I solution. All microscopy filters were placed onto Cytoclear slides and stored at –20 °C until further analysis.

2.3.3 Physicochemical parameters

Salinity, oxygen, temperature and turbidity were measured with the onboard FerryBox (Petersen et al., 2011). Bulk water was utilised to measure dissolved CO₂ and CH₄ concentrations using the headspace technique. In brief, 100 mL of water was collected in a 500 mL syringe, 400 mL of pure N₂ gas was added and the syringe vigorously shaken for 1 min. 350 mL of gas were transferred to 1 L Gas Bags and the CO₂ and CH₄ concentration measured within 12 h using an Ultraportable Los Gatos (Los Gatos Research, USA).

Dissolved organic carbon (DOC), dissolved ammonium, dissolved nitrate, dissolved nitrite, soluble reactive phosphate (SRP), and total dissolved nitrogen, phosphate, and silicate were determined in the 0.22 µm Durapore filtrate. Tests with Elbe water showed no significant carbon content difference when utilising either prewashed GF75 or prewashed Durapore 0.22

μm filtrate. DOC and total dissolved nitrogen (TDN) were measured on a Shimadzu, TOC-L, with the addition of a TNM-L module using the EN 1484 method guidelines using oxidation. Nitrate (NO_3^-) and Nitrite (NO_2^-) were measured on a FIAStar 5000 with the DIN EN ISO 13395-D28 method, while ammonium (NH_4^+) was measured with the DIN EN ISO 11732-E23 method, soluble reactive phosphate (SRP) and total dissolved phosphate (TDP) were measured with the ISO/DIS 15681-2 method, $\text{K}_2\text{S}_2\text{O}_8$ was added to TDP samples, and autoclaved before measurement, while SRP samples were measured directly after thawing. Dissolved silicate (Si) concentrations were measured with the DIN 38405-D21 method.

POC was measured from the stored GF75 filters. In brief, filters were dried for 24 h, followed by a 24 h-fumigation period in a desiccator with 1 M HCl. Filters were re-dried for 24 h, after which they were enclosed in tin capsules (5 × 9 mm, IVA Analysentechnik GmbH & Co. KG, Meerbusch, Germany). Carbon content was subsequently determined with an elemental analyser.

2.3.4 Microscopic image analysis

High quality images are vital when cell counting (Zeder et al., 2010), therefore images were manually curated for focus and artefacts. Individual filters were imaged on a Zeiss Z.1 Observer epifluorescence microscope at a 630 \times magnification on an even spread around the filter surface area using both Brightfield and FITC light (excitation 475/40, beamsplitter 500, emission 530/50). A minimum of 20 images were retained for downstream analysis, with a minimum of 350 total events for reliable data interpretation (Muthukrishnan et al., 2017). Particle size and abundance were measured using ImageJ (version 1.53q) and a custom macro script (<https://github.com/SvenTobias-Hunefeldt/ElbeParticlesDOM.git>). This was converted to $\mu\text{m}^2 \text{ L}^{-1}$, and will from here on be referred to as concentration. Most bacterial cells have a surface area $< 5 \mu\text{m}^2$, while TEP has been shown to range from a size of $\sim 5 \mu\text{m}$ to $> 100 \mu\text{m}$. (Simon et al., 2002). As such, a minimum particle size of 5.01 μm^2 was set to avoid conflicts with microorganisms, while a maximum microorganism size was set at 5 μm^2 to distinguish them from particles. Measured particle concentration was upscaled to a per Litre measurement with the following formula:

$$\begin{aligned} & [\text{Image Particle Concentration}] \times [\text{Magnification Effect}] \\ & \times [\text{Mililitre to Litre Conversion}] \end{aligned}$$

False discovery correction was applied with TEP and CSP identification macros against unstained particle filters, and calculated in R (Figure S2.1).

We utilised the allometric biomass method to provide robust biomass calculation (Norland, 1993). The derived constant bacterial biovolume ratio is 560 fg C μm^{-3} (Bratbak, 1985). Additionally, TEP and CSP particle percentage was calculated using the following particle concentration formula:

$$\frac{[\text{TEP or CSP}]}{[\text{Unstained}] + [\text{TEP}] + [\text{CSP}]}$$

2.3.5 Dissolved organic matter (DOM) analysis

DOM samples were obtained from the 0.22 µm Durapore filtrate. No significant DOM differences could be identified between 0.22 µm Durapore and GF75 filtered water samples when tested. Absorbance was measured from 190 to 800 nm using a U-2900 Spectrophotometer (Hitachi, Chiyoda City, Tokyo, Japan), while excitation (220–455 nm) and emission (290–700 nm) matrices (EEMs) were measured in 5 nm increments on a F-7000 Fluorescence Spectrophotometer (Hitachi, Chiyoda City, Tokyo, Japan) running FL Solutions 2.1. DOM analysis was carried out in R with the stardom package (version 1.1.25), following the concept of Murphy et al., (2013). EEMs underwent inner filter effect and second-order Raman and Rayleigh scattering effect correction. Blank-correction was carried out on all samples by subtracting the EEM (excitation and emission matrix) of MilliQ water (Millipore). Additional fluorescence indices were calculated.

Absorbance at 254 nm was divided by the DOC concentration (mg C L⁻¹) to determine the specific UV absorbance (SUVA₂₅₄), used as an aromaticity indicator (Weishaar et al., 2003). Additional aromaticity indicators include the UV specific absorbance at 280 nm known as ε₂₈₀ (Weishaar et al., 2003), and E₂/E₃ and E₄/E₆ ratios that are calculated from the absorbance ratio of at 250 and 365, and 465 and 665 nm, respectively (Murphy et al., 2013). Additionally, the E₂/E₃ ratio provides information on DOM molecular weight, while E₄/E₆ informs the degree of humification. Coble peaks, humification, biological freshness and the relative contribution of terrestrial and microbial sources to the DOM pool were assessed with the eemR (version 1.0.1) package (Massicotte, 2019). Relative Fluorescence Efficiency (RFE), an indicator of algal vs. non-algal DOM, calculated with the ratio of fluorescence at excitation and emission wavelengths 370 and 460 nm to absorbance at 370 nm (Downing et al., 2009), has previously identified tidal forcing effects on DOM. A higher value indicates increased terrestrial DOM. The fluorescence index is inversely related to the lignin content of DOM, in which lower values (~ 1.3) suggest a more terrestrially derived DOM source whereas higher values (~ 1.8) suggest microbial-derived DOM (McKnight et al., 2001). We measured the freshness index (β/α) which indicates recent production of DOM, with β representing more recently derived DOM and α representing relatively more decomposed DOM (Wilson and Xenopoulos 2008). The slope between 275 and 295 nm was calculated using a non-linear regression, and is used as an indicator of the terrigenous DOC percentage in river-influenced ocean margins (Fichot & Benner, 2012). The slope ratio is calculated by the non-linear regression of the slope between 275 and 295 nm, and the slope between 350 and 400 nm and indicates non-conservative processes, such as primary production and degradation (Helms et al., 2008; Sanyal et al., 2020). From the calculated slope and indices values a principle component analysis (PCA) was generated with the FactoMineR (version 2.4), normalisation utilised scaled units.

A Parallel Factor (PARAFAC) model was fitted to the data with non-negativity constraints in all modes. During data exploration, excitation at 220 nm was removed due to abnormally high leverage. Fluorescence intensity of the 4 components was reported relative to each component's maximum intensity, as well as component contribution to total sample fluorescence. The model showed a core consistency of 89.5 % and a fit of 99 %. Further model validation was carried out with a split-half analysis (Stedmon & Bro, 2008), where Tucker's congruence was equal to or above 0.95. EEMQual gave 88.6 %. Briefly, the 4 extracted model components are; C1: marine humic-like (Coble, 1996; Gold-Bouchot et al., 2021), C2:

terrestrial humic-like (Coble, 1996; Shutova et al., 2014), C3: protein (tryptophan) like (Coble, 1996; Yan et al., 2020), and C4: protein (tyrosine) like and petroleum derived (Brünjes et al., 2022; Coble, 1996). Sample component, total, and residual fluorescence patterns are available in Figure S2.2. It is difficult to assign specific molecular compounds to each DOM component, as several sources contribute to each and are therefore hard to separate (Walker et al., 2013).

2.3.6 Statistical analysis

All figures were created using ggplot2 (version 3.3.5; Wickham, 2016) and finalised with Inkscape (version 1.2.1 (9c6d41e410, 2022-07-14)) unless otherwise stated. Seasonal differences were assessed with the stats (version 4.1.2) and rstatix (version 0.7.0) packages. Correlations between two trends, differences between two group means, and pairwise differences from groups were assessed with the stats packages. More detailed R code is available at <https://github.com/SvenTobias-Hunefeldt/ElbeParticlesDOM.git>.

2.4 Results

2.4.1 Minimal salinity gradient effects on carbon abundance and characteristics

Minimal spatial patterns could be identified throughout the study period, instead most spatial patterns were limited to individual timepoints. TEP was the only particle characteristic that showed a clear spatial pattern irrespective of season. TEP decreased significantly seawards ($\eta^2 = 0.17$, $p < 0.01$), unlike CSP ($p > 0.05$) which showed no clear spatial trend (Figure 2.2). When associated with the estuarine gradient the same held true, with a significant correlation for TEP (Spearman, $\rho = -0.4$, $p < 0.01$) while CSP remained insignificant (Spearman, $p = 0.35$). Neither the dry-weight nor particle concentration (as $\mu\text{m}^2 \text{ L}^{-1}$) correlated to different stations, salinity, or temperature gradient values (Figure 2.3, ANOVA and Spearman). Although dry-weight and particle concentration correlated significantly to each other (Spearman, $p = 0.04$); dry-weight peaked at different stations during each season, with no clear spatial pattern, e.g. Feb-22 peaked at Mühlenberger Loch and Nov-22 at Twielenfleth. Turbidity (Figure 2.4) and particle concentration (Figure 2.3) are equally diverse, with no shared concentration peaks. These findings matched flow rate changes in the months quite closely, with a high flow rate associated with downstream high turbidity, and lower flow rates with more upstream high turbidity zones (Figure S2.3).

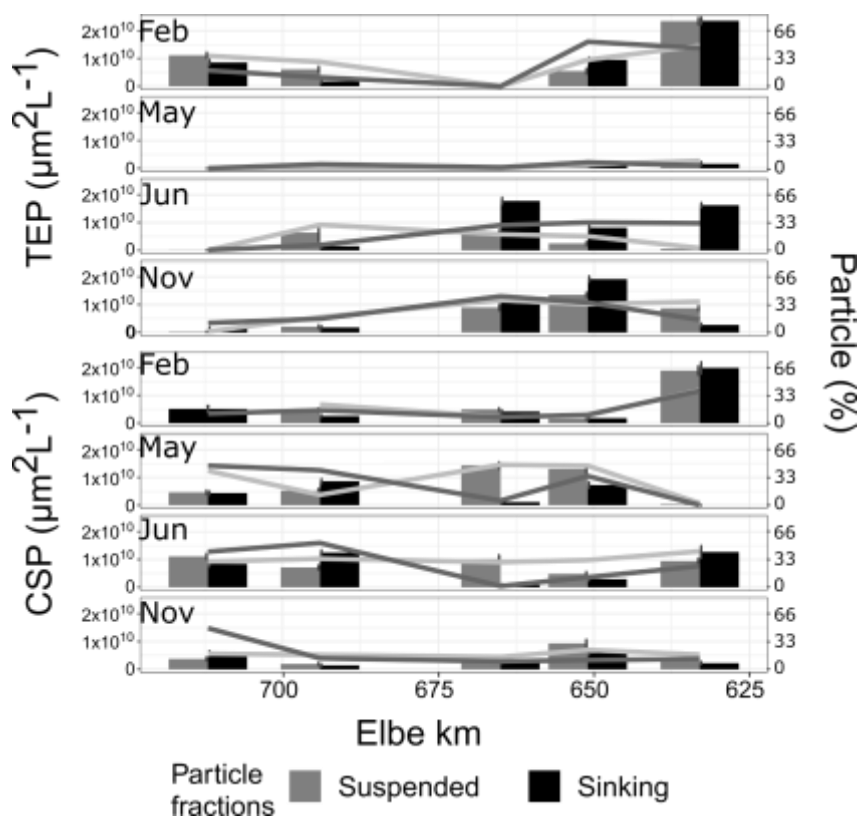


Figure 2.2. Exopolymer area and particle contribution in the Elbe estuary. Exopolymers TEP and CSP concentrations (left axis) are shown here as area per Litre (bars), and the percentage that the exopolymer area (right axis) contributed to the overall particle (unstained/TEP/CSP) area in the sample (lines). Error bars represent the standard deviation of duplicate samples. The average of parallel measurements is displayed for exopolymer concentrations.

Sinking organic particles displayed the highest standard deviation (7.32 mg C L^{-1} ; Figure 2.5), the next highest is dissolved suspended organic carbon at a standard deviation of 3.51 mg C L^{-1} . All other standard deviations are below 2.7 mg C L^{-1} . POC concentrations showed high standard deviations over the salinity gradient ($0.52\text{--}10.5 \text{ mg C L}^{-1}$). DOC did not show any consistent spatial pattern. During May and Jun-22 we did note DOC increases in May compared to Jun-22 and Nov-22. The Coble peak T (Tryptophan-like protein-like) signature was the only DOM characteristic that showed significant linear spatial differences ($p < 0.01$), decreasing seawards. A PCA assessment also failed to identify clear spatial trends (Figure 2.6). However, a quadratic assessment of DOM characteristics identified increases of non-conservative processes, such as primary production and degradation at the beginning and end of the estuary, with increases near the centre based on the slope ratio ($R^2 = 0.113$, adjusted $R^2 = 0.075$, $p < 0.02$). PARAFAC components only showed significant spatial differences when seasonality was considered (Figure 2.7). Specifically, we identified spikes of tryptophan-like C3 in the freshwater Elbe section in May and in the brackish region in Jun-22 (ANOVA, $p < 0.05$). The tyrosine-like C4 showed insignificant spikes in Nov-22 at each opposite end of the Elbe estuary, whereas it stayed consistently low otherwise.

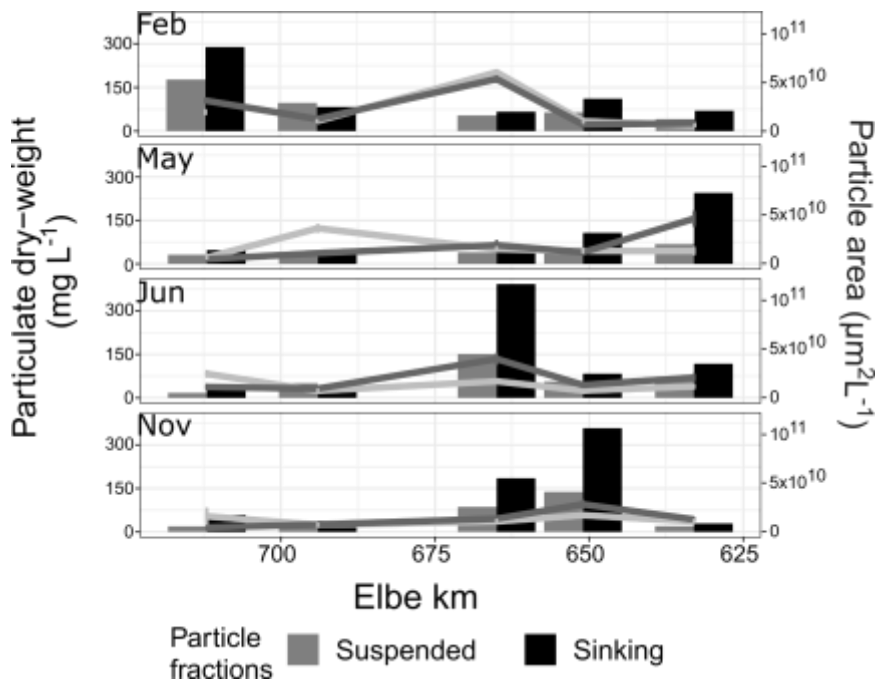


Figure 2.3. Dry-weight and particle area over the Elbe. Bars represent particulate dry-weight (mg L^{-1}), while the lines represent particle area ($\mu\text{m}^2 \text{L}^{-1}$). The average of parallel measurements is displayed.

2.4.2 Differences in bacterial particle colonisation along the Elbe estuary

Bacterial particle colonisation showed significant trends across the Elbe estuary's salinity gradient, with significantly higher bacterial colonisation of particles (ANOVA, $p < 0.01$, eta² = 0.04; Spearman, $p < 0.01$, rho = -0.21) and TEP (ANOVA, $p < 0.01$, eta² = 0.06; Spearman, $p < 0.01$, rho = -0.23) particles in the upper than lower estuary. Decreasing from 1.3×10^8 to 8.5×10^7 and 8.0×10^7 to 5.1×10^7 , for particles and TEP, respectively. Bacterial colonisation per particle showed similar trends, decreasing from 0.58 to 0.35 (ANOVA, $p < 0.01$, eta² = 0.04; Spearman, $p < 0.01$, rho = -0.22). However, bacterial particle colonisation percentages per TEP area were non-significant (Spearman, rho = -0.02) with percentages of 0.21 upstream and 0.30 downstream, although significant differences between stations were observed (ANOVA, $p < 0.01$, eta² = 0.02). CSP showed increased bacterial colonisation in the lower estuary for both total (ANOVA, $p < 0.01$, eta² = 0.02; Spearman, $p < 0.01$, rho = 0.16), and per particle colonisation (ANOVA, $p < 0.01$, eta² = 0.01; Spearman, $p < 0.01$, rho = 0.14), increasing from 9.8×10^6 and 0.0481 to 2.2×10^7 and 0.0846, respectively.

Spearman tests showed significant TEP (rho = 0.68, $p < 0.01$) and CSP (rho = -0.28, $p = 0.05$) correlations to bacterial colonisation of particles ($p < 0.05$; Figure 2.8), irrespective of sample site or time. However, no significant relationships ($\rho < 0.1$) between bacterial colonisation of TEP or CSP and particle concentration, each other, or between the visible particle concentration and unstained particle colonisation could be identified.

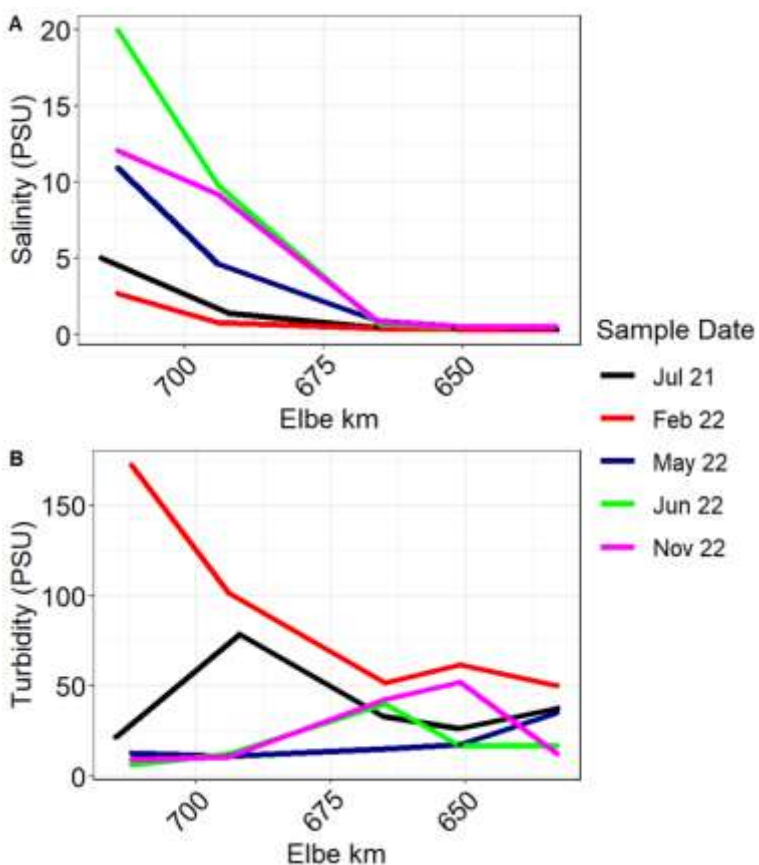


Figure 2.4. Elbe salinity and turbidity. Lines represent the measured salinity (A) and turbidity (B) of the Elbe estuary across the sample points. Colours represent the dates of sampling.

2.4.3 Strong seasonality effects on carbon dynamics

Seasonality led to strong trends in overall carbon dynamics, particulate dry weight and concentration (Figure 2.3). ANOVA tests showed a significant correlation between particle concentration and sample date ($R^2 = 0.21, p = 0.027$), strengthened via sample site interaction ($R^2 = 0.48, p < 0.01$). Meanwhile, sample date alone did not significantly correlate with dry weight ($p > 0.05$), but the interaction between sample site and date did ($R^2 = 0.08, p = 0.03$). Feb-22 represented the organic carbon maximum (10.9 mg C L⁻¹; Figure 2.5), with all other seasons displaying lower organic carbon. While seasonality affected organic particulate to dissolved carbon concentration ratios (ANOVA, $\eta^2 = 0.80, p < 0.01$), pairwise Wilcoxon tests showed no significant differences between samplings, suggesting that only a weak seasonal effect exists, and therefore only overall group effects could be identified.

Combined exopolymer concentrations showed Feb-22 had the highest exopolymer concentration throughout the study, with a mean of 8.94×10^9 (TEP) and 7.06×10^9 (CSP) $\mu\text{m L}^{-1}$. Seasonal trends differed between TEP and CSP, where TEP peaked in Feb-22 with a secondary peak in Nov-22 (Figure 2.2). CSP instead showed a primary peak in Jun-22 with a secondary peak in Feb-22, followed by a sharp decrease in Nov-22. When separating the

suspended and sinking fractions, we did see a significant difference (TEP and CSP Wilcoxon, $p < 0.01$), but fractionated and unfractionated trends remained similar. Exopolymer particle percentage (Figure 2.2) also showed strong seasonal TEP ($R^2 = 0.50$, $p < 0.01$) and CSP ($R^2 = 0.22$, $p = 0.02$) patterns. TEP and CSP particle percentage (TEP or CSP / Unstained particle concentration + TEP + CSP) showed different patterns. Both exopolymers showed similar percentage contribution patterns, with the exception of May, where TEP percentage was minimal, while CSP percentage remained high. Both exopolymer concentrations decreased from Feb-22 to May, then increased again in Jun-22, before falling in Nov-22 again.

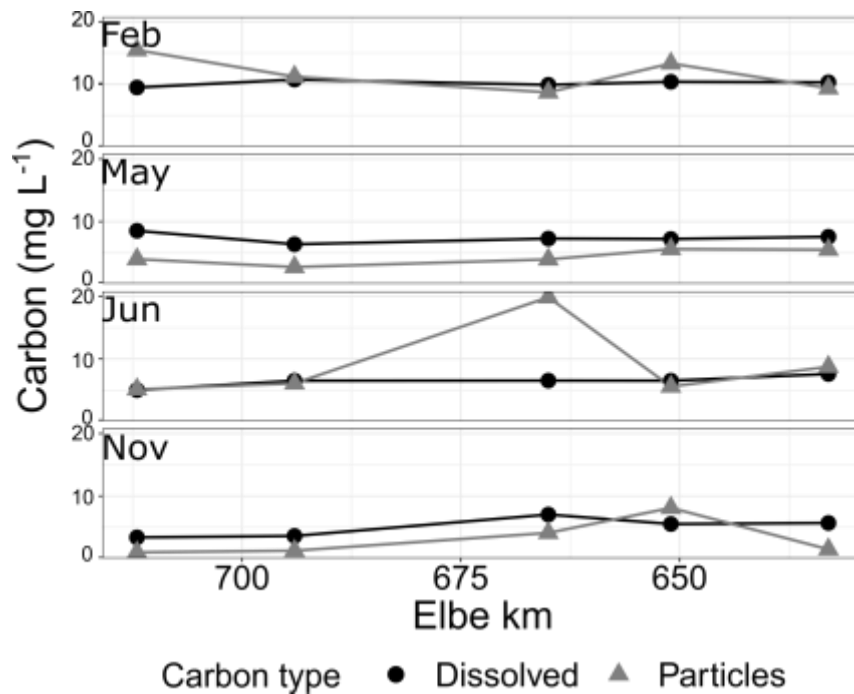


Figure 2.5. Particulate and dissolved organic carbon concentrations over the Elbe estuary. Shapes differentiate dissolved (triangles) and particulate (squares) carbon concentrations. The average of parallel measurements is displayed.

The visible particle concentration temporal pattern didn't follow that of the exopolymers. In fact, compared to the visible particles we saw a 55.7 % dissimilarity for TEP and 54 % dissimilarity for CSP in mean station particle abundance values, and a 47.5 % dissimilarity between TEP and CSP values. Unfractionated visible particle abundance peaked during Feb-22 and then steadily decreased until Nov-22. When fractions were separated we saw a small secondary peak in sinking particle abundance in Jun-22. Mean sinking particle abundance (averaged by season) remained higher than suspended particle abundance throughout the study.

A PCA of DOM peaks and indices showed no spatial, but significant seasonal patterns (Figure 2.6; ANOSIM, $R^2 = 0.55$, $p < 0.01$; adonis, $R^2 = 0.61$, $p < 0.01$). The humification index and aromaticity were the primary drivers of DOM shifts, where Nov-22 had the least humic and aromatic compounds, meanwhile Feb-22 had the most humic and aromatic compounds. Indicator values (e.g. the humification index, slope ratio, etc) showed significant (ANOVA, $p <$

0.02) seasonal trends, with the exception of the cobble T peak. Additionally, carbon to particulate matter (dry-weight) ratios agreed with aromaticity findings, with high ratios in Feb-22 and Jun-22, and lower values in May and Nov-22 (Figure. S2.4).

Our Parallel Factor (PARAFAC) analysis model identified a range of DOM compounds. Marine-like humic-like material (C1) was the most consistently abundant component (Figure 2.7), and greatest contributor to total fluorescence (42.7 %), followed by tryptophan-like material (C3) (27.5 %), terrestrial humic-like material (C2) (19.7 %), and the tyrosine-like material (C4) (10.1 %). Both marine humic-like and terrestrial humic-like material patterns were correlated throughout the study (Spearman, rho = 0.99, p < 0.01). C3 consisted of a tryptophan-like component with a high autochthonous origin and low humification signature (Yan et al., 2020) with a possible microbial origin (Coble, 1996). All components showed significant seasonal trends (ANOVA, p ≤ 0.01, eta2 = 0.21). Marine and terrestrial humic-like components displayed the same trend, with a difference of 20 % fluorescence contribution, both spiking in Feb-22 and then decreasing until Nov-22. Meanwhile, tryptophan-like C3 spikes followed a 3rd degree polynomial distribution, dipping in Feb-22 and spiking in Jun-22, while tyrosine-like C4 decreases from Jul-21 to Feb-22, and then increases until Nov-22, with a large spike from Jun-22 to Nov-22.

2.4.4 DOM interactions with particle characteristics

Significant correlations between PARAFAC identified fluorescent components and POC/DOC could be identified after Holm-Bonferroni family-wise error rate correction. Both marine and terrestrial humic-like components positively correlated with DOC (Spearman, p < 0.01), while tyrosine-like C4 negatively correlated with DOC (Spearman, p < 0.01), respectively. The marine humic-like C1 correlated with sinking POC (Spearman, p < 0.01). While the terrestrial humic-like C2 correlated with suspended POC (Spearman, p < 0.01). No PARAFAC component significantly correlated with any exopolymer fraction.

2.4.5 Few differences between suspended and sinking particles in highly mixed environments

We identified a significant (ANOVA, p = 0.03, eta2 = 0.078) difference in the dry-weight of the different particle fractions, although no significant particle area difference between suspended and sinking fractions were identified (ANOVA, p = 0.51, eta2 ≤ 0.01). This difference could represent the density differences we previously assumed took place to affect the particles sinking velocity. In fact, the sinking particle fraction has a mean dry-weight value of 103 mg L⁻¹, while suspended was only 53.7 mg L⁻¹. Therefore, with the insignificant concentration difference we can assume that sinking particles are approximately twice as dense as suspended particles.

While no significant differences could be identified, fractions were shown to favour different exopolymer types, TEP is 27 % more abundant on sinking vs. suspended particles, while CSP is 30 % more abundant on suspended vs. sinking particles. However, a Wilcoxon test showed no significant difference (p > 0.18) between the fractions for either exopolymer.

Bacterial colonisation of the suspended and sinking fractions showed significant differences between TEP (ANOVA, p < 0.01, eta2 = 0.004) and particles (ANOVA, p < 0.01, eta2 < 0.02). We identified significant bacterial colonisation differences between suspended and sinking particles for TEP (6.5×10^7 vs 7.6×10^7 microorganisms L⁻¹), although per particle

colonisation rates did not significantly differ, and unstained particles (8.9×10^7 vs. 1.4×10^8 bacteria L⁻¹; 0.36 vs 0.51 bacteria particle⁻¹). However, no significant bacteria per CSP or TEP differences could be identified between suspended and sinking particle fractions (ANOVA, eta² < 0.002).

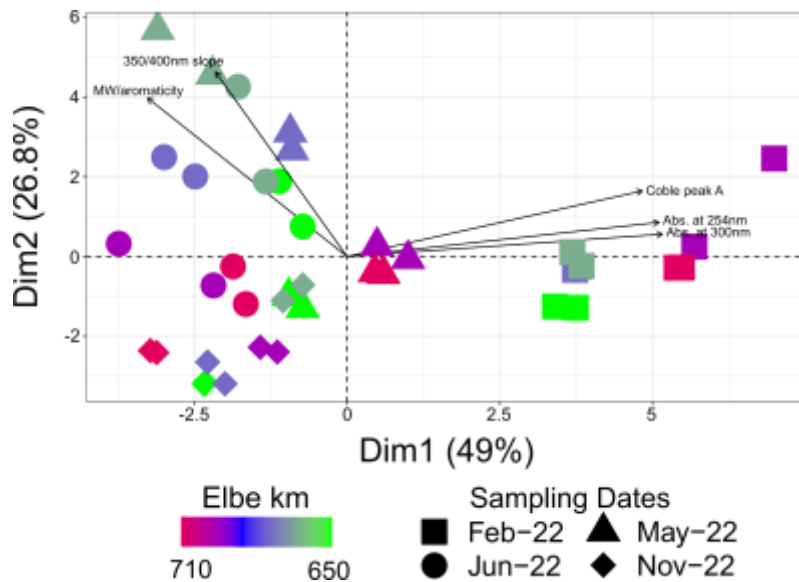


Figure 2.6. PCA biplot of DOM characteristics in the Elbe estuary. Shapes represent sample times, while the colour gradient represents sample location (in kilometre) along the Elbe estuary. The top 5 contributors are depicted to show their relation to sample distribution/dissimilarity. Coble peak A represents a humic-like signature, absorbance at 254 and 300 represent the aromatic DOM content and photooxidation, respectively, the 350/400 slope is indicative of molecular weight and aromaticity, just as MW/aromaticity does.

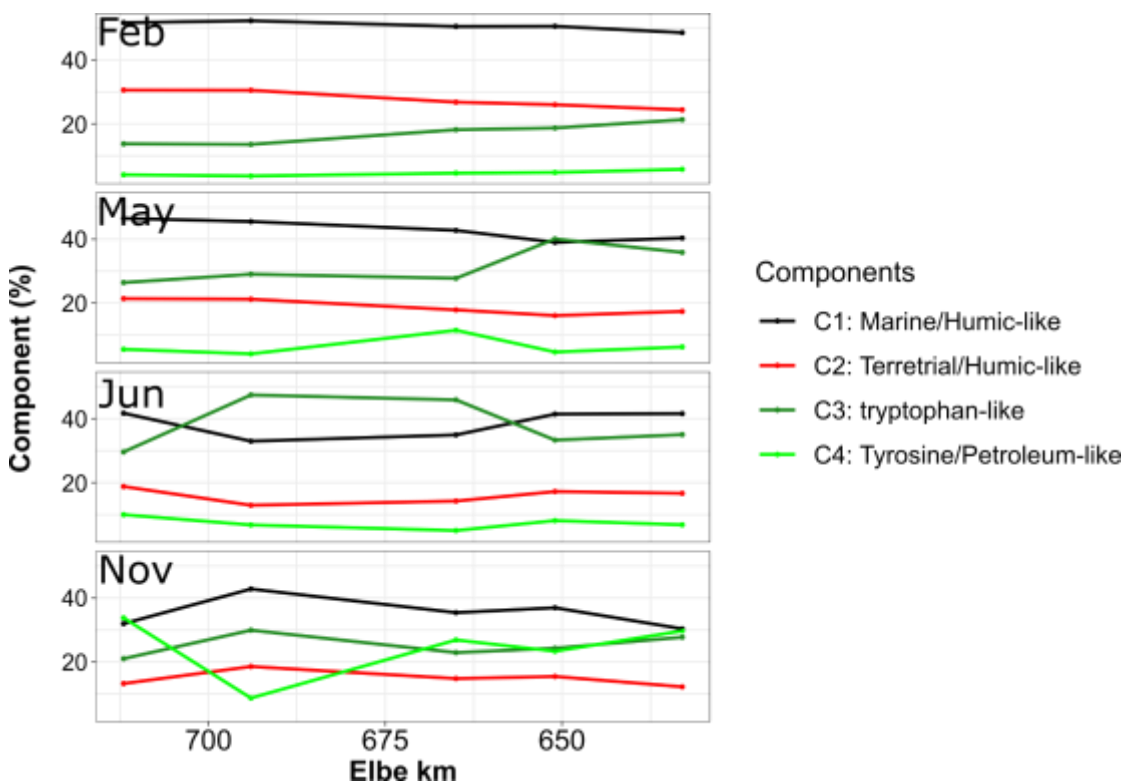


Figure 2.7. PARAFAC component contribution to total fluorescence is depicted over the Elbe estuary. Component percentage is based on component contribution to total fluorescence of the sample. Colours represent individual PARAFAC components; C1: marine humic-like, C2: terrestrial humic-like, C3: protein (tryptophan) like, and C4: protein (tyrosine) like and petroleum derived. The average of parallel measurements is displayed.

2.5 Discussion

2.5.1 Only weak interactions occur between carbon distribution and within the Elbe estuary's salinity gradient

Carbon distribution patterns are typically linked to an estuary's salinity gradient (García-Martín et al., 2021; Happ et al., 1977). Therefore, we expected decreasing POC, and increasing DOC in correspondence with increasing salinity. Our results did not follow this pattern, and only few POC/DOC characteristics shifted with the studied salinity gradient. Turbidity dependent light limitations in the brackish section reduce primary productivity, while stable salinities in the outer reaches (past Cuxhaven downstream, and past Hamburg Harbour upstream) allow for better and more stable phytoplankton growth and primary productivity. As such, the small salinity changes within the estuary would not correlate to large carbon changes, with only heterotrophic activity evident in the studied Elbe estuary section, between Mühlenberger Loch and Medemgrund. The focus on within estuary differences represents a study limitation, where exploring further upstream (past Hamburg Harbour) allows for clearer parameter associations, such as salinity linked carbon patterns.

Dissolved material makes up the majority of the carbon content within estuaries, and has been shown to shift in response to strong salinity gradients (Abril et al., 2002; Álvarez-Salgado & Miller, 1999; Y. Li et al., 2019; Madsen & Sand-Jensen, 1991; Mantoura & Woodward, 1983; Spencer et al., 2007). Salinity has also been linked to DOC shifts, with higher DOC concentrations in low salinity (<5 PSU) waters and lower DOC concentrations in intermediate salinity waters (5–12 PSU) (Abril et al., 2002; Álvarez-Salgado & Miller, 1999; Y. Li et al., 2019; Mantoura & Woodward, 1983; Spencer et al., 2007). DOC did not show significant salinity dependent spatial patterns in this study. There are many factors which could be contributing to this; primarily spatially distributed sources such as a continuous marsh exchange, and anthropogenic influences such as pollution via Hamburg Harbour and continuous dredging activities (Schöneich-Argent et al., 2020).

The lack of any clear spatial patterns in CSP is due to the continuously high and rapid production and degradation of these protein compounds (Busch et al., 2017). In contrast, TEP shows a seaward decrease that could be related to small salinity differences. Increased salinity enhances TEP aggregation properties (Decho, 1990), therefore the seawards TEP decrease and sinking particle abundance increase could be related, where TEP causes increased particle sedimentation, removing particulate carbon from the sampled Elbe surface waters. Additionally, TEP is made up of primarily surface-active acidic polysaccharides (Alldredge et al., 1993), resulting in significant stoichiometric differences between CSP and TEP. CSP has an estimated C:N ratio of 3.8:1 (Hedges et al., 2002), and TEP of 20:1 (Mari et al., 2001) and 26:1 (Engel & Passow, 2001). Bacterial colonisation of TEP and CSP indicate different microbial utilisation of the two exopolymeric compounds, with TEP concentrations increasing and CSP decreasing in response to bacterial colonisation. Previous studies have shown that exopolymers can undergo strong microbial modification and are not degraded completely (Stoderegger & Herndl, 1998). Additionally, carbohydrates are predominately respired, and not necessarily utilised for biomass production, meanwhile protein utilisation leads to bacterial growth. We propose that as TEP are modified during respiration (Passow, 2002), TEP may accumulate with increasing microbial colonisation, whereas CSP abundance decreases with its complete degradation fuelling microbial growth.

In conclusion, the lack of strong correlations between carbon distribution patterns and salinity gradient indicates that salinity represents a weak carbon driver in the studied estuary section. This indicates a departure from traditional findings in ‘anthropogenically less disturbed’ estuaries. However, studies with increased spatial and temporal resolution are required to definitely prove this.

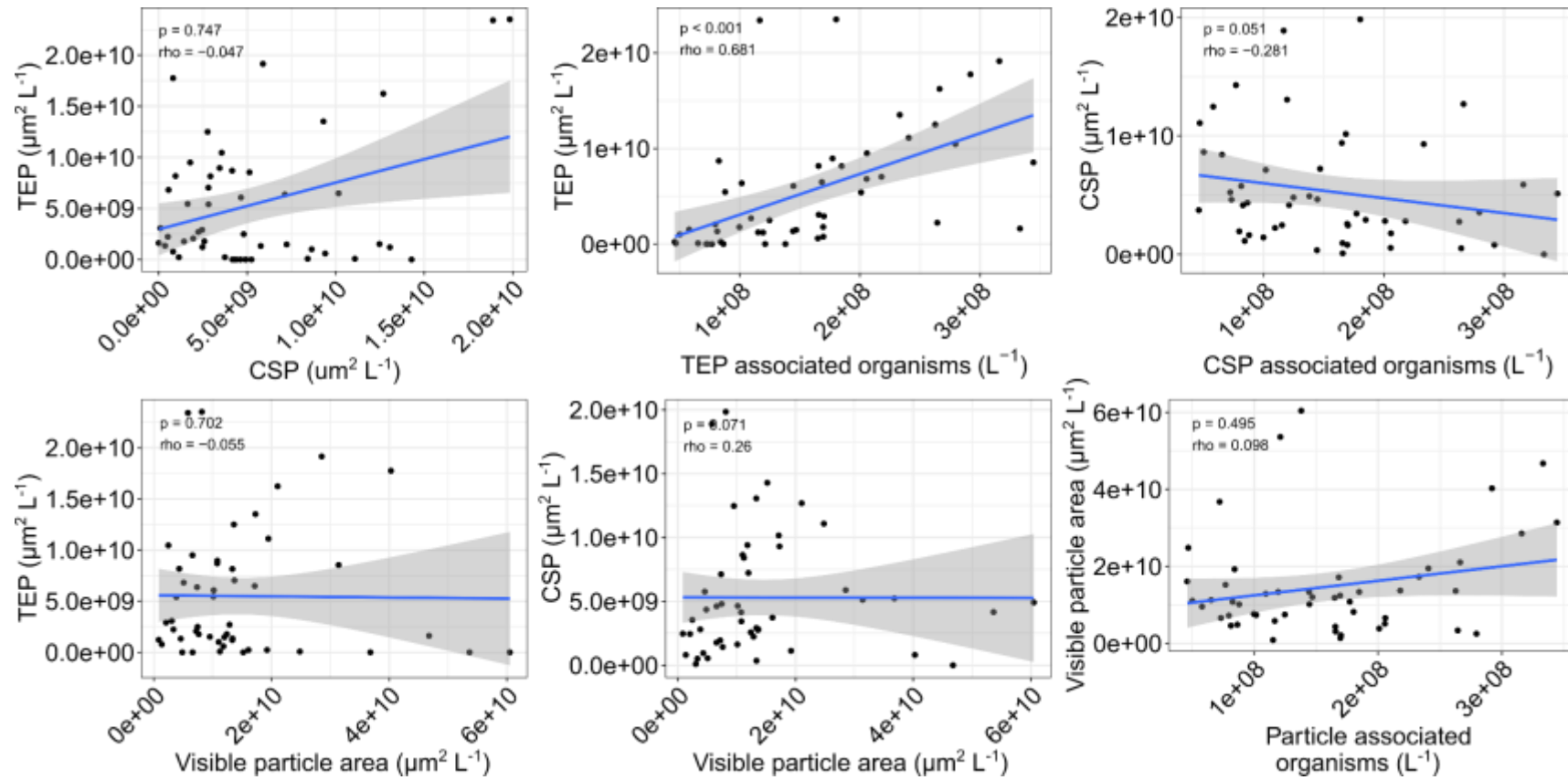


Figure 2.8. Direct correlation plots between particle characteristics. Correlations between TEP (A,B,D), CSP (A,C,E) and unstained (D,E,F) particle concentrations, and SYBR Green stained particle associated bacteria concentrations (B,C,F). Particle associated organisms are associated specifically with TEP/CSP/unstained areas. The shaded area corresponds to the 95% confidence interval, and displayed p and rho values represent a spearman correlation between the axes.

2.5.2 DOM aromaticity does not vary with salinity

Significant dissolved organic matter changes were expected across the Elbe estuarine salinity gradient. Specifically, upstream freshwater areas were hypothesised to contain more recalcitrant DOM compared to downstream marine areas, as previously shown (Asmala et al., 2016), with compounds continuously processed via heterotrophy during downstream transport. This would have been evident in an increased humification index, and decreased biological freshness indicators downstream. Instead, Coble peak T was the only spatially significant DOM indicator in respect to the estuarine salinity gradient. We attribute this to the extensive marine and terrestrial influence across the entire Elbe. Marine influence (via marine humic-like C1 signature) was initially hypothesised to be constricted to the more saline regions, instead marine DOM was the dominant component throughout the studied stretch of the estuary. Traditionally, the movement of marine material up estuaries is not considered a large influence, however, previous Elbe studies have established that the marine influence in the sediment is considerable (Kappenberg & Fanger, 2007; van Beusekom et al., 2021). This study expands on the sediment findings by identifying that marine-like material remains a relevant and major DOM source in the water column throughout the entire estuary, representing a mean 42.7 % of the fluorescing material. The terrestrial humic-like DOM compound C2 is ubiquitously present in the estuary with low variation, on account of continuous marsh-water column interactions and exchanges. Alternatively, no significant aromatic compound signature changes over the estuary could be due to dilution effects paired with local production, resulting in a net zero difference during downstream transport.

Linear components spectral signature decreases have been attributed to conservative mixing with oceanic waters, rather than due to non-conservative biotic or abiotic removal (Fellman et al., 2010; Painter et al., 2018). PARAFAC components did not linearly decrease in respect to distance from each other, in fact they did not show any significant overall pattern associated with the salinity gradient. Therefore, we conclude that our components saw non-conservative removal via abiotic and/or biotic processes, removing them from the identified PARAFAC signatures. Evidence for this exists in our Slope Ratio (an indicator of primary production and degradation), which revealed a significant quadratic relationship over the Elbe estuary. Cuxhaven and Hamburg Harbour represented minima, with increased values between them. This shows that intervening areas contain more biological activity, and that the salinity gradient does not necessarily influence DOM and microbial activity in the Elbe estuary.

2.5.3 DOM properties are affected by seasonality

The humification index and aromaticity were the primary drivers of seasonal DOM differences, with minima in Nov-22 and comparable maxima in Feb-22 and Jun-22. Previous studies have shown that spring and summer display low humification and aromaticity values on account of phytoplankton blooms and their addition of labile material to the system (Morán et al., 2013). Autumn was hypothesised to have high aromaticity and humic substance concentrations due to the gradual breakdown of phytoplankton and terrestrial (e.g. leaflitter) material. Instead we identified both high humification index and aromaticity in Jun-22 and Feb-22, and low values in Nov-22. We attribute high Jun-22 values to the presence of a previous bloom in May (Figure S2.5), indicated by the low aromaticity and humification index values. However, Jun-22 chlorophyll- α values also indicated the presence of a summer bloom, not reflected in DOC measurements. The increased DOM lability signature in Nov-22 is not related with leaf litter additions, or similar terrestrial influences, as indicated by the terrestrial humic-like C2

signature. Instead, an additional autochthonous factor caused increased DOM lability in Nov-22, such as a non-chlorophyll- α containing phytoplankton bloom. This is also reflected in a large spike in total dissolved phosphate that is not reflected in soluble reactive phosphate values (Figure S2.6). The tyrosine-like C4 spikes in Nov-22 are unrelated to increased DOM lability due to its similarity to (alkyl-substituted) benzene-derivatives, semi-biolabile nature and derivation from petroleum (Brünjes et al., 2022). Previous studies have found a negative correlation between organic carbon production and pollutants (Rewrie et al., 2023), which explains the tyrosine-like petroleum derived C4's negative correlation with DOC. Additionally, total DOC concentration decreases in Nov-22, while boat traffic and the associated petroleum pollution remains constant and high near harbours. However, based on data obtained from FGG-Elbe from 2006 to 2021 (FGG-Elbe, 2021), PAHs (Polycyclic aromatic hydrocarbons) do not experience a significant increase in winter months (Figure S2.7). Thereby, increased relative tyrosine-like C4 abundances are likely caused by an overall DOM abundance decrease, while C4 remains stable.

Humic substances show slow degradation due to high recalcitrance, therefore C1, as a marine humic-like signature, remains high. Meanwhile, protein-like components such as the tryptophan-like C3 are more labile, and therefore faster to degrade due to decreased concentrations of condensed aromatic moieties and lower C:N ratios. Consequently, high protein-like component abundances must reflect continuous input, and microbes preferentially obtain their carbon from these protein-rich compounds (H. P. Grossart & Ploug, 2001; Guillemette & del Giorgio, 2011; McKnight et al., 2001).

The tyrosine-like C4 represents a more processed protein-like material than the tryptophan-like C3, while remaining more labile than the humic-like material. Evidence for this is the timing of maxima, where the tryptophan-like C3 spiked in Jun-22 and decreased in Feb-22, while the tyrosine-like C4 spiked in Nov-22 when we expect high degradation activity. This corroborates relative abundance differences, as total sustainable biomass of higher trophic levels is lower than that of lower trophic levels, this phenomenon is known as the trophic biomass 'Pyramid'. In this case, the tryptophan-like C3 spikes represent periods and regions of high microbial activity, with increased degradable material. However, increased C3 abundance may also represent other component decreases, as fluorescence is scaled to maximum individual sample fluorescence. However, the opposite could also be true, that humic-like material abundance does not change, but instead the protein contribution varies so much seasonally that we see trends in the relative humic-like component abundances.

2.5.4 Seasonality drives particle differences, with no phytoplankton bloom link

Seasonality significantly affected total and dissolved organic carbon, where Feb-22 represented the total carbon maximum, followed by Jun-22, May, and finally Nov-22. This was unexpected, as while we hypothesised that seasonality would have a large effect, we expected spring and summer phytoplankton blooms to increase organic carbon in the system (Elovaara et al., 2020; Paczkowska et al., 2019). The high organic carbon concentrations in Feb-22 may be related to high exopolymer concentrations. It is possible that TEP present in Feb-22 represents a different chemical quality, specifically mineral vs. fresh organic matter. This has been identified in the Wadden Sea coastal areas (Fettweis et al., 2022), of which the Elbe is a tributary. The authors identified a cycle of mineral-associated TEP that is present in winter and autumn and fresh TEP in spring and summer. Therefore, it is likely that the high TEP concentrations in Feb-22 do not represent freshly generated TEP, but rather mineral-

associated TEP of bacterial origin. This may also be the reason why TEP seasonality in the Scheldt estuary was ambiguous (Horemans et al., 2021). Increased mineral-associated TEP skews total carbon concentrations not only in the Elbe estuary, but due to seaward transportation also in the Wadden Sea. During transport, TEP can be modified (as previously discussed) and microbially degraded leading to increased DOC concentrations, and high winter DOC values. Overall, we suggest that mineral-associated TEP plays a key role in the carbon cycle of the Elbe estuary, with a major influence on connecting water bodies, such as the Wadden Sea. Therefore, the expected phytoplankton bloom associated TEP increase thought to drive TEP dynamics and increases (Park et al., 2021) is rejected, instead it is more likely that mineral-associated TEP drove seasonal dynamics to a larger extent. Horemans et al., (2021) also found that modelled SPM seasonality did not require biotically induced seasonality. Suggesting that phytoplankton blooms do not necessarily play a major role in estuarine flocculation and erosion dynamics.

We conclude that while there are significant seasonal trends in particle characteristics, phytoplankton blooms did not lead to the expected organic carbon increase in spring and summer. Instead, a switch between freshly generated and mineral-associated TEP may be linked to seasonal total and dissolved carbon cycles. Therefore, placing more importance on bacterial modifications of available material than phytoplankton bloom generated compounds in seasonal carbon cycles in the Elbe.

2.5.5 Density determines suspended and sinking particle differences, with DOM compound links

We hypothesised that suspended and sinking particle concentrations, size differences and colonisation are especially pronounced in estuaries, and that different particle fractions are linked with different DOM characteristics. Specifically, we thought that suspended particles will be colonised by fewer particle associated organisms than sinking particles. To address these hypotheses, we analysed dry-weight, particle area, and particle colonisation abundance.

A consideration of our study is the shallow sample depth (~1 m), potentially omitting mature sinking material and only obtaining newly aggregated particles in our sinking particle fraction as well as missing incoming marine water along the estuary bottom. Phytoplankton bloom increased aggregation and sedimentation explaining the sudden dry-weight and particulate area decreases in May. Overall, the lack of area and exopolymer concentration differences between the fractions is presumably attributed to strong mixing forces, with some near-bottom stratification (Pein et al., 2021), rather than an effect of only sampling the estuary's surface water. Therefore, our 1 m samples remain representative of the mixed water layer.

We expected high TEP abundances on suspended particles due to their inherent buoyancy, while sinking particles contain less TEP. Instead, TEP on sinking particles was 27 % higher than on suspended particles, and CSP on suspended particles 30 % more abundant than on sinking particles (Wilcoxon $p > 0.18$). Although TEP has been shown to act as a sticking agent, and CSP is hypothesised to do the same, we could not identify a significant relationship between TEP or CSP and visible particle area. We attribute this to the high stress environment of the Elbe, where negative aggregation forces (e.g. shear stress) consistently overcome aggregation forces (TEP 'stickiness'), preventing the formation of large particles (Barton et al., 2014). Therefore, instead of exopolymers, buoyancy is dependent on density differences, identified with particle area and dry-weight mismatches. Density differences can be due to

increased degradation, or aggregation with resuspended sediments that act as ballast (Passow & De La Rocha, 2006). Stoichiometric and macromolecule differences between TEP and CSP favour TEP with lower degradation rates, which is why sinking particles contain a higher abundance of TEP. The sinking particles correlated with humic-like matter contain higher abundances of the less ‘attractive’ TEP, even though it has been shown that TEP acts as a buoyancy agent due to its lower than water density (Mari et al., 2017). As a result, TEP and CSP differences do not contribute to the particle fraction differences in the Elbe estuary. Instead, particle density is indicated as the driving factor between suspended and sinking particle fractions.

Humic-substances exhibit a stabilising effect on particles in the presence of salinity (Lasareva et al., 2023), with low salinities decreasing correlation strengths. Consequently, we suggest that the particulate organic matter is either a source of humic-like material or made up of similarly humic-like material. The marine-like component correlated with sinking POC, while the terrestrial-like component correlated with the suspended POC. This suggests an interaction, with sinking material more marine derived, potentially resuspended from deeper bottom water, while suspended material seems to be of a terrestrial origin. We are therefore tracking two separate humic-like matter pools, i.e. marine and terrestrial derived humic matter - potentially originating from particles with different sinking velocities and characteristics. Our study indicates that marine particles, if resuspended, are prone to re-sinking. Meanwhile terrestrial material is washed in from top-soil or the top marsh layer and remains suspended and continuously refreshed due to continuous marsh exchanges. This agrees with previous findings that Elbe sediments contain marine material, even significantly upstream, past Hamburg Harbour (Schoer, 1990). High marine content sediments explain the lack of fraction carbon content differences, as resuspended sediment is involved in estuarine aggregation dynamics (X. Wang & Andutta, 2013). This resuspended sediment would show a higher proportion of carbon compared to more labile material, substantially increasing sinking material carbon content. However, this is not freshly fixed material headed for long-term storage, but rather remains involved in the aquatic carbon cycle. Resuspended sediments have previously been shown to act as ballast material (M. Kim et al., 2020) so may help increase carbon sedimentation, especially under low current conditions.

Overall, we find that the Elbe estuary's particles are heterotrophic with their organic portion making up either marine-like or terrestrial-like signatures, and are highly subject to physical alteration and influences, such as current velocity affected by rainfall changes under climate change conditions.

2.5.6 Bacterial particle colonisation significantly differs in response to the estuarine gradient

We hypothesised that bacterial colonisation in the upper estuary would be significantly higher than in the lower Elbe estuary. Our results verify this, as we identified a significant seawards bacterial colonisation increase on unstained particles. Previous studies identified regional differences in bacterial colonisation between the upper and lower Elbe estuary (Zimmermann, 1997), however we identified a linear decrease in bacterial particle colonisation across the Elbe estuary indicative of decreased microbial particle degradation, and potential shifts in community composition and functions. While heterotrophic activity was not assessed, decreased bacterial abundance is indicative of either decreased bacterial growth rates or increased zooplankton predation (L. Silva et al., 2019).

Generally, freshwater particles were more colonised than brackish or marine particles. Reasons for colonisation differences include differences in nutrient availability, osmotic pressure due to changing salinities, and particle characteristics along the estuarine gradient. The best way to identify changes due to nutrient availability and osmotic pressure changes includes analysing the microbial community composition and their functional potential. The salinity gradient stresses freshwater organisms, reducing growth rates and potentially killing (micro-)organisms, thereby decreasing microbial colonisation rates (Painchaud et al., 1995). By identifying transporters known to increase survivability in saline waters (Jurdzinski et al., 2023) in the community's functional potential we could assess if the salinity gradient is responsible for decreased bacterial colonisation rates. Previously, a switch from a freshwater to estuarine, low to high phosphate, environment, supported the growth of primary producers and heterotrophs (Tee et al., 2021) that typically utilise low-affinity phosphate transporters. Selecting for specific (micro-)organisms and functional profiles, shifting community composition and its functional potential. Particle characteristics in association with colonisation have been discussed above.

In conclusion, we identified a significant linear trend of decreasing particle colonisation by microbes along the Elbe estuary. This is indicative of decreased microbial degradation, and shifts in microbial community composition and functions. Such a shift can be important as degradation rates affect greenhouse gas emissions which is especially relevant for estuaries. However, further microbiome studies are required to definitively identify the precise cause, as decreased bacterial colonisation may not necessarily affect particle degradation rates if individual cell activity would increase.

2.6 Conclusion

We identified evidence that TEP and CSP follow different patterns, and are not associated specifically with either suspended or sinking particles. Instead, Elbe estuary particles are heterotrophic with correlations between their organic content and either marine-like (sinking) or terrestrial-like (suspended) signatures.

While salinity was not a primary carbon driver in the studied Elbe estuary section, PARAFAC analyses identified brackish Elbe estuary areas as more biologically active, and that the salinity gradient does not necessarily influence the DOM, and microbial activity, in the Elbe estuary. This is important as decreased degradation rates reduce associated greenhouse gas emissions, and especially relevant for the disproportionate greenhouse gas emissions producing estuaries. However, further microbiome studies are required to definitively identify the cause, as decreased colonisation may not necessarily affect degradation rates if per cell activity is increased.

Overall, our findings concerning the ubiquitous marine and terrestrial carbon source contributions, aromaticity, humification index, and bioavailability are important policy indicators, affecting dissolved and particulate matter dynamics within the Elbe estuary, e.g. dredging activity effects on particles, links between water-column activity and marine particles and terrestrial run-off, and terrestrial run-off mitigation as terrestrial DOM remains largely suspended and would contributing to atmospheric exchanges.

Future studies should investigate the estuarine microbiome and functional differences in this highly variable environment. Additionally, while the metabolic potential may remain constant

between particle fractions due to high mixing and stochastic colonisation, gene transcription could differ significantly between particle fractions in response to particle characteristics, thereby affecting carbon fate, with implications for organic matter and carbon cycling, and climate feedbacks; affecting management and mitigation strategies.

Chapter 3: Suspended and sinking particle-associated microbiomes exhibit distinct lifestyles

This chapter's figure and section numbers have been modified to integrate the publication into the thesis and is currently under review as: Tobias-Hünefeldt, S.P., Woodhouse, J.N., Ruscheweyh, H.-J., Sunagawa, S., Russnak, V., Streit, W.R., Grossart, H.-P., 2024. Microbial organic carbon processing along the Elbe Estuary is driven by salinity and salinity sensitive organisms.

3.1 Abstract

Estuaries are important components of the global carbon cycle as they exchange large amounts of carbon between aquatic, atmospheric, and terrestrial environments, making them important loci for blue carbon storage and greenhouse gas emissions. Estuarine particles are especially important due to their role in microbial transformation and vertical/horizontal transport of organic matter. Particulate organic matter fate in estuaries is largely driven by structural changes in polymers, which modify buoyancy and determine the proportions of sinking or suspended organic matter. Less, however, is known about how microbial community structure and function differs between particle fractions. We used metagenomes and metatranscriptomes to assess changes in free-living and sinking/suspended particle-associated microbial community composition and functioning across the Elbe Estuary over 16 months.

The Elbe Estuary salinity gradient's impact was evident, with strong influences on microbiome composition and function, independent of temperature, oxygen, and dissolved/particulate nutrients. Free-living vs. particle-associated functional patterns significantly differed, with nitrogen fixation genes found on particles with no preferential transcription, resulting in higher net nitrogen fixation on particles, compared to the free-living fraction. To better differentiate particle-associated microbiomes, suspended and sinking particle fractions were separated. Although sinking particle-associated transcripts expressed coenzyme M biosynthesis, required for methanogenesis, suspended particle-associated transcripts favoured energy acquisition and growth. Our findings suggest that environmental changes such as dredging, projected sea-level rise, and decreased freshwater run-off, have a strong impact on dissolved greenhouse gas concentrations due to decreased methane oxidation, and higher suspended-sinking particle ratios, via reduced dredging, may reduce methane concentrations.

3.2 Introduction

Aquatic environments act as CO₂ storage and processing centres, as well as organic matter (OM) production, utilisation, and transportation hubs (Gao et al., 2022), linking terrestrial and oceanic ecosystems (Regnier et al., 2022), and drive terrestrial-atmosphere transfers (Liu et al., 2022). In particular, estuaries represent critical environmental carbon hotspots due to their disproportionate carbon cycling influence (Hutchings et al., 2020). Estuaries are characterised by distinct salinity gradients and dynamic environmental conditions including freshwater flow and marine intrusions which shape their biodiversity, heterotrophy rates, food-web efficiency, and nutrient/carbon transport (Chilton et al., 2021; Gillanders & Kingsford, 2002). Salinity gradients represent dynamic conditions based on tidal and a mixture of freshwater and marine influence (Wells, 1995) and may even create a barrier that freshwater organisms cannot overcome. As a consequence, phytoplankton bloom intensity, and thereby productivity, may

be spatially constrained, leading to localised oxygen depletion following bloom-collapse, with hypoxic areas increasing in prevalence and size over time (Sanders et al., 2023). Oxygen depletion creates a hostile environment, killing or isolating endemic species, and shifting ecosystem conditions, e.g. redox conditions affecting biogeochemical processes such as carbon and nitrogen cycling. For instance, during productive seasons (i.e. spring and summer), estuaries can act as carbon sinks. Yet, the high CO₂ production in freshwater areas leads to an overall net annual CO₂ production (Zimmermann-Timm, 2002). As a result, estuaries influence carbon transport and have large salinity-dependent carbon footprints (Khatiwala et al., 2013; Rackley, 2010), playing a key role in greenhouse gas emissions and climate change feedback (Ren et al., 2022). Moreover, biogeochemical dynamics and carbon exchanges, both atmospheric and seawards, are altered by intense human activities and climate change. This often leads to pollution and eutrophication further intensifying hostile conditions, e.g. lack of oxygen and presence of hydrogen sulphide. Consequently, estuaries represent dynamic and complex ecosystems where physical, chemical, and biological processes are highly interdependent, shaping biota and their related biochemical processes both in space and time.

Particles represent major carbon sources in estuarine ecosystems. Particles transport carbon between pelagic, benthic, and aquatic environments with sequestration in estuarine and marsh sediments, mobilised by massive resuspension under high discharge conditions. The Elbe Estuary (Germany) has a catchment of 140,268 km², making it the second largest German River to discharge into the North Sea (Boehlich & Strotmann, 2019) and thus an important system for the analysis of particles and dissolved organic matter (DOM) dynamics (Tobias-Hünefeldt et al., 2024). It also supports a wide range of species and habitats, while heavily anthropogenically impacted, e.g. shipping and industrial activities. Numerous attempts have been made to understand the source and fate of inorganic/organic carbon in the Elbe Estuary (Matoušů et al., 2018; Ploug et al., 2002; Tobias-Hünefeldt et al., 2024), although freshwater rather than brackish zones was the usual focus (Amann et al., 2012; Jürgens et al., 1997; Zimmermann-Timm, 2002). Previously, differences between suspended and sinking particles have been identified both in the Wadden Sea, and within the Elbe Estuary (Lunau et al., 2004; Tobias-Hünefeldt et al., 2024). Elbe particles differed in density and POC, linking to either marine-like (sinking) or terrestrial-like (suspended) humic-like dissolved organic matter (DOM). Additionally, Elbe particles were highly variable due to a range of influences, such as dredging, tidal marsh and harbour exchanges, and seasonal phytoplankton and zooplankton dynamics. Resulting in significant particle differences between upper and lower Elbe Estuary regions.

Bacterial OM transformation and degradation processes play a central role in particle degradation and DOM turnover. Microbial particle degradation is a major source of CO₂ (Cai, 2011; Simon et al., 2002) and an essential biogeochemical driver (Jiao et al., 2010; Longhurst & Glen Harrison, 1989), especially with the increased metabolic potential and activity compared to free-living organisms (Grossart et al., 2007; Nguyen et al., 2022; Wang et al., 2024). While estuarine effects (i.e. the associated nutrient/salinity gradient) on microbial particle degradation and therefore the carbon cycle have been explored (Lin et al., 2024), studies on estuaries have yet to integrate physicochemical profiles, microbial community compositions, functional potential, metatranscriptomes, DOM profiles, and particle characteristics. Although studies have identified shifts in the particle-associated community composition and colonisation in response to the estuarine gradient (Jürgens et al., 1997;

Tobias-Hünefeldt et al., 2024), the microbiome composition represents only one aspect of the numerous variable factors. Therefore, it is important to understand simultaneously which microorganisms and genes are present, their metabolic capabilities and ‘lifestyle’, and establish links between taxonomies and specific functions to gain a more comprehensive understanding on the carbon transfer through the system (Trevathan-Tackett et al., 2019; Urvoy et al., 2022; Zoccarato et al., 2022).

To achieve this goal, this study explores spatiotemporal gene patterns in the Elbe Estuary, comparing microbial community composition and functions between particles-associated and free-living microbiomes, while integrating particulate (POC) and dissolved organic carbon (DOC) dynamics. We hypothesise that osmoregulation gene limitations will spatially constrain taxa involved in CO₂ and CH₄ processing, driving shifts in microbiome composition and functionality, losing important roles previously linked to freshwater Elbe regions, e.g. nitrification (Sanders et al., 2018). Our data also enable a detailed analysis of free-living vs. particle-associated lifestyles in a highly turbid and turbulent estuary (Schröder & Siedler, 1989). We hypothesise that particle-associated microbiomes play a greater role in complex polymer degradation than free-living bacteria. Additionally, we expect suspended particles to be enriched for genes involved in labile organic matter degradation, while sinking particles are linked to recalcitrant compound (i.e. aromatic) degradation. We expand on previous findings by incorporating both particulate and dissolved variables, as well as microbial community composition, functional potential, and transcription profiles across the Elbe Estuary’s salinity gradient. Leading to conclusions such as elevated coenzyme M expression on sinking particles contribute to methane concentrations, and a reduction of sinking particles, such as via decreased dredging, may decrease methanogenesis.

3.3 Materials and Methods

3.3.1 Sampling

Samples were taken from the River Elbe Estuary in the main channel, Germany, in May-21, Jul-21, Feb-22, May-22, Jun-22, and Nov-22 at 5 stations (Mühlenberger Loch [53.54907, 9.82338], Twielenfleth [53.60921, 9.56536], Schwarztonnensand [53.71442, 9.46976], Brunsbüttel [53.88742, 9.19429], and Medemgrund [53.8363, 8.88777]; Figure 3.1). Samples were taken with a horizontal sampler (Lunau et al., 2004) at a depth of 1 m, due to very high turbidity in the Elbe Estuary that rapidly decreases primary production over depth. Suspended and sinking particles were allowed to vertically separate for 30 minutes (Figure 3.1), and downstream particle analyses were carried out on each separate fraction. Free-living microbes were captured on 0.22 µm Durapore filters, using the filtrate from the particle-associated microbes, captured on 5-µm Durapore filters. All samples were collected in duplicate, unless otherwise stated.

Particle characteristics were obtained by filtering samples onto pre-weighed and rinsed GF75 ADVANTEC filters, followed by another rinsing to remove salts, to determine their particulate matter dry weight and particulate total and organic carbon contents (PTC and POC). Before use, filters were pre-combusted for 5 hrs at 400 °C to remove any residual carbon.

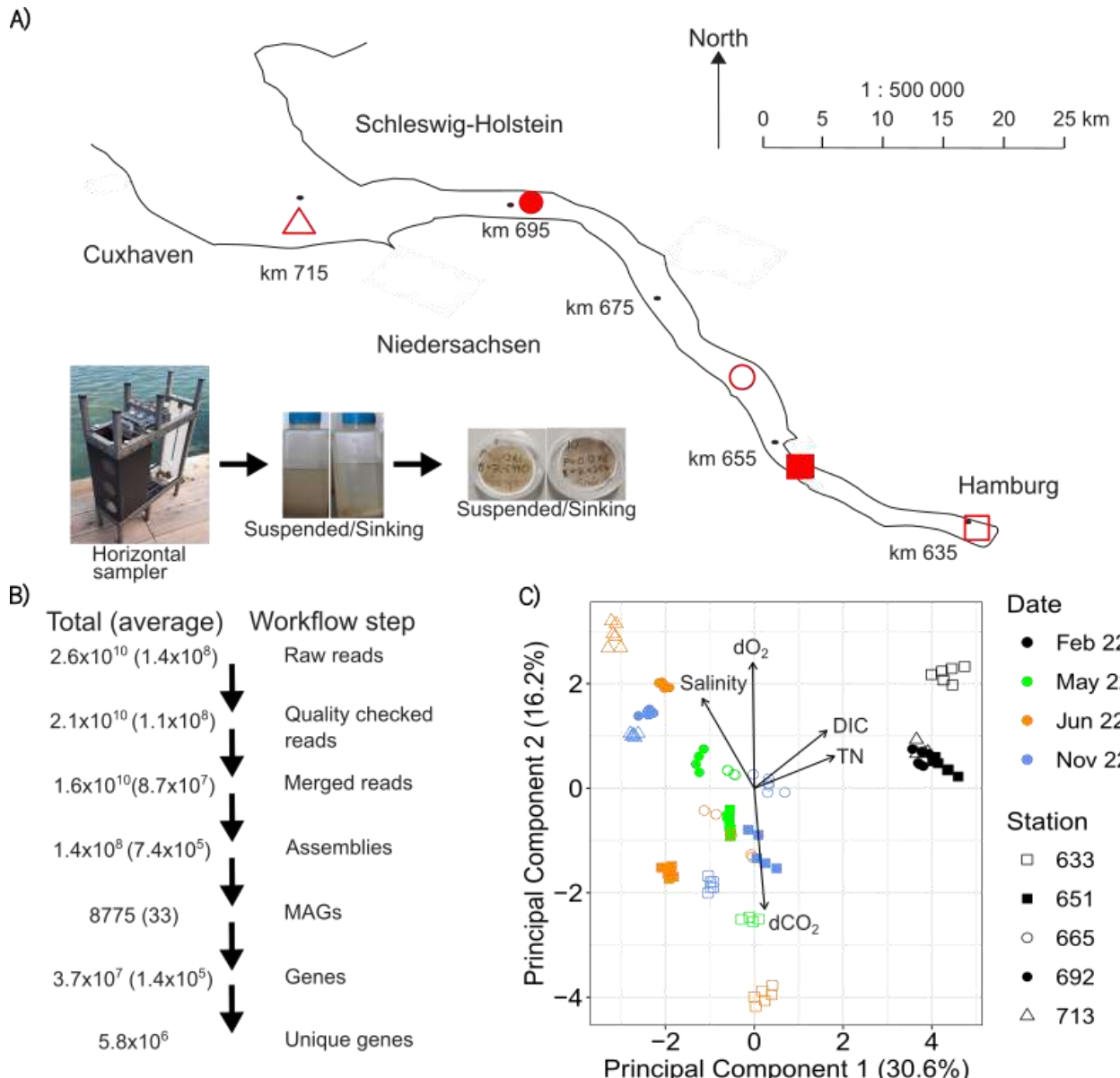


Figure 3.1. Elbe Estuary map. The map (A) depicts the outline of the Elbe Estuary, from Hamburg Harbour to Cuxhaven, with marks of the Elbe Estuary length (in kilometre) shown as black circles. Sample stations are depicted as red shapes, used throughout the manuscript, with pictures depicting the horizontal sampler, suspended/sinking particle separation and filtration results. The sequencing workflow (B) with the total and average number of raw, quality checked, and merged reads, assemblies, MAGs, and genes per sample. The PCA (C) depicts environmental changes across the study period during sample acquisition, only 2022 samples are shown due to their complete physicochemical profiles. The top 5 contributors to sample dissimilarity are shown. Adapted from Tobias-Hünefeldt et al. (2024).

3.3.2 DNA extraction and sequencing

DNA was extracted using the method described in Nercessian et al. (2005). In brief, cells were lysed with zirconia-silica beads (0.1-1 mm) suspended in cetyltrimethyl ammoniumbromide (CTAB). Sodium dodecyl sulfate and N-Lauroylsarcosine (anion surfactants), and proteinase K and phenol-chloroform-isoamyl alcohol were added. Chloroform-isoamyl alcohol and polyethylene glycol (PEG) was used for DNA purification, and precipitation at 4°C, ethanol

washing air-drying and finally dissolving in Tris (Tris-hydroxymethyl-aminomethane). Metagenomic sequencing was performed at Ramaciotti Centre for Genomics (Sydney, Australia) and the Competence Centre for Genomic Analysis Kiel (Kiel, Germany). Samples were prepared for sequencing with the Illumina DNA prep kit, and sequenced on a NovaSeq 6000 platform (Illumina, San Diego, CA, USA). Raw sequences are available on NCBI under BioProject accession number PRJEB54081 (BioSamples: SAMEA110290250 – SAMEA110290357 and SAMEA112714775 – SAMEA112714862).

Metagenomic and metatranscriptomic sequences were processed as outlined in (Paoli et al., 2022). Details are available in the Supplementary Methods. In brief, sequences were quality filtered with BBMap (v.38.79; <https://sourceforge.net/projects/bbmap/>), assembled with metaSPAdes (v.3.15.2, (Nurk et al., 2017), reads mapped to scaffolds with BWA (v.0.7.17-r1188; Li & Durbin, 2009), and depth quantified and individual samples binned with MetaBAT2 (v.2.12.1; Kang et al., 2019). Bin qualities were assessed with CheckM (v.1.1.3; Parks et al., 2015) and Anvi'o (v.7.1; Eren et al., 2015), keeping bins above $\geq 50\%$ completeness/completion (cpl) and a contamination/redundancy (ctn) of $\leq 10\%$. MAG taxonomy was assigned with GTDB-Tk (v.2.1.0; Chaumeil et al., 2020) against the GTDB R214 release (Parks et al., 2018). Gene sequences were predicted with Prodigal (v2.6.3; Hyatt et al., 2010).

Viral MAGs and genes were identified with VIBRANT (v1.3.1; Kieft et al., 2020) via the ViWrap pipeline (v1.3.0; Zhou et al., 2023), and quality checked with CheckV (v1.0.1; Nayfach et al., 2021). Genes were clustered at 95% with CD-HIT (v4.8.1, Fu et al., 2012) and aligned and classified against KEGG (Kyoto Encyclopedia of Genes and Genomes; v2019-03-20; Kanehisa, 2019; Kanehisa et al., 2023; Kanehisa & Goto, 2000), Pfam (v32; Mistry et al., 2021; Paysan-Lafosse et al., 2025), and VOG (release 94; Trgovec-Greif et al., 2024) databases using DIAMOND (v2.0.15; Buchfink et al., 2021). Gene-length normalised read abundances were converted to per-cell gene copy number using single-copy marker genes (Ruscheweyh et al., 2022). Meanwhile, rRNA sequences were extracted with Barrnap (v0.9; Seemann, 2013; <https://github.com/tseemann/barrnap>), and taxonomic profiling extended the mOTUs database (v3.1; Ruscheweyh et al., 2022) with prokaryotic MAGs. Additional MAG dereplication was performed with dRep (v3.0.0; Olm et al., 2017).

Total and median read and gene abundances, as well as MAG numbers are displayed in Figure 3.1. With an emphasis on processes involved in the processing of monomeric and polymeric organic carbon substrates, we established an extensive genome and gene catalogue to understand shifts in composition and function of free-living, suspended, and sinking particle-associated microbiomes.

The CO₂ and CH₄ gene database was manually curated based on the Kyoto Encyclopedia of Genes and Genomes database (Kanehisa, 2019; Kanehisa et al., 2023; Kanehisa & Goto, 2000), extracting all CO₂ (C00011) and CH₄ (C01438) associated genes. Osmoregulation genes were classified based on KEGG annotations or prior identification in Jurdzinski et al., (2023).

3.3.3 Physicochemical parameters

Salinity, oxygen, temperature and turbidity were measured with the onboard FerryBox (Petersen et al., 2011). Bulk water was utilised to measure dissolved CO₂ and CH₄

concentrations using the headspace technique. In brief, 100 mL of water was collected in a 500 mL syringe, 400 mL of pure N₂ gas was added and the syringe vigorously shaken for 1 minute. 350 mL of gas were transferred to 1 L Gas Bags and the CO₂ and CH₄ concentration measured within 12 hours using an Ultraportable Los Gatos (Los Gatos Research, USA), as described in Kang et al. (2024). POC, PTC, DOC, dissolved ammonium, dissolved nitrate, dissolved nitrite, soluble reactive phosphate (SRP), and total dissolved nitrogen, phosphate, and silicate were determined as outlined in Tobias-Hünefeldt et al. (2024).

3.3.4 Statistical analysis

All figures were created using ggplot2 (version 3.5.1; Wickham, 2016) and finalised with Inkscape (version 1.3.2) unless otherwise stated. The prcomp() function from the stats package (version 4.1.2) was used to generate the physicochemical PCA figure. Group differences were assessed with the ANOSIM and PERMANOVA tests with the vegan package (version 2.6-6.1), and ANOVA tests from the stats package; eta_squared() from the rstatix package (version 0.7.0) assessed the correlation strength of ANOVA tests. Differences between two group means were assessed with wilcoxon.test() from the stats package, pairwise Wilcoxon tests from the stats vegan package identified pairwise differences from groups. Spearman tests with cor.test() from the stats package assessed correlations between two trends. Network analyses were carried out with the WGCNA package (version 1.72-5) in R, genes that were excluded from the network are removed from subsequent statistical analyses. Gephi (version 0.10.1) was used to visualise the network. Mantel tests from the vegan package (version 2.6-6.1) were used to compare distance matrices (generated using dist()) between mOTUs, metagenomes, and transcripts per genome, and their network module eigenvalues. Metatranscriptome derived mOTUs could not be utilised, due to the low number of matches between metatranscriptomes and marker genes, therefore all mOTUs are derived from metagenomic data. All code is available at <https://github.com/SvenTobias-Hunefeldt/ElbeMicrobiome>.

3.4 Results and Discussion

Globally, estuaries are hotspots of organic matter cycling, remineralising >70% of terrestrial organic matter entering riverine ecosystems, primarily driven by microorganisms, particularly those colonising particles (Liu et al., 2020; Middelburg & Herman, 2007). Thus, it is critical to understand how microbial processes might be impacted by changes in the structure of organic matter, salinity and temperature. With this in mind, we performed regular sampling along five sites in the Elbe Estuary, one of the largest estuaries in Europe, between Hamburg and the North Sea, assessing how environmental change impacts both particulate and dissolved carbon (POC and DOC) cycling dynamics.

In total, 30 discrete water samples were collected from the Elbe Estuary, representing five sites and six time-points (Figure 3.1A). Discrete water samples were separated into free-living, suspended and sinking particle-associated fractions (Figure 3.1A; Lunau et al., 2004). Metagenomic and metatranscriptome sequencing (Figure 3.1B) allows us to relate changes in community composition, functional composition and transcription (Salazar et al., 2021) to differences in physicochemical parameters. Measured environmental variables (i.e. temperature, salinity, nutrients, DOC quantity and quality, POC quantity and quality, CO₂, etc.), exhibited a high degree of both spatial and temporal variation (Figure 3.1C; Tobias-Hünefeldt et al., 2024). Many of these parameters (i.e. salinity, dCO₂ and pH) exhibited strong

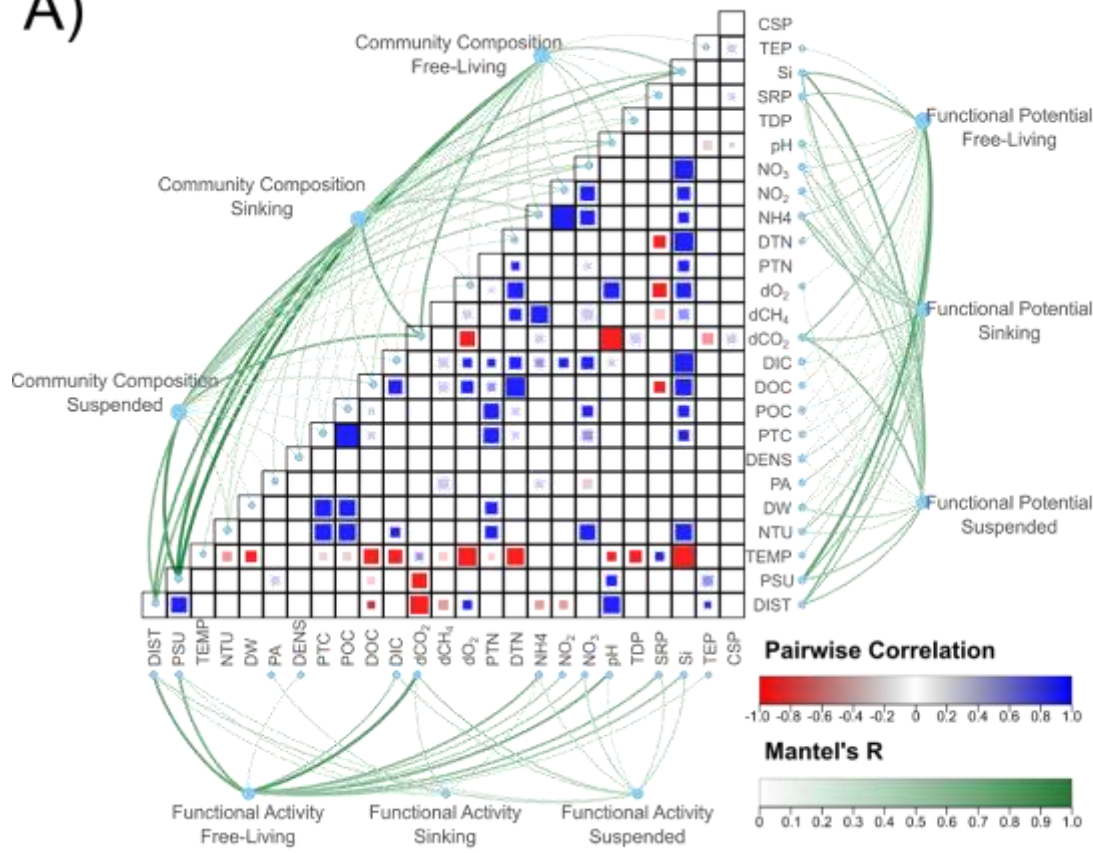
spatial patterns and were correlated with distance along the Elbe Estuary (km), whereas temperature, dissolved nutrients and turbidity tended to correlate with the sample date, indicating greater seasonal influence (Figure 3.2A).

We next sought to understand to what extent aspects of the microbial community, amongst the different fractions, were influenced by spatial and temporal environment variations. We identified significant differences between free-living and particle-associated microbiomes in terms of their community composition, functional potential, and transcription profiles (Figure 3.2B; ANOSIM, $R > 0.07$, $p < 0.01$; PERMANOVA, $R > 0.06$, $p < 0.01$). Pairwise PERMANOVA analyses reiterated differences between each particle fraction and the free-living microbiome ($p < 0.05$). We did not observe strong fractionation between sinking and suspended particle communities (Figure 3.2B, $p > 0.05$). We had hypothesised that structural differences between sinking and suspended particles alter the community composition and function of associated microbial populations. However, high turbulence in the Elbe Estuary keeps particles in suspension longer with irregular aggregation-disaggregation dynamics, minimising differences between suspended and sinking fractions (Tobias-Hünefeldt et al., 2024). For instance, turbulent kinetic energy in the turbidity maximum zone (TMZ) can be 240 times higher in the Elbe Estuary (Schröder & Siedler, 1989) than in the Wadden Sea (Stanev et al., 2007) due to tidal and flow rate influences. On the other hand, in both the Wadden Sea (Stanev et al., 2007) and Elbe Estuary (Tobias-Hünefeldt et al., 2024) sinking and suspended particulate fractions exhibited distinct biochemical properties. Our results suggest in agreement with others (Alcolombri et al., 2021; Huston & Deming, 2002) that these differences are not a function of differences in microbial composition or functional potential but rather in differences in colonisation rate and density.

3.4.1 Salinity and osmoregulation genes drive dissolved CO₂ and CH₄ processing gene profiles

Across the estuary, we observed consistent spatiotemporal impacts of physicochemical parameters on community composition, functional potential, and transcription, independent of fraction (Figure 3.2). A strong temporal differentiation was evident, with significant differences over time (ANOSIM, $R > 0.37$, $p < 0.01$; PERMANOVA, $R^2 > 0.31$, $p < 0.01$). Transcription profiles were significantly different over time (ANOSIM, $R = 0.13$, $p < 0.01$; PERMANOVA, $R^2 = 0.09$, $p < 0.01$), although spatial partitioning was more pronounced (ANOSIM, $R = 0.34$, $p < 0.01$;

A)



B)

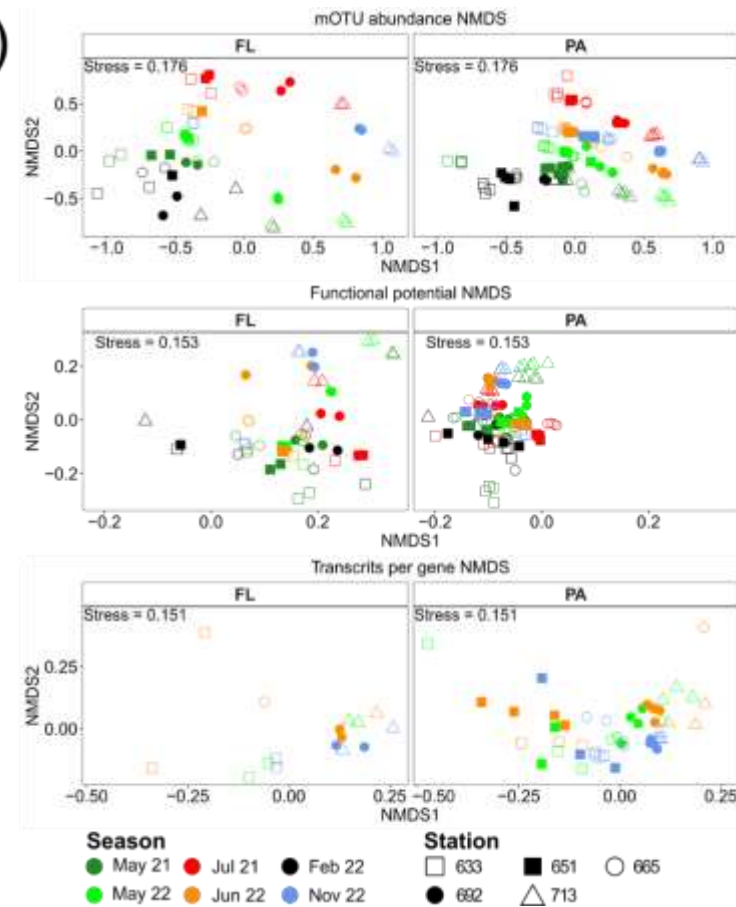


Figure 3.2. Microbiome aspects in the ecosystem. Pairwise correlations between the microbial community composition, functional potential, and transcription profiles (A) using Mantel tests. Colours represent the pairwise correlation, and alpha the Mantels R value. Non-significant interactions (corrected $p > 0.05$) are not shown. DIST = Elbe Estuary kms, PSU = Salinity (practical salinity units), TEMP = temperature ($^{\circ}$ Celsius), NTU = Turbidity (Nephelometric Turbidity Units), DW = Particulate Dry Weight (mg L^{-1}), PA = Particle Area ($\mu\text{m}^2 \text{L}^{-1}$), DENS = particle density, PTC = Particulate Total Carbon (mg L^{-1}), POC = Particulate Organic Carbon (mg L^{-1}), DOC = Dissolved Organic Carbon (mg L^{-1}), DIC = Dissolved Inorganic Carbon (mg L^{-1}), dCO₂ = Dissolved CO₂ concentration (μM), dCH₄ = Dissolved CH₄ concentration (μM), dO₂ = Dissolved Oxygen concentration (μM), PTN = Particulate Total Nitrogen (mg L^{-1}), DTN = Dissolved Total Nitrogen (mg L^{-1}), NH₄ = Dissolved Ammonium (mg L^{-1}).

NO_3 = Dissolved Nitrate (mg L^{-1}), NO_2 = Dissolved Nitrite (mg L^{-1}), TDP = Total Dissolved Phosphate (mg L^{-1}), SRP = Soluble Reactive Phosphate (mg L^{-1}), Si = Dissolved Silicate (mg L^{-1}), TEP = Transparent Exopolymer Particles ($\mu\text{m}^2 \text{L}^{-1}$), CSP = Coomassie Stainable Protein ($\mu\text{m}^2 \text{L}^{-1}$). **(B)** NMDs plots of microbiome mOTUs, functional potential, and transcripts per gene, with free-living (FL) and particle-associated (PA) samples separated. Colours represent sample dates, and shape sample stations along the Elbe Estuary. Outliers have been removed.

PERMANOVA, $R^2 = 0.41$, $p < 0.01$). KEGG Orthology term aggregation during the analysis may have reduced temporal variation due to functional redundancy over time (Ramond et al., 2025) and a strong selection of key processes along the estuary gradient (Levipan et al., 2024).

Salinity was the dominant physicochemical driver (Figure 3.2), with high community composition and functional potential, and weak transcription correlations. Its variation, driven by intrusion, tides and upstream flow rates, complicated spatial and temporal differentiation. Composition and function varied between mesohaline/polyhaline (downstream) and oligohaline/freshwater (upstream) sites, with Schwarztannensand oscillating between them.

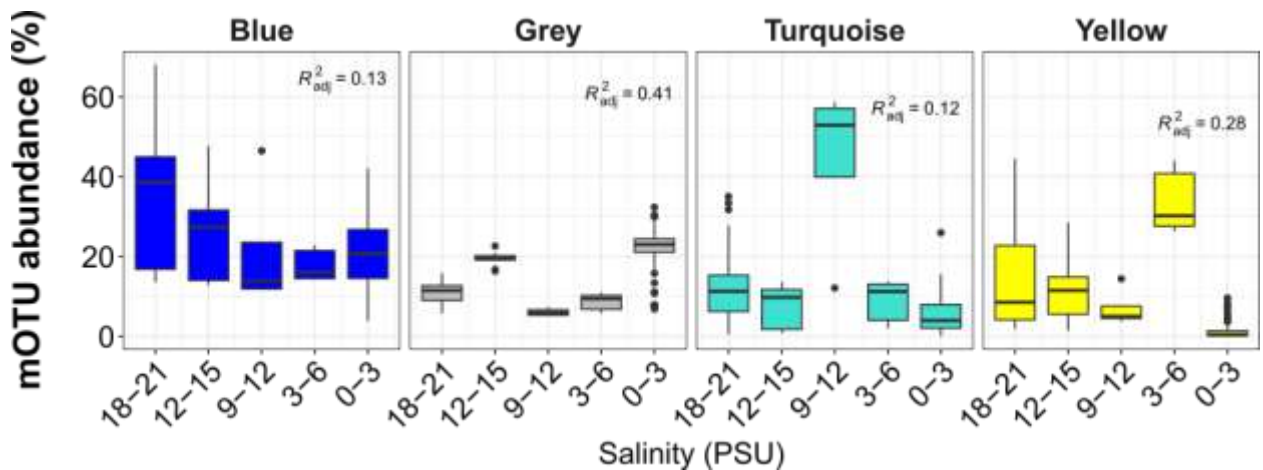


Figure 3.3. WGCNA mOTU module abundance in relation to salinity. Total module mOTU (**A, C**) and genes per genome (**B, D**) abundance is shown in relation to Elbe km (**A, B**) and sample dates (**C, D**). Additionally, Total mOTU module abundance is shown against salinity, binned every 3 PSU, with an adjusted R^2 value.

A network-based weighted gene co-expression network analysis (WGCNA) identified four salinity-correlated mOTU modules (Figure 3.3, S3.1, S3.2). Only the grey mOTU module, predominantly comprised of freshwater and non-salinity associated taxa such as bacteria affiliated with Limnohabitans (Kasalický et al., 2017), Pseudoholngiellaceae (Dong et al., 2023), and Burkholderiaceae (Coenye & Vandamme, 2003; Sawana et al., 2014), declined with salinity (Figure 3.3). In contrast, turquoise, blue, and yellow mOTU modules all included halophilic-halotolerant Rhodobacteraceae (Simon et al., 2017) and Flavobacteriaceae (Bernardet & Bowman, 2015; Bowman, 2006).

To confirm the freshwater vs salinity tolerant module distribution, we examined mOTUs for osmoregulation genes. In freshwater-associated and negatively correlated modules 4-16.8% of mOTUs contained osmoregulation genes, versus 23-32% of positively correlated modules. Showcasing that increased osmoregulation gene abundance is associated with salinity tolerance. The Elbe estuary freshwater section (<0.5 PSU) contained five distinct genera, based on WGCNA (Figure S3.1) and indicator analyses, previously identified in other freshwater environments: *CAIRTT01*, *Aquirufa* (Pitt et al., 2019), *Flavobacterium* (Kang et al., 2013), *Zoogloea* (Dugan et al., 1992; Shi et al., 2023), and *UBA953* (Moncadas et al., 2024).

Nitrogen cycling transcription showed similar salinity dependent localisation to freshwater areas, specifically transcription localisation of: UMPS (*de novo* pyrimidine biosynthesis; Suttle et al., 1988), narB (nitrate assimilation; Allen et al., 2001), and nifD (nitrogen fixation; Raymond et al., 2004). Preferential nitrate assimilation gene transcription can be attributed to high nitrate concentrations in limnetic Elbe zones (Ingeniero et al., 2024) as a result of remineralisation/nitrification activity near Hamburg Harbour, and upstream phytoplankton growth (Sanders et al., 2018).

Considering salinity's strong impact on microbiome composition, carbon processing, and nitrogen cycling we conclude that salinity shifts, such as a result of marine-intrusions as an effect of droughts, would broadly affect estuarine microbiome distribution, disrupting distinct freshwater microbes and associated activities. Including heterotrophy-autotrophy dynamics, nitrate assimilation, nitrogen accumulation, and *de novo* pyrimidine biosynthesis, resulting in decreased nitrate assimilation, and decreased heterotrophy.

The salinity-dCO₂ correlation suggests that salinity influences net production/consumption of dCO₂ in the Elbe estuary via localised heterotrophy-autotrophy balance. Van Beusekom et al., (2021) has shown increased upstream heterotrophy with the largest shift in the turbidity maximum zone (TMZ). This relationship was seasonally influenced, with stronger spatial patterns in summer, suggesting increased upstream heterotrophy. Bacterial carbon utilisation drives the spatial pattern, as salinity does not impact phytoplankton abundance or production (Figure S3.3H), but influences specific taxa occurrence (Martens, Biederbick, et al., 2024).

WGCNA also associated the green mOTU module with dCO₂ (Figure S3.1), consisting of diverse taxonomies, including phytoplankton (*Microcystis*: freshwater cyanobacteria, *Cyanobium*: low salinity; Budinoff, 2005), reiterating the salinity dependent heterotrophy-autotrophy balance that determines dCO₂ concentrations. Given dCO₂ freshwater accumulation, we considered whether dark CO₂ fixation pathways may be promoted. Indeed, freshwater sites experienced seasonally independent ATP-citrate lyases (rTCA) increases (Figure S3.3) that may be linked to *Nitrospirota* dependent denitrification, a dominant process in Hamburg Harbour (Figure S3.4; Grüterich et al., 2024; Sanders et al., 2023). The Harbour may also be a confounding factor in terms of our most upstream dCO₂ concentrations, as Hamburg Harbour, a known heterotrophic area (Goosen et al., 1999), may increase dCO₂ levels due to proximity. Future experiments pairing salinity tolerance with activity tests would provide direct mechanistic evidence of what we inferred based on sequenced-based molecular data.

Previous studies have pointed to salinisation of estuaries as having a positive side-effect of reducing methane emissions across the estuary (Liu et al., 2019; Poffenbarger et al., 2011; Soued et al., 2024). Here our findings agreed, and with negatively correlated salinity and dissolved CH₄ concentrations (spearman, rho = -0.15, p < 0.01; Figure 3.2A). Our findings suggest this is most likely due to an impact on methanogenesis as particulate methane monooxygenase (*pmoA*) genes per genome (spearman, rho = -0.49, p < 0.01) and transcripts per gene increased in freshwater areas (spearman, rho = -0.62, p < 0.01; Figure 3.4) and were positively correlated with methane concentrations, suggesting accumulation of methane drives the occurrence and activity of methanotrophs. Salinity has been shown to reduce the abundance of methanogen and methanotrophic taxa in aquatic (S. Chen et al., 2020) and terrestrial (Poffenbarger et al., 2011) estuarine ecosystems. This might partly explain the localisation of methanotrophic taxa such as *Methylococcaceae* (Chen et al., 2020; Taubert et

al., 2019), and *Methylomonadaceae* (Bussmann et al., 2021) to oligohaline conditions (0.5-5 PSU; Figure S3.5). A single dCH₄-correlated mOTU module (brown) was identified, primarily consisting of *Bacteroidia*, along with *Planctomycetota* and *Verrucomicrobiota*. Many remain undescribed, but taxa like *Saprospiraceae* (McIlroy & Nielsen, 2014), *Emticicia* (Mayrberger, Jenifer M., 2011; Whitman, 2015), and *Novosphingobium* (Sohn et al., 2004) suggest complex carbon degradation capabilities. However, no methanotroph or methanogen was associated with the brown module, indicating that dCH₄ originates from the sediment (Chen et al., 2020b), distributed via diffusive fluxes, microbubbles, fluvial inflows and tidal induced advective mixing (Borges et al., 2018; Wang, et al., 2021; Zhan, et al., 2021; Steinsdóttir et al., 2022; Wells et al., 2020). From this we can ascertain that decreased methane emissions due to increased salt-water intrusions and decreased freshwater flows are most likely a function of inhibition of sediment derived methane production. However, further research is needed to assess methanogen patterns that influence net production, utilisation, and atmospheric exchange. Especially as CH₄ sources include terrestrial exchange, sediments, side-channels, and anoxic harbour waters (Borges et al., 2018; Steinsdóttir et al., 2022; Wells et al., 2020).

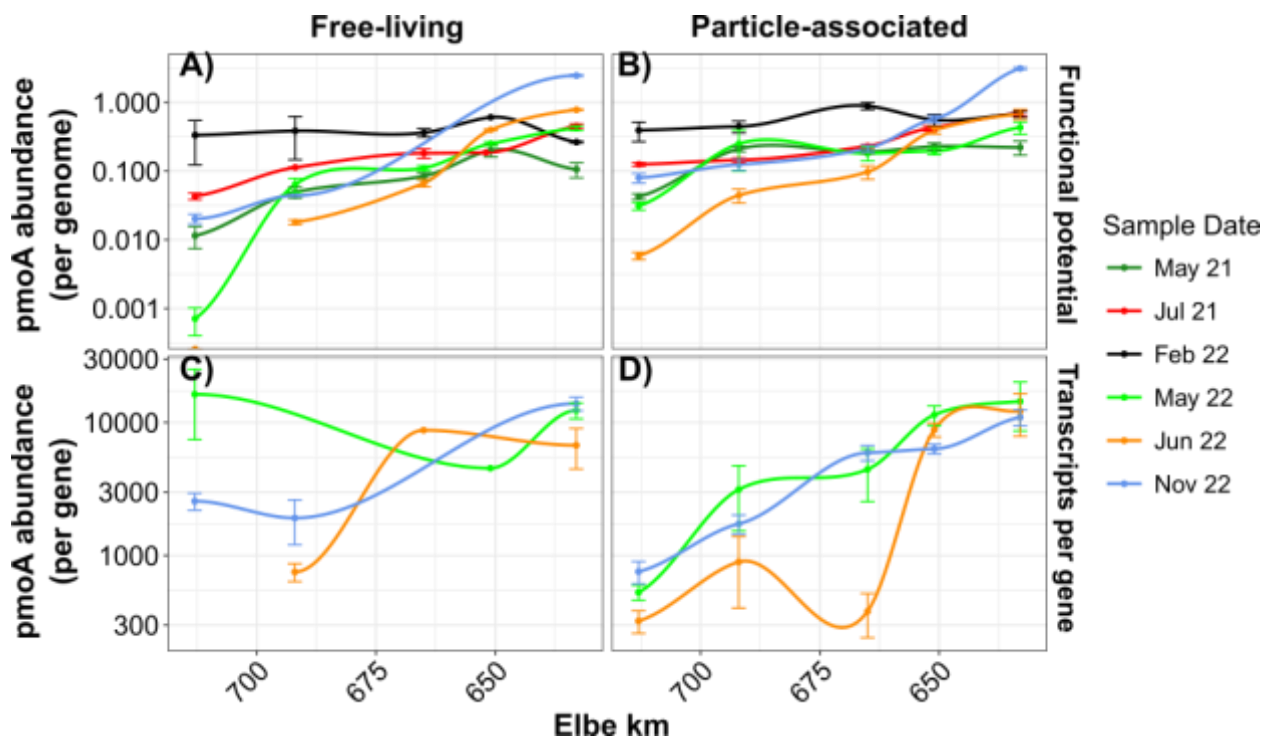


Figure 3.4. Particulate methane monooxygenase subunit A (*pmoA*) abundance in the Elbe Estuary for functional potential per genome and transcription per gene. The mean of two samples *pmoA* (**A, B**) functional potential and (**C, D**) transcripts per gene are shown across the Elbe Estuary. *pmoA* abundance has been taxonomically corrected against *amoA*. Colours depict sample dates and standard errors are shown as error bars and free-living (**A, C**) and particle-associated (**B, D**) abundances have been divided.

3.4.2 Exopolymer TEP correlated taxa are salinity specific, unlike CSP

We speculated that transparent exopolymer particles (TEP) and Coomassie stainable particles (CSP) significantly impact microbial activity and function due to two main reasons. First, both polymers are produced and modified by phytoplankton and prokaryotes (Allredge et al., 1993; Decho, 1990; Simon et al., 2002). Second, TEP abundance has previously been shown to decrease with salinity in the Elbe Estuary (Tobias-Hünefeldt et al. 2024).

Whilst both exopolymers are abundant in the estuary, only TEP showed significant microbiome associations with the microbiome composition (Mantel, $R = 0.11$, $p < 0.01$), functional potential (Mantel, $R = 0.16$, $p < 0.01$) and transcription (Mantel, $R = 0.19$, $p = 0.02$; Figure 3.2). The lack of CSP associations suggests that either CSPs protein fraction does not influence microbes uniformly or its turnover is rapid and continuous, as previously suggested (Tobias-Hünefeldt et al. 2024). TEP, meanwhile, was correlated with the free-living fraction specifically (Figure 3.2). We suggest this is due to the free-living fraction producing EPS, including TEP, while particle-associated microbes participate in production-utilisation cycles, masking TEP correlations unless taxa are individually assessed (Jayathilake et al., 2017). Especially as prokaryotes can modify TEP without affecting its abundance (Stoderegger & Herndl, 1998).

As predicted, the 148 TEP-correlated particle-associated bacterial genera ($<0.8\%$ median abundance) peaked freshwater or brackish regions, but remaining undetectable above 20 PSU (Figure S3.6); underscoring the salinity-dependent nature of TEP and its associated taxa in Elbe Estuary. Genomic comparisons revealed GH65 and GT51 carbohydrate active enzyme families (glycoside hydrolases and glycosyltransferases) were significantly enriched in TEP-correlated genomes. These gene families, essential for glycosidic bond synthesis and degradation (R. N. Silva et al., 2014), play key roles in EPS, and presumably TEP, turnover by catalysing the hydrolysis, reversible phosphorylation, and/or synthesis of various α -glucosides (typically α -glucobioses or their derivatives; De Beul et al., 2024; Mohapatra, 2024; Yuan et al., 2007), obscuring TEP-particle correlations as predicted.

3.4.3 Particle-associated activity is split into growth vs. methanogenesis focuses

We identified significant spatial and temporal drivers of microbiome composition and functions. However, a broad approach masks local drivers, such as free-living vs. particle-associated microbiomes, or distinct particle fractions. Our study design addresses these finer scale questions, such as free-living vs. particle associated microbiomes, offering insights into estuarine carbon processing essential to predict system responses to ongoing anthropogenic and climate changes. It has been well established that free-living and particle-associated microbiomes differ significantly in taxonomy and functions (Middelboe et al., 1995; Rösel & Grossart, 2012; Urvoy et al., 2022). While most studies focus on specific conditions, such as phytoplankton blooms, single seasons, or particular processes, we aimed to identify consistent carbon processing differences across a highly turbid and mixed estuary across multiple seasons. This approach provides a broader understanding of free-living vs. particle-associated, and suspended vs. sinking particle microbiomes.

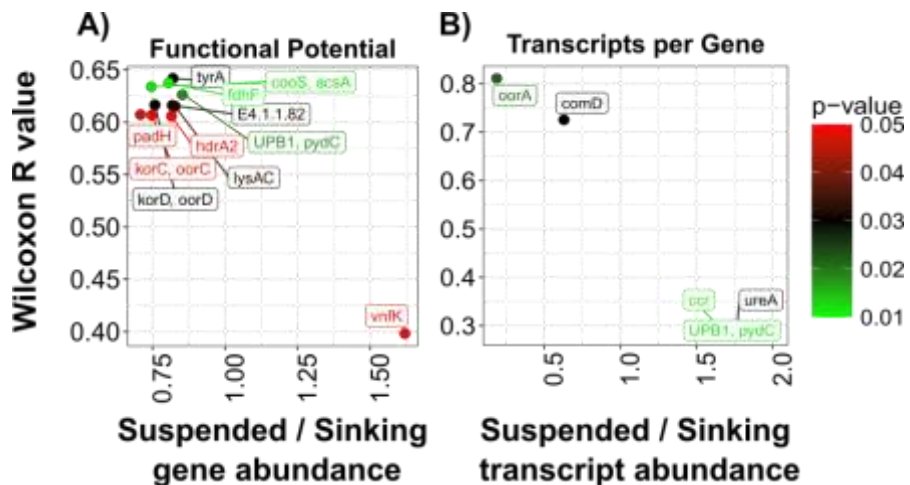


Figure 3.5. Lifestyle differences between suspended vs. sinking particle-associated functional potential and transcripts per gene. Significantly different functional potential genes (**A**) and transcripts per gene (**B**) are depicted, based on Wilcoxon tests. Colour denotes the Mantel p-value, with the y-axis representing the Wilcoxon R value, and x-axis the ratio between suspended to sinking abundance.

WGCNA revealed one mOTU module (turquoise) negatively associated with the free-living fraction, while no functional potential modules were associated with the free-living fraction or displayed equal trends for particle fractions. Indicator species analysis identified 49 free-living mOTUs and 257 particle-associated mOTUs (Table S3.1), but none appeared in the turquoise mOTU module. Free-living indicator taxa included *Planktophila* (freshwater bacterioplankton; (Jezbera et al., 2009; S. Kim et al., 2019), *Pelagibacter* (marine plankton; (Fernández-Gómez et al., 2013), and *Rickettsiales* (obligate intracellular-symbionts; Cruz-Flores & Cáceres-Martínez, 2020). Particle-associated mOTUs spanned a wide taxonomic range – from *Verrucomicrobia* to *Pseudomonadota* – prompting us to focus on functional indicators. Although no carbon processing or nitrogen cycling genes were indicative of free-living functional potential, 31 genes indicated a particle-associated lifestyle (Table S3.1). Key indicators included nitrogen fixation (*nifHDK*; Fani et al., 2000), anaerobic growth on plant organic acid facilitator *oorAB* (Pierce et al., 2010), CO₂ production and methanogenesis genes *fdhAB* and *fmdCE* (Costa et al., 2013; Lupa et al., 2008; Vorholt et al., 1996), and antibiotic degradation and biosynthesis genes (e.g. *bacA*, *antA*, and *cadA*). Although *nifHDK* was not a transcription indicator, particle microenvironments may mitigate oxygen inhibition of nitrogenases (Goldberg et al., 1987; Riemann et al., 2022), enhancing net nitrogen fixation – although free-living organisms would also contribute during seasonal oxygen minima (Figure S3.7). This has important implications for eutrophication, as hypoxia promotes nitrogen retention, exacerbating estuarine eutrophication over time (Crump & Bowen, 2024). Moreover, *oorAB* presence suggests that plant-associated taxa from terrestrial sources are common on particles (Tobias-Hünefeldt et al., 2024). In contrast, indicator transcript analyses showed that antibiotic genes (*andAd*; Chang et al., 2003; Gai et al., 2010), and enzyme 4.1.1.64 (Bailey & Dempsey, 1967; Kamenik et al., 2015), and components of the reductive TCA cycle (*fhdF*) were elevated in the free-living fraction (Table S3.1).

Given the abundance of particle-associated indicator genes, we investigated functional distributions between suspended and sinking particles. Indicator analyses did not identify preferentially associations; however, abundance based Wilcoxon tests (Figure 3.5A) showed significant increases of *vnfK* (nitrogen fixation; Eady et al., 1988) on suspended particles, whereas sinking particles exhibited increased growth related genes such as *korC* (TCA involvement; Tersteegen et al., 1997), *tyrA* (amino acid biosynthesis; Bonner et al., 2004), and *pydC* (pyrimidine degradation; Kao & Hsu, 2003). Notably, *hdrA2* – a key methanogenesis intermediate (Mander et al., 2004) – was enriched on sinking particles, predisposing them to methanogenesis.

We followed up on functional potential by assessing transcription differences. Indicator analysis only marked *tyrA* (amino acid biosynthesis; Bonner et al., 2004) as suspended particle associated. In contrast, Wilcoxon tests (Figure 3.5B) associated sinking particles with *oorA* (energy involvement) and *comD* (coenzyme M biosynthesis, a key methanogenesis cofactor gene; Graupner et al., 2000), and suspended particles with *ccr* (antibiotic synthesis; Erb et al., 2007), *ureA* (arginine biosynthesis and xenobiotic degradation; Cruz-Ramos et al., 1997), and *pydC* (pyrimidine degradation). We conclude that growth related gene transcription is elevated on suspended particles, and sinking particles show increased transcription of methanogenesis-associated genes.

Overall, our findings show that although taxonomic differences between particle fractions are minimal, functional profiles diverge. Suspended particles transcribe growth related pathways, whereas sinking particle microbiomes are predominantly involved in methanogenesis.

3.5 Conclusion

The Elbe Estuary's microbiome is shaped by its physicochemical profile, with salinity crucial to understanding carbon processing profiles. Salinity drives significant spatiotemporal microbiome composition and functional shifts; where increased marine intrusion disrupts freshwater nitrate assimilation, growth processes (e.g. de novo pyrimidine biosynthesis), and methane accumulation. Further research, including microbial sediment analysis, is required. Salinity also influences TEP and its associated taxa, which become undetectable above 20 PSU, indicating diminished downstream aggregation leading to reduced carbon sedimentation.

Salinity independent analysis included the assessment of free-living vs. particle-associated where particle-associated microbiomes may fix more nitrogen due to increased *nifHDK* genes with equal transcripts per gene, and contain more bacteria from a terrestrial origin. Transcription patterns revealed distinct lifestyles between particle fractions: sinking particle transcripts are linked to methanogenesis, whereas suspended particle-associated microbiomes preferentially transcribe growth-associated genes. Our findings suggest that increased methane concentrations may be related to an abundance of sinking particles through elevated coenzyme M gene expression. This is especially relevant in the highly turbid Elbe Estuary, where urban activities (e.g. dredging) may greatly affect greenhouse gas emissions. Future studies should examine the underlying mechanism and controlling variables in greater detail, especially in the context of climate predictions. Our findings highlight potential climate impacts, including methanogen dependent methane emission decreases, and consequent carbon processing impairments.

Chapter 4: General Discussion

My thesis aims to characterise microbial carbon cycling and processing in the Elbe Estuary. Specifically, exploring particulate-dissolved carbon dynamics, the impact of exopolymers, and how microbiomes interact and are affected by both. Firstly, I address the lack of research on dissolved and particulate carbon interactions over spatiotemporally dynamic conditions with the use of a wide range of techniques, from spectrophotometry to microscopy. Secondly, I connect carbon dynamics to carbon processing mechanisms via microbiome community composition and functionality, with the inclusion of metagenomic and metatranscriptomic analyses.

Below I address the research questions raised in section 1.8, by integrating each chapter's key findings via their discussion, followed by establishing connections between them leading to a comprehensive overarching result. Finally, limitations and implications of this thesis are discussed, together with the identification of knowledge gaps for future research, and the presentation of the overall thesis conclusion. Figure 4.1 graphically summarizes the major findings and conclusion of this study and thus provides an overview of the Thesis' key findings.

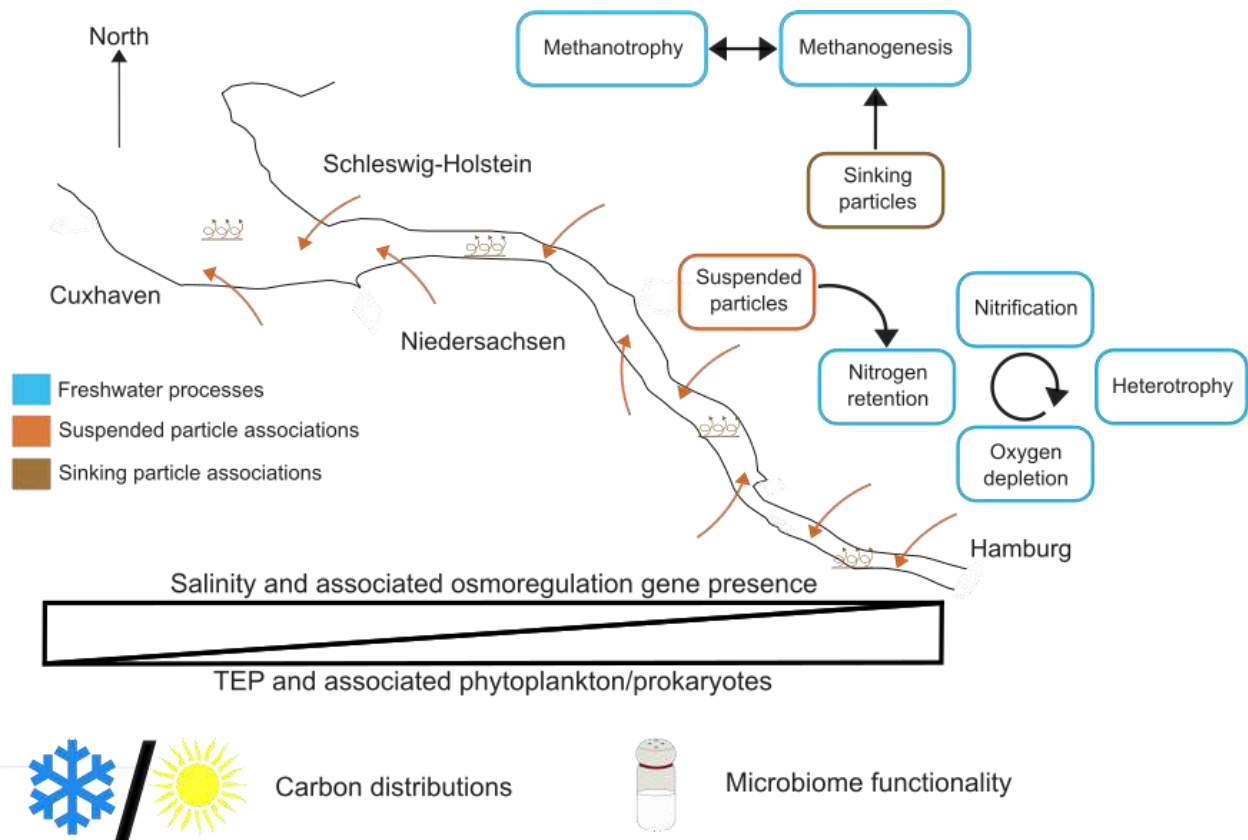


Figure 4.1. Overview of key findings. Processes localised to freshwater areas are surrounded by light-blue boxes. Source contributions of suspended and sinking particles are shown in orange and brown, representing terrestrial wash-in and resuspended sediments. Sun and snowflakes represent the predominantly temporal influence on carbon, while a salt shaker represents the primarily salinity dependent microbiome functionality. Black triangles show how the spatially dependent salinity drives associated osmoregulation genes and functionality, while TEP and its associated phytoplankton/prokaryote distributions are shown to localise to

their area of influence (i.e. freshwater areas). Please note that findings are highly simplified for clarity.

4.1 Key Findings

4.1.1 Spatiotemporal carbon and microbiome dynamics

Microbial communities and carbon concentrations are tightly interwoven (Cai, 2011; Figueroa et al., 2021), with microbes processing carbon and shuttling carbon and organic matter across trophic levels (Brankovits et al., 2017). Given their interdependence, I expected that they would share primary drivers. Findings however, reveal that while seasonality is the primary driver of carbon profiles – and significantly contribute to microbial profiles – salinity is the most influential microbiome driver. I further explore these differences by examining concentrations of different carbon pools, the microbiome, and carbon-processing genes.

Phytoplankton play important roles in estuarine carbon dynamics (Bukaveckas, 2022), introducing new particulate and dissolved carbon into the system seasonally (Thornton, 2014). In previous studies, DOM humification and aromaticity are at their minimum in spring and summer due to the primary phytoplankton production of labile material (Moran et al., 2022; Morán et al., 2013). However, Elbe Estuary summer samples contain highly humic and aromatic DOM. Attributed to extensive degradation/heterotrophy of phytoplankton and/or terrestrial carbon, also explaining the lack of high Chl-a to DOC increases. Phytoplankton are commonly identified in heterotrophic areas (Street & Paytan, 2005), supplying metabolites to heterotrophic microbes (Ferrer-González et al., 2021), often leading to oxygen depletion (Sun et al., 2022). The Elbe Estuary contains *Microcystis* and *Cyanobium* – freshwater and oligohaline phytoplankton – in these areas. Both are associated with high dCO₂ concentrations, suggesting a role in the oxygen minima by supporting heterotrophic activity. Heterotrophic activity requires transcription, translation, and growth, and therefore nitrogen. I have identified nitrogen genes in the Elbe Estuary that facilitate nitrogen accumulation in the environment (*nifD*; Raymond et al., 2004), nitrogen integration into the cell (*narB*; Allen et al., 2001), followed by pyrimidine biosynthesis (*UMPS*; (Suttle et al., 1988), essential for cell replication and growth. My findings agree with previous studies that the Elbe Estuary's freshwater/oligohaline region is a remineralisation/nitrification hotspot. Meanwhile, the TMZ represents a secondary, lower, peak (Sanders et al., 2018) due to increased nitrification furthest from the ocean and resuspended sediments doubling surface water nitrification rates (Damashek et al., 2016), even with a turbidity minima. This remains consistent with other studies that documented high nitrification and mineralisation rates in the TMZ that often correlate with particle and resuspended sediment abundances (Hollibaugh & Wong, 1999). Freshwater localised nitrogen integration and nitrate fixation are connected to increased heterotrophy and the eventual formation of a seasonal oxygen minima. These conditions exacerbate eutrophication, as hypoxia promotes nitrogen retention, leading to a positive feedback loop (Crump & Bowen, 2024).

Dark CO₂ fixation pathways may also drive localised carbon increases in the estuary's highly turbid environment. However, ATP-citrate lyases (rTCA components) increases in a seasonally independent manner and is linked to Nitrospirota dependent denitrification, a dominant process in Hamburg Harbour (Grüterich et al., 2024; Sanders et al., 2023).

Increased spring and summer oxygen depletions can be attributed to the activity of specific phytoplankton which play a significant role in DOM quantity and properties. However, confirmation requires phytoplankton monitoring and salinity tolerance and activity experiments. Particle properties, meanwhile, show no consistent phytoplankton link, with no ubiquitously present phytoplankton (Martens, Biederick, et al., 2024; Martens, Russnak, et al., 2024). While TEP (phytoplankton produced and predominately polysaccharide; (Alldredge et al., 1993) does display seasonal differences. Patterns are primarily attributed to shifts of mineral-associated TEP of bacterial origin (Fettweis et al., 2022). Additional POC drivers include light and terrestrial exchanges. Light inhibits protein synthesis (Santos et al., 2012) and degrades OM (Dalzell et al., 2009) as reflected in CSP profiles, as CSP mainly consists of proteins (Long & Azam, 1996). However, the high turbidity means that light plays a negligible role in the Elbe Estuary. Whereas continuous terrestrial exchanges across the estuarine gradient are suggested based on previous DOM signatures and, most importantly, the identification of terrestrial genes such as those involved in plant organic acid utilisation. In the end, while phytoplankton remain an important TEP source, they do not drive seasonal POC dynamics in the Elbe Estuary's surface waters (Horemans et al., 2021).

Spatial carbon dynamics are challenging to untangle. While my findings align with previous studies (Middelburg & Herman, 2007), focusing solely on the Elbe Estuary may limit observable spatial differences. Expanding sampling upstream of Hamburg Harbour and downstream of Cuxhaven could reveal clearer spatial patterns across the salinity gradient. Salinity is a key spatial driver in dynamic environments (Rieck et al., 2015; Telesh & Khlebovich, 2010; Tobias-Hünefeldt et al., 2019) and increases are typically associated with decreasing POC and variable DOC responses (Abril et al., 2002; Álvarez-Salgado & Miller, 1999; Y. Li et al., 2019; Madsen & Sand-Jensen, 1991; Mantoura & Woodward, 1983; Spencer et al., 2007). In the Elbe Estuary, only TEP and tryptophan-like DOM signatures decrease with salinity, while biological activity peaks in mesohaline areas. A closer examination of TEP-associated taxa reveals localisation to freshwater and oligohaline conditions and the uniquely present GH65 and GT51 carbohydrate active enzyme families (glycoside hydrolases and glycosyltransferases). Other studies also identified TEP producing phytoplankton (Guinardia; (Berman-Frank et al., 2016; Martens, Russnak, et al., 2024) in the Elbe Estuary's freshwater regions. Both enzyme families play a key role during exopolymer turnover (De Beul et al., 2024; Mohapatra, 2024; Silva et al., 2014; Yuan et al., 2007). Thus, osmotic pressure likely drives spatial TEP patterns, although anthropogenic influences such as Hamburg Harbour effluents and dredging activities (Schöneich-Argent et al., 2020), or a dominant marine influence throughout the estuary, must also be considered. This means that a loss of this freshwater region may severely affect particle aggregation and sedimentation dynamics with decreased TEP production, an important aggregation agent.

Kappenberg & Fanger (2007) and van Beusekom et al. (2021) proved that sediments may be predominately marine derived throughout an estuarine area. The noted marine-like influence may denote a resuspension of marine-derived sediment. Both microbiome and DOM analyses support this conclusion: anoxic sediment and soil associated genes appear in particle-associated microbiomes regardless of salinity, and no TEP-associated organisms have previously been identified in marine environments (Alldredge et al., 1993; Claquin et al., 2008), and marine-like DOM signatures remain consistent, indicative of a ubiquitous source. These results imply that marine intrusions are of great concern, affecting upstream sediments and the water column, with dredging intensifying marine-like influence. Although marine intrusions

may result in effects separate from the current marine influence in the Elbe Estuary. Further studies are needed to assess how marine intrusions impact biological activity – especially if the highly active mesohaline region merges with the active Hamburg Harbour (Norbisrath et al., 2022) – as this may profoundly affect heterotrophic activity, oxygen distributions, and overall ecosystem functions, resulting oxygen depletions, high heterotrophic activities, and food-web changes.

Overall, seasonal and spatial drivers both shape carbon profiles. Estuarine models support our findings: hydrodynamics determining winter DOC dynamics, while biogeochemical processes drive summer dynamics (Yao et al., 2024), with microbes acting as summer carbon sinks (Jiao & Zheng, 2011; Yao et al., 2024).

The Elbe Estuary microbiome shows strong seasonally dependent compositional and functional potential trends, but weak transcription trends. Salinity, however, dominates transcription patterns and strongly influences composition and functional potential, emerging as the primary microbiome driver. Although functional redundancy must be increasingly considered over time (Ramond et al., 2025), the selection of key processes along the estuary gradient (Levitan et al., 2024) weakens temporal patterns. This redundancy and process selection is evident in my transcription profiles, which actively responds to estuarine gradients, while carbon profiles, and microbiome composition and functional potential represent long-term trends. For instance, bacteria may be transported from oligo- to mesohaline conditions, altering osmoregulation gene transcription while the organism's genome remains unchanged. Therefore, spatial differences are largely driven by osmoregulation: colonisation decreasing with salinity as taxa with high osmoregulation gene abundance dominate saline conditions, while those lacking osmoregulation genes are confined to freshwater areas. Examples include *Limnohabitans* (Kasalický et al., 2017), *Pseudoholngiellaceae* (Dong et al., 2023), *Burkholderiaceae* (Coenye & Vandamme, 2003; Sawana et al., 2014), *CAIRTT01*, *Aquirufa* (Pitt et al., 2019), and *Flavobacterium* (Kang et al., 2013). However, salinity was not the sole spatial determiner. *Zoogloea* are a good example, while found in freshwater conditions they may also represent effluent contamination from wastewater treatment (Dugan et al., 1992; Shi et al., 2023).

An ecologically important consideration concerns CH₄ production and utilisation, especially as salinisation reduces methane emissions and dCH₄ concentrations (L. Liu et al., 2019; Poffenbarger et al., 2011; Soued et al., 2024). Freshwater areas represent *pmoA* gene and transcript abundance maxima, high methane concentrations potentially driving methanotroph activity and presence (Methylococcaceae: Chen et al., 2020; Taubert et al., 2019; Methylomonadaceae: Bussmann et al., 2021). However, while methanotrophs and methanogenesis cofactors are seen, methanogens and key methanogenesis genes (e.g. *mcrA*) could not be identified in surface waters. Suggesting that the sediment (Chen et al., 2020b) was the primary CH₄ source. The lack of surface water methanogenesis suggests that in the Elbe Estuary salinity-dependent dCH₄ concentrations likely result from an inhibition of sediment production, or another upstream source. Further research should compare methanogen and methanotroph activity in sediments vs. the water column to confirm our findings. Especially as the detection of methanogenesis cofactors and intermediates (*hdrA2*, *comD*, and *fmdCE*) on particles suggests that microenvironment activity and detection limits may apply. Therefore, qPCR approaches may be the most suitable. Studies will have to be environmentally specific, as increased methanotrophy, rather than decreased

methanogenesis, was responsible for decreased dCH₄ concentrations in salt ponds (J. Zhou et al., 2022).

My findings indicate that carbon and microbiome profiles should be assessed independently; seasonality primarily shapes organic carbon distributions, while salinity – and the presence of osmoregulation genes – drives microbial profiles. Their integration enables better contextualisation of findings, placing them into an ecological framework for future models and policy decisions, showing the value of multifaceted approaches. For instance, freshwater input prevents the fusion of two high-activity areas, and the marine-like influence originates from marine-sediment-derived materials rather than marine-phytoplankton-derived organic.

4.1.2 Carbon and microbiome dependent fraction differences

Localised microbiome differences are often obscured in broad spatiotemporal studies or those focussed on specific conditions, e.g. phytoplankton blooms, single seasons, or particular processes (Middelboe et al., 1995; Rösel & Grossart, 2012; Urvoy et al., 2022). Meanwhile, my study design lets me identify consistent carbon property and processing differences between fractions, independent of spatiotemporal considerations.

Free-living microbes include the expected planktonic genera such as *Planktophila* and *Pelagibacter*, as well as intracellular eukaryotic symbionts (*Rickettsiales*). In contrast, particle-associated microbiomes span diverse taxa, from *Verrucomicrobia* to *Pseudomonadota*. Functional assessments show that particle-associated microbiomes are preferentially involved in nitrogen fixation, plant organic acid utilisation, and represent methanogenesis cofactors. The presence of plant organic acid utilising genes reinforces the link between terrestrial-like DOM and the particle fraction, emphasizing the role of terrestrial exchanges in Elbe Estuary carbon processing.

Initial hypotheses associated suspended particles with autochthonous DOM, and sinking particles with aromatic DOM, based on previous Wadden Sea studies (Lunau et al., 2004). However, terrestrial-like humic-like DOM correlates with suspended POC, while marine-like humic-like DOM aligns with sinking POC. This argues against a suspended-autochthonous connection as both are humic-like, although the degree of humification remains debatable. Based on this finding I predicted an upregulation of terrestrial-associated genes and taxa abundance on the suspended fraction, and more sediment associated genes and taxa in the sinking fraction. While no terrestrial specific process could be identified, growth related pathways are upregulated (i.e. amino acid biosynthesis and nitrogen recycling genes) on the suspended fraction, with *oorA* – typical of terrestrial-associated genomes (Pierce et al., 2010) – even upregulated in the sinking fraction. Meanwhile, the sinking fraction displays tentative sediment links via the presence and transcription of methanogenesis cofactors, a process usually associated with anoxic sediments and soils. My findings are consistent with previous studies, where resuspended particles in the Elbe Estuary experience periodical anoxia on the sediment surface before resuspension (Eisma et al., 1982, 1994; Rolinski, 1999).

Thus, suspended particles may drive new nitrogen input, and sinking microbiomes are more likely to utilise methanogenesis as a final electron acceptor. If associations remain true, as suspended particle abundance increases with increased terrestrial input (e.g. bank erosion or extreme weather events), nitrogen availability and atmospheric exchange rates also increase, leading to increased eutrophication and heterotrophic activity. Focused studies are required

to assess this in more detail and offer deeper insights into estuarine carbon processes, essential to predict system responses to ongoing anthropogenic and climate changes, such as increased marine intrusions and terrestrial input.

4.1.3 How does particle colonisation change across estuarine gradients?

Particle-associated organisms play a significant role across estuarine surface water gradients, predominantly due to increased activity compared to free-living organisms (Rieck et al., 2015). Free-living vs. particle associated microbial differences are well established. I set out to determine what separates suspended and sinking particle-associated microbiomes in more detail, including what leads to colonisation differences, if any exist.

Upstream freshwater/oligohaline region particles were expected to be more labile due to an increased link to autochthonous production, i.e. phytoplankton and phytoplankton-derived TEP, and thus preferentially colonised, based on upper vs. lower Elbe estuary region studies (Zimmermann, 1997). Bacterial colonisation decreases with salinity, matching the hypothesis. However, numerous factors play a role, including nutrient availability, decreased osmotic tolerance (Painchaud et al., 1995), increased zooplankton predation (Silva et al., 2019), colonising taxa growth rate reductions, etc. Colonisation reduction suggests community composition and functions are also affected by the salinity gradient, shown with the presence of osmoregulation genes that are responsible for spatial differences. Osmoregulation likely also plays a key role in colonisation, although its relative importance requires further studies due to the presence of microenvironments protecting against osmotic pressure.

Differences between suspended and sinking particles are challenging to determine in the highly turbulent Elbe Estuary (Tobias-Hünefeldt et al., 2024). Presence-absence based indicator tests failed to identify particle fraction differences, while abundance-based Wilcoxon tests could identify some significant differences. This indicates that differences in colonisation rate and subsequent growth may determine suspended vs. sinking particle microbiome differences, with stochastic mechanisms determining initial settlement. I initially hypothesised that deterministic processes such as increased exopolymer concentrations on suspended particles would enhance colonisation, but while TEP supports this hypothesis, CSP did not. Direct colonisation assessments indicate that colonisation differences likely stem from buoyant effects, rather than direct exopolymer colonisation. CSP is not associated with colonisation as its degradation fuels growth. CSP's rapid turnover and variable utilisation (Busch et al., 2017) prevents robust field-based observation, although numerous studies have confirmed CSP's involvement with phytoplankton and bacterial communities (Allredge et al., 1993; Bar-Zeev & Rahav, 2015; de Moreno et al., 1986; Decho, 1990; H.-P. Grossart et al., 1997, 2006; Logan et al., 1994; Roux et al., 2021; Simon et al., 2002; Stoderegger & Herndl, 1998; Thornton, 2018).

In summary, differences between TEP and CSP arise from distinct bacterial utilisation: the predominately polysaccharide TEP accumulates with colonisation while acting as an aggregation agent, while the protein heavy CSP supports growth through its degradation.

4.3 Challenges and limitations

My study explores knowledge gaps using a multitude of biogeochemical and molecular approaches, nonetheless, limitations must be acknowledged and considered. Limitations include a limited spatial range, low temporal resolution, the presence of neutrally buoyant

particles, limitations inherent in particle studies, a lack of depth profile, and not accounting for dredging during sampling campaigns.

Primary productivity and phytoplankton growth are typically promoted under conditions of low turbidity and stable salinity. Our study site between Hamburg Harbour and Cuxhaven, is strongly impacted by marine intrusions which create conditions of varying salinity (0.3 to 20 PSU) and large quantities of resuspended sediment. As such, primary productivity is rather limited within the Elbe Estuary, whereas upstream of Hamburg Harbour in the Elbe River, and in the North Sea outside Cuxhaven, primary productivity is much higher. This results in higher contributions of autochthonous carbon into the aquatic ecosystem (Sugie et al., 2020; Zander et al., 2020) relative to the highly turbid estuarine environment, dominated by allochthonous carbon. Expanding the study area to account for these more productive areas would have facilitated clearer parameter associations, potentially increasing the strength of carbon-salinity associations. However, a focus on the limited shifting salinity region allows us to focus on what drives these shifts, such as heterotrophy in the oxygen minima.

Heterotrophy-autotrophy dynamics are often temporally dependent. I was limited to only a single sample per season. Increased temporal resolution facilitates a closer examination of trends and the identification of intricate carbon processing details with increased reliability. A multi-year assessment, such as over 5-years, would also allow us to draw clearer seasonal conclusions. Annual differences are common in estuaries, with long-term studies still able to identify seasonal trends over long time periods (Rösel et al., 2012; Vance et al., 2024), with the potential to miss more intricate components of the dynamics. A more consistent sampling schedule, such as weekly, or bi-weekly, would ideally capture more temporal details.

To assess differences in sinking and suspended particles, I adopted an instrument previously deployed in the Wadden Sea. This device allows for separation of positively and negatively buoyant particles. However, I was unable to effectively quantify neutrally buoyant particles, which are distributed throughout both the suspended and sinking particle fractions. As such, I could not sufficiently determine what proportions of the collected fractions constituted these neutral particles, and the impact that this had in masking differences in the occurrence and abundance of specific taxa and functional processes. Presence/absence analysis are still informative as they identify taxa and genes unique to each fraction, excluding neutrally buoyant particle-associated taxa and functions, however are less powerful in highly mixed environments with stochastic settlements. Abundance based differences are also more challenging with statistical power increases required to overcome neutrally buoyant particle microbiome baselines. A more comprehensive approach requires the isolation of individual particles, measuring sinking velocity and classifying them as suspended, neutral, or sinking. Particles are highly heterogeneous, so this approach would also provide a clearer picture of what is occurring on each particle. However, characterising single-particles in the Elbe Estuary encounters severe technical limitations. Elbe Estuary particles are far too abundant and small to isolate, measure, characterise, and extract the DNA/RNA of a representative amount. Additionally, a shallow sampling depth (~1m) potentially omits mature sinking material, obtaining only newly aggregated particles. This can be seen in May, where dry-weight and particle area decreases due to a potential phytoplankton bloom increasing aggregation and sedimentation, removing them from the shallow sampling depth at increased rates. A depth profile would help answer this, and explore what effect the stratification of the Elbe Estuary has, and if the high mixing rates are reflected in marine-sediment influences.

Dredging exhibits the opposite effect, increasing turbidity and particle abundance and can even prevent algal bloom damage by affecting core species abundance (Wan et al., 2023). While dredging events close to sampling sites were recorded, accounting for all dredging efforts in the Elbe Estuary would allow us to account for manifested impacts such as decreased primary production and increased aggregation leading to increased sinking particle abundance. This would require extensive data access, including displacement abundances, from the barges carrying out dredging activities and their schedules to properly account for dredging effects. This would then need to be compared to times where no dredging took effect, which is challenging as the Elbe Estuary is continuously dredged and conditions continuously change (Winterscheid et al., 2019).

4.4 Conclusions and Outlook

Throughout this thesis I show that carbon and microbial dynamics are inherently linked and respond to many of the same physical/chemical drivers. A notable distinction was that carbon dynamics are more strongly driven by seasonal fluctuations, and the microbiome and functional composition are instead driven by spatial salinity variations. This thesis shows how carbon and microbiome profiles are deeply connected, integrating particulate and dissolved carbon profiles, and microbiome composition, functional potential, and transcription profiles. Such a multifaceted approach allows us to determine localisation of methanotrophy to the Elbe Estuary's freshwater areas, where production and release of methane from freshwater sediments has been shown to occur, unimpeded by high salt concentrations. This is important as estuaries represent hotspots of organic matter cycling, with microbes influencing carbon concentrations across the estuarine gradient. Utilising the available carbon for growth, competition via antibiotic biosynthesis and degradation, and as waste products. Future studies should examine if increased methane concentrations are related to the abundance of sinking particles and the resuspension of marine-derived sediments, studying the underlying mechanism and controlling variables in greater detail, especially in the context of climate predictions.

Findings also further highlight areas for future study, including the integration of inorganic carbon profiles beyond dCO₂, greenhouse gas flux measurements, and assessing alkalinity (Norbisrath et al., 2022) to better assess carbon profiles and the ability of the estuarine channels to store, process, and/or emit greenhouse gases. Especially if marine intrusions lead to the merging of the mesohaline high activity zone, and Hamburg Harbour. Based on our conclusions it is suggested that increased phytoplankton monitoring and phytoplankton salinity acclimation paired with their activity experiments should be carried out to assess if seasonal oxygen depletion can be attributed to the degradation of specific phytoplankton. Currently phytoplankton monitoring only reaches freshwater regions (Martens, Russnak, et al., 2024), peripherally near where oxygen minima develop. Meanwhile, salinity tolerance tests would address if their activity is likely to continue under increased marine intrusion scenarios, and if indeed TEP abundance and its role as an aggregation agent is affected like I predict.

This thesis demonstrates the importance of understanding, integrating, and contextualising carbon profiles, microbiome compositions, functional potential, and transcription in a comprehensive framework to reach robust conclusions. Providing insights into future estuarine condition changes and their effects, e.g. marine intrusions with rising sea levels. Further proving that the multifaceted approach, integrating usually separately assessed components, allows us to better understand the current dynamics, and predict future changes.

Bibliography

- Abril, G., Nogueira, M., Etcheber, H., Cabeçadas, G., Lemaire, E., & Brogueira, M. J. (2002). Behaviour of Organic Carbon in Nine Contrasting European Estuaries. *Estuarine, Coastal and Shelf Science*, 54(2), 241–262. <https://doi.org/10.1006/ecss.2001.0844>
- Alcolombri, U., Peaudcerf, F. J., Fernandez, V. I., Behrendt, L., Lee, K. S., & Stocker, R. (2021). Sinking enhances the degradation of organic particles by marine bacteria. *Nature Geoscience*, 14(10), 775–780. <https://doi.org/10.1038/s41561-021-00817-x>
- Alfonso, M. B., Lindsay, D. J., Arias, A. H., Nakano, H., Jandang, S., & Isobe, A. (2023). Zooplankton as a suitable tool for microplastic research. *Science of The Total Environment*, 905, 167329. <https://doi.org/10.1016/j.scitotenv.2023.167329>
- Allredge, A. L., Passow, U., & Logan, B. E. (1993). The abundance and significance of a class of large, transparent organic particles in the ocean. *Deep Sea Research Part I*, 40(6), 1131–1140.
- Allen, A. E., Booth, M. G., Frischer, M. E., Verity, P. G., Zehr, J. P., & Zani, S. (2001). Diversity and Detection of Nitrate Assimilation Genes in Marine Bacteria. *Applied and Environmental Microbiology*, 67(11), 5343–5348.
<https://doi.org/10.1128/AEM.67.11.5343-5348.2001>
- Álvarez-Salgado, X. A., & Miller, A. E. J. (1999). Dissolved Organic Carbon in a Large Macrotidal Estuary (the Humber, UK): Behaviour During Estuarine Mixing. *Marine Pollution Bulletin*, 37(3), 216–224. [https://doi.org/10.1016/S0025-326X\(98\)00156-8](https://doi.org/10.1016/S0025-326X(98)00156-8)
- Amann, T., Weiss, A., & Hartmann, J. (2012). Carbon dynamics in the freshwater part of the Elbe estuary, Germany: Implications of improving water quality. *Estuarine, Coastal and Shelf Science*, 107, 112–121. <https://doi.org/10.1016/j.ecss.2012.05.012>
- Amann, T., Weiss, A., & Hartmann, J. (2015). Inorganic Carbon Fluxes in the Inner Elbe Estuary, Germany. *Estuaries and Coasts*, 38(1), 192–210.
<https://doi.org/10.1007/s12237-014-9785-6>
- Asmala, E., Kaartokallio, H., Carstensen, J., & Thomas, D. N. (2016). Variation in Riverine

Inputs Affect Dissolved Organic Matter Characteristics throughout the Estuarine Gradient. *Frontiers in Marine Science*, 2.

<https://www.frontiersin.org/articles/10.3389/fmars.2015.00125>

Bailey, G. B., & Dempsey, W. B. (1967). Purification and Properties of an α -Dialkyl Amino Acid Transaminase*. *Biochemistry*, 6(5), 1526–1533.

<https://doi.org/10.1021/bi00857a039>

Balch, W. M., & Mitchell, C. (2023). Remote sensing algorithms for particulate inorganic carbon (PIC) and the global cycle of PIC. *Earth-Science Reviews*, 239, 104363.

<https://doi.org/10.1016/j.earscirev.2023.104363>

Barendrecht, M. H., Matanó, A., Mendoza, H., Weesie, R., Rohse, M., Koehler, J., de Ruiter, M., Garcia, M., Mazzoleni, M., Aerts, J. C. J. H., Ward, P. J., Di Baldassarre, G., Day, R., & Van Loon, A. F. (2024). Exploring drought-to-flood interactions and dynamics: A global case review. *WIREs Water*, 11(4), e1726. <https://doi.org/10.1002/wat2.1726>

Barton, A. D., Ward, B. A., Williams, R. G., & Follows, M. J. (2014). The impact of fine-scale turbulence on phytoplankton community structure. *Limnology and Oceanography: Fluids and Environments*, 4(1), 34–49. <https://doi.org/10.1215/21573689-2651533>

Bar-Zeev, E., & Rahav, E. (2015). Microbial metabolism of transparent exopolymer particles during the summer months along a eutrophic estuary system. *Frontiers in Microbiology*, 0(MAY), 403. <https://doi.org/10.3389/FMICB.2015.00403>

Baumann, M., Paul, A. J., Taucher, J., Bach, L. T., Goldenberg, S., Stange, P., Minutolo, F., & Riebesell, U. (2023). Drivers of particle sinking velocities in the Peruvian upwelling system. *Biogeosciences*, 20(13), 2595–2612. <https://doi.org/10.5194/bg-20-2595-2023>

Baumas, C. M. J., Le Moigne, F. A. C., Garel, M., Bhairy, N., Guasco, S., Riou, V., Armougom, F., Grossart, H. P., & Tamburini, C. (2021). Mesopelagic microbial carbon production correlates with diversity across different marine particle fractions. *ISME Journal*. <https://doi.org/10.1038/s41396-020-00880-z>

Becker, J. W., Berube, P. M., Follett, C. L., Waterbury, J. B., Chisholm, S. W., DeLong, E. F.,

& Repeta, D. J. (2014). Closely related phytoplankton species produce similar suites of dissolved organic matter. *Frontiers in Microbiology*, 5.

<https://doi.org/10.3389/fmicb.2014.00111>

Bergemann, M., & Gaumert, T. (2010). *Elbebericht 2008*. FGG-Elbe. [https://www.fgg-](https://www.fgg-elbe.de/files/Download-)

Archive/Gewaesserguete/Elbeberichte_ab_2008/08Elbebericht.pdf

Berman-Frank, I., Spungin, D., Rahav, E., Van Wambeke, F., Turk-Kubo, K., & Moutin, T. (2016). Dynamics of transparent exopolymer particles (TEP) during the VAHINE mesocosm experiment in the New Caledonian lagoon. *Biogeosciences*, 13(12), 3793–3805. <https://doi.org/10.5194/bg-13-3793-2016>

Bernardet, J.-F., & Bowman, J. P. (2015). Flavobacterium. In *Bergey's Manual of Systematics of Archaea and Bacteria* (pp. 1–75). John Wiley & Sons, Ltd.

<https://doi.org/10.1002/9781118960608.gbm00312>

Bernát, N., Köpcke, B., Yasseri, S., Thiel, R., & Wolfstein, K. (1994). Tidal variation in bacteria, phytoplankton, zooplankton, mysids, fish and suspended particulate matter in the turbidity zone of the Elbe estuary; Interrelationships and causes. *Netherlands Journal of Aquatic Ecology*, 28(3–4), 467–476. <https://doi.org/10.1007/BF02334218>

Bianchi, D., Weber, T. S., Kiko, R., & Deutsch, C. (2018). Global niche of marine anaerobic metabolisms expanded by particle microenvironments. *Nature Geoscience*, 11(4), 263–268. <https://doi.org/10.1038/s41561-018-0081-0>

Bižić-Ionescu, M., Ionescu, D., & Grossart, H. P. (2018). Organic particles: Heterogeneous hubs for microbial interactions in aquatic ecosystems. *Frontiers in Microbiology*, 9(OCT), 1–15. <https://doi.org/10.3389/fmicb.2018.02569>

Boehlich, M. J., & Strotmann, T. (2019). *Das Elbeästuar*.

<https://hdl.handle.net/20.500.11970/107117>

Bogard, M. J., del Giorgio, P. A., Boutet, L., Chaves, M. C. G., Prairie, Y. T., Merante, A., & Derry, A. M. (2014). Oxic water column methanogenesis as a major component of aquatic CH₄ fluxes. *Nature Communications*, 5(1), 5350.

<https://doi.org/10.1038/ncomms6350>

- Boller, M., & Blaser, S. (1998). Particles under stress. *Water Science and Technology*, 37(10), 9–29. [https://doi.org/10.1016/S0273-1223\(98\)00303-5](https://doi.org/10.1016/S0273-1223(98)00303-5)
- Bonner, C. A., Jensen, R. A., Gander, J. E., & Keyhani, N. O. (2004). A core catalytic domain of the TyrA protein family: Arogenate dehydrogenase from Synechocystis. *Biochemical Journal*, 382(1), 279–291. <https://doi.org/10.1042/BJ20031809>
- Borges, A. V., & Abril, G. (2011). 5.04—Carbon Dioxide and Methane Dynamics in Estuaries. In E. Wolanski & D. McLusky (Eds.), *Treatise on Estuarine and Coastal Science* (pp. 119–161). Academic Press. <https://doi.org/10.1016/B978-0-12-374711-2.00504-0>
- Borges, A. V., Abril, G., & Bouillon, S. (2018). Carbon dynamics and CO₂ and CH₄ outgassing in the Mekong delta. *Biogeosciences*, 15(4), 1093–1114. <https://doi.org/10.5194/bg-15-1093-2018>
- Bowman, J. P. (2006). The Marine Clade of the Family Flavobacteriaceae: The Genera Aequorivita, Arenibacter, Cellulophaga, Croceibacter, Formosa, Gelidibacter, Gillisia, Maribacter, Mesonia, Muricauda, Polaribacter, Psychroflexus, Psychroserpens, Robiginitalea, Salegentibacter, Tenacibaculum, Ulvibacter, Vitellibacter and Zobellia. In M. Dworkin, S. Falkow, E. Rosenberg, K.-H. Schleifer, & E. Stackebrandt (Eds.), *The Prokaryotes: Volume 7: Proteobacteria: Delta, Epsilon Subclass* (pp. 677–694). Springer. https://doi.org/10.1007/0-387-30747-8_26
- Brankovits, D., Pohlman, J. W., Niemann, H., Leigh, M. B., Leewis, M. C., Becker, K. W., Iliffe, T. M., Alvarez, F., Lehmann, M. F., & Phillips, B. (2017). Methane- and dissolved organic carbon-fueled microbial loop supports a tropical subterranean estuary ecosystem. *Nature Communications*, 8(1), 1835. <https://doi.org/10.1038/s41467-017-01776-x>
- Bratbak, G. (1985). Bacterial Biovolume and Biomass Estimations. *Applied and Environmental Microbiology*, 49(6), 1488–1493. <https://doi.org/10.1128/AEM.49.6.1488-1493.1985>

- Bratbak, G., Egge, J. K., & Heldal, M. (1993). Viral mortality of the marine alga *Emiliania huxleyi* (Haptophyceae) and termination of algal blooms. *Marine Ecology Progress Series*, 93(1/2), 39–48.
- Braun, A., Spona-Friedl, M., Avramov, M., Elsner, M., Baltar, F., Reinthaler, T., Herndl, G. J., & Griebler, C. (2021). Reviews and syntheses: Heterotrophic fixation of inorganic carbon – significant but invisible flux in environmental carbon cycling. *Biogeosciences*, 18(12), 3689–3700. <https://doi.org/10.5194/bg-18-3689-2021>
- Brünjes, J., Seidel, M., Dittmar, T., Niggemann, J., & Schubotz, F. (2022). Natural Asphalt Seeps Are Potential Sources for Recalcitrant Oceanic Dissolved Organic Sulfur and Dissolved Black Carbon. *Environmental Science & Technology*, 56(12), 9092–9102. <https://doi.org/10.1021/acs.est.2c01123>
- Buchfink, B., Reuter, K., & Drost, H.-G. (2021). Sensitive protein alignments at tree-of-life scale using DIAMOND. *Nature Methods*, 18(4), 366–368. <https://doi.org/10.1038/s41592-021-01101-x>
- Budinoff, C. R. (2005). *Ecophysiology of a mono lake Cyanobacterium* [MSc]. The University of Georgia.
- Bukaveckas, P. A. (2022). Carbon dynamics at the river–estuarine transition: A comparison among tributaries of Chesapeake Bay. *Biogeosciences*, 19(17), 4209–4226. <https://doi.org/10.5194/bg-19-4209-2022>
- Burd, A. B., & Jackson, G. A. (2009). Particle Aggregation. *Annual Review of Marine Science*, 1(Volume 1, 2009), 65–90. <https://doi.org/10.1146/annurev.marine.010908.163904>
- Busch, K., Endres, S., Iversen, M. H., Michels, J., Nöthig, E.-M., & Engel, A. (2017). Bacterial Colonization and Vertical Distribution of Marine Gel Particles (TEP and CSP) in the Arctic Fram Strait. *Frontiers in Marine Science*, 4. <https://www.frontiersin.org/articles/10.3389/fmars.2017.00166>
- Bussmann, I., Horn, F., Hoppert, M., Klings, K.-W., Saborowski, A., Warnstedt, J., & Liebner, S. (2021). *Methylomonas albis* sp. nov. and *Methylomonas fluvii* sp. nov.: Two cold-

adapted methanotrophs from the river Elbe and emended description of the species *Methylovulum psychrotolerans*. *Systematic and Applied Microbiology*, 44(6), 126248. <https://doi.org/10.1016/j.syapm.2021.126248>

Cael, B. B., Cavan, E. L., & Britten, G. L. (2021). Reconciling the Size-Dependence of Marine Particle Sinking Speed. *Geophysical Research Letters*, 48(5), e2020GL091771. <https://doi.org/10.1029/2020GL091771>

Cai, W. J. (2011). Estuarine and coastal ocean carbon paradox: CO₂ sinks or sites of terrestrial carbon incineration? *Annual Review of Marine Science*, 3, 123–145. <https://doi.org/10.1146/annurev-marine-120709-142723>

Casas-Ruiz, J. P., Bodmer, P., Bona, K. A., Butman, D., Couturier, M., Emilson, E. J. S., Finlay, K., Genet, H., Hayes, D., Karlsson, J., Paré, D., Peng, C., Striegl, R., Webb, J., Wei, X., Ziegler, S. E., & del Giorgio, P. A. (2023). Integrating terrestrial and aquatic ecosystems to constrain estimates of land-atmosphere carbon exchange. *Nature Communications*, 14(1), 1571. <https://doi.org/10.1038/s41467-023-37232-2>

Chang, H.-K., Mohseni, P., & Zylstra, G. J. (2003). Characterization and Regulation of the Genes for a Novel Anthranilate 1,2-Dioxygenase from *Burkholderia cepacia* DBO1. *Journal of Bacteriology*, 185(19), 5871–5881. <https://doi.org/10.1128/jb.185.19.5871-5881.2003>

Chaumeil, P.-A., Mussig, A. J., Hugenholtz, P., & Parks, D. H. (2020). GTDB-Tk: A toolkit to classify genomes with the Genome Taxonomy Database. *Bioinformatics*, 36(6), 1925–1927. <https://doi.org/10.1093/BIOINFORMATICS/BTZ848>

Chen, F., Zheng, Y., Hou, L., Zhou, J., Yin, G., & Liu, M. (2020). Denitrifying anaerobic methane oxidation in marsh sediments of Chongming eastern intertidal flat. *Marine Pollution Bulletin*, 150, 110681. <https://doi.org/10.1016/j.marpolbul.2019.110681>

Chen, S., Wang, P., Liu, H., Xie, W., Wan, X. S., Kao, S.-J., Phelps, T. J., & Zhang, C. (2020). Population dynamics of methanogens and methanotrophs along the salinity gradient in Pearl River Estuary: Implications for methane metabolism. *Applied Microbiology and Biotechnology*, 104(3), 1331–1346. <https://doi.org/10.1007/s00253-019-09612-w>

019-10221-6

- Chilton, D., Hamilton, D. P., Nagelkerken, I., Cook, P., Hipsey, M. R., Reid, R., Sheaves, M., Waltham, N. J., & Brookes, J. (2021). Environmental Flow Requirements of Estuaries: Providing Resilience to Current and Future Climate and Direct Anthropogenic Changes. *Frontiers in Environmental Science*, 9.
<https://doi.org/10.3389/fenvs.2021.764218>
- Christensen, O. B., & Christensen, J. H. (2004). Intensification of extreme European summer precipitation in a warmer climate. *Global and Planetary Change*, 44(1), 107–117.
<https://doi.org/10.1016/j.gloplacha.2004.06.013>
- Ciais, P., Sabine, C., Bala, G., Bopp, L., Brovkin, V., Canadell, J., Chhabra, A., DeFries, R., Galloway, J., Heimann, M., Jones, C., Quéré, C. L., Myneni, R. B., Piao, S., & Thornton, P. (2013). The physical science basis. Contribution of working group I to the fifth assessment report of the intergovernmental panel on climate change. *Change, IPCC Climate*, 465–570. <https://doi.org/10.1017/CBO9781107415324.015>
- Cisternas-Novoa, C., Lee, C., & Engel, A. (2015). Transparent exopolymer particles (TEP) and Coomassie stainable particles (CSP): Differences between their origin and vertical distributions in the ocean. *Marine Chemistry*, 175, 56–71.
<https://doi.org/10.1016/j.marchem.2015.03.009>
- Claquin, P., Probert, I., Lefebvre, S., & Veron, B. (2008). Effects of temperature on photosynthetic parameters and TEP production in eight species of marine microalgae. *Aquatic Microbial Ecology*, 51(1), 1–11.
<https://doi.org/10.3354/ame01187>
- Coble, P. G. (1996). Characterization of marine and terrestrial DOM in seawater using excitation-emission matrix spectroscopy. *Marine Chemistry*, 51(4), 325–346.
[https://doi.org/10.1016/0304-4203\(95\)00062-3](https://doi.org/10.1016/0304-4203(95)00062-3)
- Coenye, T., & Vandamme, P. (2003). Diversity and significance of Burkholderia species occupying diverse ecological niches. *Environmental Microbiology*, 5(9), 719–729.
<https://doi.org/10.1046/j.1462-2920.2003.00471.x>

- Cole, J. J., & Prairie, Y. T. (2014). Dissolved CO₂ in Freshwater Systems☆. In *Reference Module in Earth Systems and Environmental Sciences*. Elsevier.
<https://doi.org/10.1016/B978-0-12-409548-9.09399-4>
- Cole, J. J., Prairie, Y. T., Caraco, N. F., McDowell, W. H., Tranvik, L. J., Striegl, R. G., Duarte, C. M., Kortelainen, P., Downing, J. A., Middelburg, J. J., & Melack, J. (2007). Plumbing the global carbon cycle: Integrating inland waters into the terrestrial carbon budget. *Ecosystems*, 10(1), 171–184. <https://doi.org/10.1007/s10021-006-9013-8>
- Costa, K. C., Lie, T. J., Xia, Q., & Leigh, J. A. (2013). VhuD Facilitates Electron Flow from H₂ or Formate to Heterodisulfide Reductase in *Methanococcus maripaludis*. *Journal of Bacteriology*, 195(22), 5160–5165. <https://doi.org/10.1128/jb.00895-13>
- Crump, B. C., & Baross, J. A. (1996). Particle-attached bacteria and heterotrophic plankton associated with the Columbia River estuarine turbidity maxima. *Marine Ecology Progress Series*, 138(1–3), 265–273. <https://doi.org/10.3354/meps138265>
- Crump, B. C., & Bowen, J. L. (2024). The Microbial Ecology of Estuarine Ecosystems. *Annual Review of Marine Science*, 16(1), null. <https://doi.org/10.1146/annurev-marine-022123-101845>
- Cruz-Flores, R., & Cáceres-Martínez, J. (2020). Rickettsiales-like organisms in bivalves and marine gastropods: A review. *Reviews in Aquaculture*, 12(4), 2010–2026. <https://doi.org/10.1111/raq.12419>
- Cruz-Ramos, H., Glaser, P., Wray, L. V., & Fisher, S. H. (1997). The *Bacillus subtilis* ureABC operon. *Journal of Bacteriology*, 179(10), 3371–3373. <https://doi.org/10.1128/jb.179.10.3371-3373.1997>
- Dähnke, K., Sanders, T., Voynova, Y., & Wankel, S. D. (2022). Nitrogen isotopes reveal a particulate-matter driven biogeochemical reactor in a temperate estuary. <https://doi.org/10.5194/bg-2022-123>
- Dalzell, B. J., Minor, E. C., & Mopper, K. M. (2009). Photodegradation of estuarine dissolved organic matter: A multi-method assessment of DOM transformation. *Organic*

- Geochemistry*, 40(2), 243–257. <https://doi.org/10.1016/j.orggeochem.2008.10.003>
- Damashek, J., Casciotti, K. L., & Francis, C. A. (2016). Variable Nitrification Rates Across Environmental Gradients in Turbid, Nutrient-Rich Estuary Waters of San Francisco Bay. *Estuaries and Coasts*, 39(4), 1050–1071. <https://doi.org/10.1007/s12237-016-0071-7>
- De Beul, E., Franceus, J., & Desmet, T. (2024). The many functions of carbohydrate-active enzymes in family GH65: Diversity and application. *Applied Microbiology and Biotechnology*, 108(1), 476. <https://doi.org/10.1007/s00253-024-13301-4>
- de Moreno, M. R., Smith, J. F., & Smith, R. V. (1986). Mechanism Studies of Coomassie Blue and Silver Staining of Proteins. *Journal of Pharmaceutical Sciences*, 75(9), 907–911. <https://doi.org/10.1002/jps.2600750919>
- Decho, A. W. (1990). Microbial exopolymer secretions in ocean environments: Their role (s) in food webs and marine processes. *Oceanogr. Mar. Biol. Annu. Rev*, 28(7), 73--153.
- Dong, X., Zhu, L., He, Y., Li, C., & Li, D. (2023). Salinity significantly reduces plastic-degrading bacteria from rivers to oceans. *Journal of Hazardous Materials*, 451, 131125. <https://doi.org/10.1016/j.jhazmat.2023.131125>
- Downing, B. D., Boss, E., Bergamaschi, B. A., Fleck, J. A., Lionberger, M. A., Ganju, N. K., Schoellhamer, D. H., & Fujii, R. (2009). Quantifying fluxes and characterizing compositional changes of dissolved organic matter in aquatic systems in situ using combined acoustic and optical measurements. *Limnology and Oceanography: Methods*, 7(1), 119–131. <https://doi.org/10.4319/lom.2009.7.119>
- Dugan, P. R., Stoner, D. L., & Pickrum, H. M. (1992). The Genus Zoogloea. In A. Balows, H. G. Trüper, M. Dworkin, W. Harder, & K.-H. Schleifer (Eds.), *The Prokaryotes: A Handbook on the Biology of Bacteria: Ecophysiology, Isolation, Identification, Applications* (pp. 3952–3964). Springer. https://doi.org/10.1007/978-1-4757-2191-1_58
- Dürr, H. H., Laruelle, G. G., van Kempen, C. M., Slomp, C. P., Meybeck, M., & Middelkoop, H. (2011). Worldwide Typology of Nearshore Coastal Systems: Defining the

Estuarine Filter of River Inputs to the Oceans. *Estuaries and Coasts*, 34(3), 441–458.

<https://doi.org/10.1007/s12237-011-9381-y>

Eady, R. R., Richardson, T. H., Miller, R. W., Hawkins, M., & Lowe, D. J. (1988). The vanadium nitrogenase of *Azotobacter chroococcum*. Purification and properties of the Fe protein. *Biochemical Journal*, 256(1), 189–196. <https://doi.org/10.1042/bj2560189>

Eisma, D. (1993). *Suspended Matter in the Aquatic Environment*.

Eisma, D., Cadee, G., & Laane (RIP), R. W. P. M. (1982). Supply of suspended matter and particulate and dissolved organic carbon from the Rhine to the coastal North Sea. *Transport of Carbon and Minerals in Major World Rivers*, 52, 483–505.

Eisma, D., Chen, S., & Li, A. (1994). Tidal variations in suspended matter floc size in the Elbe river and Dollard estuaries. *Netherlands Journal of Aquatic Ecology*, 28(3), 267–274. <https://doi.org/10.1007/BF02334194>

Elovaara, S., Degerlund, M., Franklin, D. J., Kaartokallio, H., & Tamelander, T. (2020). Seasonal variation in estuarine phytoplankton viability and its relationship with carbon dynamics in the Baltic Sea. *Hydrobiologia*, 847(11), 2485–2501.

<https://doi.org/10.1007/s10750-020-04267-1>

Engel, A., & Passow, U. (2001). Carbon and nitrogen content of transparent exopolymer particles (TEP) in relation to their Alcian Blue adsorption. *Marine Ecology Progress Series*, 219(1977), 1–10. <https://doi.org/10.3354/meps219001>

Erb, T. J., Berg, I. A., Brecht, V., Müller, M., Fuchs, G., & Alber, B. E. (2007). Synthesis of C5-dicarboxylic acids from C2-units involving crotonyl-CoA carboxylase/reductase: The ethylmalonyl-CoA pathway. *Proceedings of the National Academy of Sciences*, 104(25), 10631–10636. <https://doi.org/10.1073/pnas.0702791104>

Eren, A. M., Esen, Ö. C., Quince, C., Vineis, J. H., Morrison, H. G., Sogin, M. L., & Delmont, T. O. (2015). Anvi'o: An advanced analysis and visualization platform for 'omics data. *PeerJ*, 3, e1319. <https://doi.org/10.7717/peerj.1319>

Fani, R., Gallo, R., & Liò, P. (2000). Molecular Evolution of Nitrogen Fixation: The Evolutionary History of the nifD, nifK, nifE, and nifN Genes. *Journal of Molecular*

Evolution, 51(1), 1–11. <https://doi.org/10.1007/s002390010061>

Fast, T., & Kies, L. (1990). Biomass and production of phytoplankton in the Elbe estuary.

Estuarine Water Quality Management, 395–398. <https://doi.org/10.1029/ce036p0395>

Feldewert, C., Lang, K., & Brune, A. (2020). The hydrogen threshold of obligately methyl-reducing methanogens. *FEMS Microbiology Letters*, 367(17), fnaa137.

<https://doi.org/10.1093/femsle/fnna137>

Fellman, J. B., Spencer, R. G. M., Hernes, P. J., Edwards, R. T., D'Amore, D. V., & Hood, E. (2010). The impact of glacier runoff on the biodegradability and biochemical composition of terrigenous dissolved organic matter in near-shore marine ecosystems. *Marine Chemistry*, 121(1), 112–122.

<https://doi.org/10.1016/j.marchem.2010.03.009>

Fernández-Gómez, B., Richter, M., Schüler, M., Pinhassi, J., Acinas, S. G., González, J. M., & Pedrós-Alió, C. (2013). Ecology of marine bacteroidetes: A comparative genomics approach. *ISME Journal*, 7(5), 1026–1037. <https://doi.org/10.1038/ismej.2012.169>

Ferrer-González, F. X., Widner, B., Holdeman, N. R., Glushka, J., Edison, A. S., Kujawinski, E. B., & Moran, M. A. (2021). Resource partitioning of phytoplankton metabolites that support bacterial heterotrophy. *The ISME Journal*, 15(3), 762–773.

<https://doi.org/10.1038/s41396-020-00811-y>

Fettweis, M., Schartau, M., Desmit, X., Lee, B. J., Terseleer, N., Van der Zande, D., Parmentier, K., & Riethmüller, R. (2022). Organic Matter Composition of Biomineral Flocs and Its Influence on Suspended Particulate Matter Dynamics Along a Nearshore to Offshore Transect. *Journal of Geophysical Research: Biogeosciences*, 127(1), e2021JG006332. <https://doi.org/10.1029/2021JG006332>

FGG-Elbe. (2021). *Datenportal der FGG Elbe* [Website]. <https://www.elbedatenportal.de/FisFggElbe/content/start/BesucherUnbekannt.action>

Fichot, C. G., & Benner, R. (2012). The spectral slope coefficient of chromophoric dissolved organic matter (S_{275–295}) as a tracer of terrigenous dissolved organic carbon in river-influenced ocean margins. *Limnology and Oceanography*, 57(5), 1453–1466.

<https://doi.org/10.4319/lo.2012.57.5.1453>

- Figueroa, D., Capo, E., Lindh, M. V., Rowe, O. F., Paczkowska, J., Pinhassi, J., & Andersson, A. (2021). Terrestrial dissolved organic matter inflow drives temporal dynamics of the bacterial community of a subarctic estuary (northern Baltic Sea). *Environmental Microbiology*, 23(8), 4200–4213. <https://doi.org/10.1111/1462-2920.15597>
- Fu, L., Niu, B., Zhu, Z., Wu, S., & Li, W. (2012). CD-HIT: Accelerated for clustering the next-generation sequencing data. *Bioinformatics*, 28(23), 3150–3152. <https://doi.org/10.1093/bioinformatics/bts565>
- Fugate, D. C., & Friedrichs, C. T. (2003). Controls on suspended aggregate size in partially mixed estuaries. *Estuarine, Coastal and Shelf Science*, 58(2), 389–404. [https://doi.org/10.1016/S0272-7714\(03\)00107-0](https://doi.org/10.1016/S0272-7714(03)00107-0)
- Gai, Z., Wang, X., Liu, X., Tai, C., Tang, H., He, X., Wu, G., Deng, Z., & Xu, P. (2010). The Genes Coding for the Conversion of Carbazole to Catechol Are Flanked by IS6100 Elements in *Sphingomonas* sp. Strain XLDN2-5. *PLOS ONE*, 5(4), e10018. <https://doi.org/10.1371/journal.pone.0010018>
- Gao, Y., Jia, J., Lu, Y., Sun, K., Wang, J., & Wang, S. (2022). Carbon transportation, transformation, and sedimentation processes at the land-river-estuary continuum. *Fundamental Research*. <https://doi.org/10.1016/j.fmre.2022.07.007>
- García-Martín, E. E., Sanders, R., Evans, C. D., Kitidis, V., Lapworth, D. J., Rees, A. P., Spears, B. M., Tye, A., Williamson, J. L., Balfour, C., Best, M., Bowes, M., Breimann, S., Brown, I. J., Burden, A., Callaghan, N., Felgate, S. L., Fishwick, J., Fraser, M., ... Mayor, D. J. (2021). Contrasting Estuarine Processing of Dissolved Organic Matter Derived From Natural and Human-Impacted Landscapes. *Global Biogeochemical Cycles*, 35(10), e2021GB007023. <https://doi.org/10.1029/2021GB007023>
- Giblin, A. E., Weston, N. B., Banta, G. T., Tucker, J., & Hopkinson, C. S. (2010). The Effects of Salinity on Nitrogen Losses from an Oligohaline Estuarine Sediment. *Estuaries and Coasts*, 33(5), 1054–1068. <https://doi.org/10.1007/s12237-010-9280-7>

- Gillanders, B., & Kingsford, M. (2002). Impact of Changes in Flow of Freshwater on Estuarine and Open Coastal Habitats and the Associated Organisms. *Oceanography and Marine Biology: An Annual Review*, 40, 233–309.
<https://doi.org/10.1201/9780203180594.ch5>
- Goldberg, I., Nadler, V., & Hochman, A. (1987). Mechanism of nitrogenase switch-off by oxygen. *Journal of Bacteriology*, 169(2), 874–879.
- Gold-Bouchot, G., Polis, S., Castañon, L. E., Flores, M. P., Alsante, A. N., & Thornton, D. C. O. (2021). Chromophoric dissolved organic matter (CDOM) in a subtropical estuary (Galveston Bay, USA) and the impact of Hurricane Harvey. *Environmental Science and Pollution Research International*, 28(38), 53045–53057.
<https://doi.org/10.1007/s11356-021-14509-x>
- Goosen, N. K., Kromkamp, J., Peene, J., Van Rijswijk, P., & Van Breugel, P. (1999). Bacterial and phytoplankton production in the maximum turbidity zone of three European estuaries: The Elbe, Westerschelde and Gironde. *Journal of Marine Systems*, 22(2–3), 151–171. [https://doi.org/10.1016/S0924-7963\(99\)00038-X](https://doi.org/10.1016/S0924-7963(99)00038-X)
- Graupner, M., Xu, H., & White, R. H. (2000). Identification of the Gene Encoding Sulfopyruvate Decarboxylase, an Enzyme Involved in Biosynthesis of Coenzyme M. *Journal of Bacteriology*, 182(17), 4862–4867. <https://doi.org/10.1128/jb.182.17.4862-4867.2000>
- Grossart, H. P. (1999). Interactions between marine bacteria and axenic diatoms (*Cylindrotheca fusiformis*, *Nitzschia laevis*, and *Thalassiosira weissflogii*) incubated under various conditions in the lab. *Aquatic Microbial Ecology*, 19(1), 1–11.
<https://doi.org/10.3354/ame019001>
- Grossart, H. P., Hietanen, S., & Ploug, H. (2003). Microbial dynamics on diatom aggregates in Øresund, Denmark. *Marine Ecology Progress Series*, 249, 69–78.
<https://doi.org/10.3354/meps249069>
- Grossart, H. P., Kiørboe, T., Tang, K., & Ploug, H. (2003). Bacterial colonization of particles: Growth and interactions. *Applied and Environmental Microbiology*, 69(6), 3500–3509.

<https://doi.org/10.1128/AEM.69.6.3500-3509.2003>

Grossart, H. P., & Ploug, H. (2001). Microbial degradation of organic carbon and nitrogen on diatom aggregates. *Limnology and Oceanography*, 46(2), 267–277.

<https://doi.org/10.4319/lo.2001.46.2.0267>

Grossart, H.-P., Berman, T., Simon, M., & Pohlmann, K. (1998). Occurrence and microbial dynamics of macroscopic organic aggregates (lake snow) in Lake Kinneret, Israel, in fall. *Aquatic Microbial Ecology*, 14(1), 59–67. <https://doi.org/10.3354/ame014059>

Grossart, H.-P., Czub, G., & Simon, M. (2006). Algae-bacteria interactions and their effects on aggregation and organic matter flux in the sea. *Environmental Microbiology*, 8(6), 1074–1084. <https://doi.org/10.1111/j.1462-2920.2006.00999.x>

Grossart, H.-P., Simon, M., & Logan, B. E. (1997). Formation of macroscopic organic aggregates (lake snow) in a large lake: The significance of transport exopolymer particles, phytoplankton, and zooplankton. *Limnology and Oceanography*, 42(8), 1651–1659.

Grossart, H.-P., Tang, K. W., Kiørboe, T., & Ploug, H. (2007). Comparison of cell-specific activity between free-living and attached bacteria using isolates and natural assemblages. *FEMS Microbiology Letters*, 266(2), 194–200.

<https://doi.org/10.1111/j.1574-6968.2006.00520.x>

Grüterich, L., Woodhouse, J. N., Mueller, P., Tiemann, A., Ruscheweyh, H.-J., Sunagawa, S., Grossart, H.-P., & Streit, W. R. (2024). Assessing environmental gradients in relation to dark CO₂ fixation in estuarine wetland microbiomes. *Applied and Environmental Microbiology*, 91(1), e02177-24. <https://doi.org/10.1128/aem.02177-24>

Guillemette, F., & del Giorgio, P. A. (2011). Reconstructing the various facets of dissolved organic carbon bioavailability in freshwater ecosystems. *Limnology and Oceanography*, 56(2), 734–748. <https://doi.org/10.4319/lo.2011.56.2.0734>

Hansell, D. A., & Carlson, C. A. (2014). *Biogeochemistry of Marine Dissolved Organic Matter*. Academic Press.

Happ, G., Gosselink, J. G., & Day, J. W. (1977). The seasonal distribution of organic carbon

in a Louisiana estuary. *Estuarine and Coastal Marine Science*, 5(6), 695–705.

[https://doi.org/10.1016/0302-3524\(77\)90042-1](https://doi.org/10.1016/0302-3524(77)90042-1)

Hedges, J. I., Baldock, J. A., Gélinas, Y., Lee, C., Peterson, M. L., & Wakeham, S. G.

(2002). The biochemical and elemental compositions of marine plankton: A NMR perspective. *Marine Chemistry*, 78(1), 47–63. [https://doi.org/10.1016/S0304-4203\(02\)00009-9](https://doi.org/10.1016/S0304-4203(02)00009-9)

Helms, J. R., Stubbins, A., Ritchie, J. D., Minor, E. C., Kieber, D. J., & Mopper, K. (2008).

Absorption spectral slopes and slope ratios as indicators of molecular weight, source, and photobleaching of chromophoric dissolved organic matter. *Limnology and Oceanography*, 53(3), 955–969. <https://doi.org/10.4319/lo.2008.53.3.0955>

Hillebrand, G., Hardenbicker, P., Fischer, H., Otto, W., & Vollmer, S. (2018). Dynamics of total suspended matter and phytoplankton loads in the river Elbe. *Journal of Soils and Sediments*, 18(10), 3104–3113. <https://doi.org/10.1007/s11368-018-1943-1>

Hinson, K. E., Friedrichs, M. A. M., Najjar, R. G., Bian, Z., Herrmann, M., St-Laurent, P., & Tian, H. (2024). Response of hypoxia to future climate change is sensitive to methodological assumptions. *Scientific Reports*, 14(1), 17544.

<https://doi.org/10.1038/s41598-024-68329-3>

Hollibaugh, J. T., & Wong, P. S. (1999). Microbial processes in the San Francisco Bay estuarine turbidity maximum. *Estuaries*, 22(4), 848–862.

<https://doi.org/10.2307/1353066>

Horemans, D. M. L., Dijkstra, Y. M., Schuttelaars, H. M., Sabbe, K., Vyverman, W., Meire, P., & Cox, T. J. S. (2021). Seasonal Variations in Flocculation and Erosion Affecting the Large-Scale Suspended Sediment Distribution in the Scheldt Estuary: The Importance of Biotic Effects. *Journal of Geophysical Research: Oceans*, 126(4), e2020JC016805. <https://doi.org/10.1029/2020JC016805>

Huang, S., Krysanova, V., & Hattermann, F. (2015). Projections of climate change impacts on floods and droughts in Germany using an ensemble of climate change scenarios. *Regional Environmental Change*, 15(3), 461–473. <https://doi.org/10.1007/s10113-014-0700-0>

014-0606-z

- Huang, Y., & An, S. (2022). Weak Hypoxia Enhanced Denitrification in a Dissimilatory Nitrate Reduction to Ammonium (DNRA)-Dominated Shallow and Eutrophic Coastal Waterbody, Jinhae Bay, South Korea. *Frontiers in Marine Science*, 9.
- <https://doi.org/10.3389/fmars.2022.897474>
- Huston, A. L., & Deming, J. W. (2002). Relationships between microbial extracellular enzymatic activity and suspended and sinking particulate organic matter: Seasonal transformations in the North Water. *Deep Sea Research Part II: Topical Studies in Oceanography*, 49(22), 5211–5225. [https://doi.org/10.1016/S0967-0645\(02\)00186-8](https://doi.org/10.1016/S0967-0645(02)00186-8)
- Hutchings, J. A., Bianchi, T. S., Najjar, R. G., Herrmann, M., Kemp, W. M., Hinson, A. L., & Feagin, R. A. (2020). Carbon Deposition and Burial in Estuarine Sediments of the Contiguous United States. *Global Biogeochemical Cycles*, 34(2), e2019GB006376.
- <https://doi.org/10.1029/2019GB006376>
- Hyatt, D., Chen, G.-L., LoCascio, P. F., Land, M. L., Larimer, F. W., & Hauser, L. J. (2010). Prodigal: Prokaryotic gene recognition and translation initiation site identification. *BMC Bioinformatics*, 11(1), 119. <https://doi.org/10.1186/1471-2105-11-119>
- Iglesias, I., Almeida, C. M. R., Teixeira, C., Mucha, A. P., Magalhães, A., Bio, A., & Bastos, L. (2020). Linking contaminant distribution to hydrodynamic patterns in an urban estuary: The Douro estuary test case. *Science of The Total Environment*, 707, 135792. <https://doi.org/10.1016/j.scitotenv.2019.135792>
- Ingeniero, R. C. O., Schulz, G., & Bange, H. W. (2024). Dissolved nitric oxide in the lower Elbe Estuary and the Port of Hamburg area. *Biogeosciences*, 21(14), 3425–3440.
- <https://doi.org/10.5194/bg-21-3425-2024>
- Jackson, G. A., & Burd, A. B. (2015). Simulating aggregate dynamics in ocean biogeochemical models. *Progress in Oceanography*, 133, 55–65.
- <https://doi.org/10.1016/j.pocean.2014.08.014>
- Jayathilake, P. G., Jana, S., Rushton, S., Swailes, D., Bridgens, B., Curtis, T., & Chen, J. (2017). Extracellular Polymeric Substance Production and Aggregated Bacteria

Colonization Influence the Competition of Microbes in Biofilms. *Frontiers in Microbiology*, 8, 1865. <https://doi.org/10.3389/fmicb.2017.01865>

Jezbera, J., Sharma, A. K., Brandt, U., Doolittle, W. F., & Hahn, M. W. (2009). 'Candidatus Planktophila limnetica', an actinobacterium representing one of the most numerically important taxa in freshwater bacterioplankton. *International Journal of Systematic and Evolutionary Microbiology*, 59(11), 2864–2869.

<https://doi.org/10.1099/ijss.0.010199-0>

Jiao, N., Herndl, G. J., Hansell, D. A., Benner, R., Kattner, G., Wilhelm, S. W., Kirchman, D. L., Weinbauer, M. G., Luo, T., Chen, F., & Azam, F. (2010). Microbial production of recalcitrant dissolved organic matter: Long-term carbon storage in the global ocean.

Nature Reviews Microbiology, 8(8), 593–599. <https://doi.org/10.1038/nrmicro2386>

Jiao, N., & Zheng, Q. (2011). The microbial carbon pump: From genes to ecosystems.

Applied and Environmental Microbiology, 77(21), 7439–7444.

<https://doi.org/10.1128/AEM.05640-11>

Jurdzinski, K. T., Mehrshad, M., Delgado, L. F., Deng, Z., Bertilsson, S., & Andersson, A. F. (2023). Large-scale phylogenomics of aquatic bacteria reveal molecular mechanisms for adaptation to salinity. *Science Advances*, 9(21), eadg2059.

<https://doi.org/10.1126/sciadv.adg2059>

Jürgens, K., Arndt, H., & Zimmermann, H. (1997). Impact of metazoan and protozoan grazers on bacterial biomass distribution in microcosm experiments. *Aquatic Microbial Ecology*, 12(2), 131–138. <https://doi.org/10.3354/ame012131>

Kamenik, Z., Kadlcik, S., Radojevic, B., Jiraskova, P., Kuzma, M., Gazak, R., Najmanova, L., Kopecky, J., & Janata, J. (2015). Deacetylation of mycothiol-derived 'waste product' triggers the last biosynthetic steps of lincosamide antibiotics. *Chemical Science*, 7(1), 430–435. <https://doi.org/10.1039/C5SC03327F>

Kanehisa, M. (2019). Toward understanding the origin and evolution of cellular organisms.

Protein Science: A Publication of the Protein Society, 28(11), 1947–1951.

<https://doi.org/10.1002/pro.3715>

- Kanehisa, M., Furumichi, M., Sato, Y., Kawashima, M., & Ishiguro-Watanabe, M. (2023). KEGG for taxonomy-based analysis of pathways and genomes. *Nucleic Acids Research*, 51(D1). <https://doi.org/10.1093/nar/gkac963>
- Kanehisa, M., & Goto, S. (2000). KEGG: Kyoto encyclopedia of genes and genomes. *Nucleic Acids Research*, 28(1). <https://doi.org/10.1093/nar/28.1.27>
- Kang, D. D., Li, F., Kirton, E., Thomas, A., Egan, R., An, H., & Wang, Z. (2019). MetaBAT 2: An adaptive binning algorithm for robust and efficient genome reconstruction from metagenome assemblies. *PeerJ*, 7, e7359. <https://doi.org/10.7717/peerj.7359>
- Kang, J. Y., Chun, J., & Jahng, K. Y. (2013). Flavobacterium aciduliphilum sp. Nov., isolated from freshwater, and emended description of the genus Flavobacterium. *International Journal of Systematic and Evolutionary Microbiology*, 63(Pt_5), 1633–1638. <https://doi.org/10.1099/ijns.0.044495-0>
- Kang, M., Liu, L., & Grossart, H.-P. (2024). Spatio-temporal variations of methane fluxes in sediments of a deep stratified temperate lake. *iScience*, 27(4), 109520. <https://doi.org/10.1016/j.isci.2024.109520>
- Kao, C.-H., & Hsu, W.-H. (2003). A gene cluster involved in pyrimidine reductive catabolism from *Brevibacillus agri* NCHU1002. *Biochemical and Biophysical Research Communications*, 303(3), 848–854. [https://doi.org/10.1016/S0006-291X\(03\)00439-X](https://doi.org/10.1016/S0006-291X(03)00439-X)
- Kappenberg, J., & Fanger, H.-U. (2007). *Sedimenttransportgeschehen in der tidebeeinflussten Elbe, der Deutschen Bucht und in der Nordsee* [Report]. <https://publications.hereon.de/id/25898/>
- Karl, D. M., Beversdorf, L., Björkman, K. M., Church, M. J., Martinez, A., & Delong, E. F. (2008). Aerobic production of methane in the sea. *Nature Geoscience*, 1(7), 473–478. <https://doi.org/10.1038/ngeo234>
- Kasalický, V., Zeng, Y., Piwoz, K., Šimek, K., Kratochvílová, H., & Koblížek, M. (2017). Aerobic Anoxygenic Photosynthesis Is Commonly Present within the Genus Limnohabitans. *Applied and Environmental Microbiology*, 84(1), e02116-17. <https://doi.org/10.1128/AEM.02116-17>

- Kennish, M. J. (2005). Estuaries, Anthropogenic Impacts. In M. L. Schwartz (Ed.), *Encyclopedia of Coastal Science* (pp. 434–436). Springer Netherlands.
https://doi.org/10.1007/1-4020-3880-1_140
- Kerner, M. (2007). Effects of deepening the Elbe Estuary on sediment regime and water quality. *Estuarine, Coastal and Shelf Science*, 75(4), 492–500.
<https://doi.org/10.1016/j.ecss.2007.05.033>
- Khatriwala, S., Tanhua, T., Mikaloff Fletcher, S., Gerber, M., Doney, S. C., Graven, H. D., Gruber, N., McKinley, G. A., Murata, A., Ríos, A. F., & Sabine, C. L. (2013). Global ocean storage of anthropogenic carbon. *Biogeosciences*, 10(4), 2169–2191.
<https://doi.org/10.5194/bg-10-2169-2013>
- Kieft, K., Zhou, Z., & Anantharaman, K. (2020). VIBRANT: Automated recovery, annotation and curation of microbial viruses, and evaluation of viral community function from genomic sequences. *Microbiome*, 8(1), 90. <https://doi.org/10.1186/s40168-020-00867-0>
- Kies, L., Fast, T., Wolfstein, K., & Hoberg, M. (1996). On the role of algae and their exopolymers in the formation of suspended particulate matter in the Elbe estuary (Germany). *Advances in Limnology* 47, 47(1), 93–103.
- Kim, M., Kim, Y.-I., Hwang, J., Choi, K. Y., Kim, C. J., Ryu, Y., Park, J.-E., Park, K.-A., Park, J.-H., Nam, S., Haghipour, N., & Eglinton, T. I. (2020). Influence of Sediment Resuspension on the Biological Pump of the Southwestern East Sea (Japan Sea). *Frontiers in Earth Science*, 8.
<https://www.frontiersin.org/articles/10.3389/feart.2020.00144>
- Kim, S., Kang, I., Seo, J.-H., & Cho, J.-C. (2019). Culturing the ubiquitous freshwater actinobacterial acl lineage by supplying a biochemical ‘helper’ catalase. *The ISME Journal*, 13(9), 2252–2263. <https://doi.org/10.1038/s41396-019-0432-x>
- Klawonn, I., Van den Wyngaert, S., Iversen, M. H., Walles, T. J. W., Flintrop, C. M., Cisternas-Novoa, C., Nejstgaard, J. C., Kagami, M., & Grossart, H.-P. (2023). Fungal parasitism on diatoms alters formation and bio–physical properties of sinking

aggregates. *Communications Biology*, 6(1), Article 1. <https://doi.org/10.1038/s42003-023-04453-6>

LaBrie, R., Lapierre, J.-F., & Maranger, R. (2020). Contrasting Patterns of Labile and Semilabile Dissolved Organic Carbon From Continental Waters to the Open Ocean. *Journal of Geophysical Research: Biogeosciences*, 125(2), e2019JG005300. <https://doi.org/10.1029/2019JG005300>

Laruelle, G. G., Rosentreter, J. A., & Regnier, P. (2023). *Extrapolation based regionalized re-evaluation of the global estuarine surface area*.

<https://eartharxiv.org/repository/view/5086/>

Lasareva, E. V., Parfenova, A. M., Lasareva, E. V., & Parfenova, A. M. (2023). *Influence of Organic Matter on the Transport of Mineral Colloids in the River-Sea Transition Zone*. IntechOpen. <https://doi.org/10.5772/intechopen.110247>

Lee, H.-S., Hur, J., & Shin, H.-S. (2021). Dynamic exchange between particulate and dissolved matter following sequential resuspension of particles from an urban watershed under photo-irradiation. *Environmental Pollution*, 283, 117395. <https://doi.org/10.1016/j.envpol.2021.117395>

Levin, L. A., Boesch, D. F., Covich, A., Dahm, C., Erséus, C., Ewel, K. C., Kneib, R. T., Moldenke, A., Palmer, M. A., Snelgrove, P., Strayer, D., & Weslawski, J. M. (2001). The Function of Marine Critical Transition Zones and the Importance of Sediment Biodiversity. *Ecosystems*, 4(5), 430–451. <https://doi.org/10.1007/s10021-001-0021-4>

Levitan, H. A., Opazo, L. F., Arenas-Uribe, S., Wicki, H., Marchant, F., Florez-Leiva, L., & Avendaño-Herrera, R. (2024). Estimating taxonomic and functional structure along a tropical estuary: Linking metabolic traits and aspects of ecosystem functioning.

Microbiology Spectrum, 12(10), e03886-23. <https://doi.org/10.1128/spectrum.03886-23>

Li, B., Wang, H., Lai, A., Xue, J., Wu, Q., Yu, C., Xie, K., Mao, Z., Li, H., Xing, P., & Wu, Q. L. (2023). Hydrogenotrophic pathway dominates methanogenesis along the river-estuary continuum of the Yangtze River. *Water Research*, 240, 120096.

<https://doi.org/10.1016/j.watres.2023.120096>

Li, H., & Durbin, R. (2009). Fast and accurate short read alignment with Burrows–Wheeler transform. *Bioinformatics*, 25(14), 1754–1760.

<https://doi.org/10.1093/bioinformatics/btp324>

Li, X., Li, Y., Gao, D., Liu, M., & Hou, L. (2022). Methane Production Linked to Organic Matter Molecule and Methanogenic Community in Estuarine Benthic Sediments.

Journal of Geophysical Research: Biogeosciences, 127(12), e2022JG007236.

<https://doi.org/10.1029/2022JG007236>

Li, Y., Fichot, C. G., Geng, L., Scarratt, M. G., & Xie, H. (2020). The Contribution of Methane Photoproduction to the Oceanic Methane Paradox. *Geophysical Research Letters*, 47(14), e2020GL088362. <https://doi.org/10.1029/2020GL088362>

Li, Y., Song, G., Massicotte, P., Yang, F., Li, R., & Xie, H. (2019). Distribution, seasonality, and fluxes of dissolved organic matter in the Pearl River (Zhujiang) estuary, China. *Biogeosciences*, 16(13), 2751–2770. <https://doi.org/10.5194/bg-16-2751-2019>

Li, Y., Wang, D., Chen, Z., Chen, J., Hu, H., & Wang, R. (2021). *Methane Emissions during the Tide Cycle of a Yangtze Estuary Salt Marsh*.

Li, Y., Zhan, L., Chen, L., Zhang, J., Wu, M., & Liu, J. (2021). Spatial and temporal patterns of methane and its influencing factors in the Jiulong River estuary, southeastern China. *Marine Chemistry*, 228, 103909.

<https://doi.org/10.1016/j.marchem.2020.103909>

Lian, Z., Jiang, Z., Huang, X., Liu, S., Zhang, J., & Wu, Y. (2018). Labile and recalcitrant sediment organic carbon pools in the Pearl River Estuary, southern China. *Science of the Total Environment*, 640–641, 1302–1311.

<https://doi.org/10.1016/j.scitotenv.2018.05.389>

Lin, G., Gao, D., Yang, P., Liu, S., Sun, D., & Lin, X. (2024). Editorial: Linking microbial-driven key processes with carbon and nitrogen cycling in estuarine, coastal, and the nearshore areas. *Frontiers in Microbiology*, 15.

<https://doi.org/10.3389/fmicb.2024.1382148>

- Liu, H., Pan, Z., Bai, Y., Xu, S., Wu, Z., Ma, J., Wang, Z., Tian, Z., & Chen, Y. (2024). Methanogens dominate methanotrophs and act as a methane source in aquaculture pond sediments. *Ecotoxicology and Environmental Safety*, 288, 117317. <https://doi.org/10.1016/j.ecoenv.2024.117317>
- Liu, L., Wang, D., Chen, S., Yu, Z., Xu, Y., Li, Y., Ge, Z., & Chen, Z. (2019). Methane Emissions from Estuarine Coastal Wetlands: Implications for Global Change Effect. *Soil Science Society of America Journal*, 83(5), 1368–1377. <https://doi.org/10.2136/sssaj2018.12.0472>
- Liu, S., Kuhn, C., Amatulli, G., Aho, K., Butman, D. E., Allen, G. H., Lin, P., Pan, M., Yamazaki, D., Brinkerhoff, C., Gleason, C., Xia, X., & Raymond, P. A. (2022). The importance of hydrology in routing terrestrial carbon to the atmosphere via global streams and rivers. *Proceedings of the National Academy of Sciences*, 119(11), e2106322119. <https://doi.org/10.1073/pnas.2106322119>
- Liu, Y., Lin, Q., Feng, J., Yang, F., Du, H., Hu, Z., & Wang, H. (2020). Differences in metabolic potential between particle-associated and free-living bacteria along Pearl River Estuary. *Science of The Total Environment*, 728, 138856. <https://doi.org/10.1016/j.scitotenv.2020.138856>
- Logan, B. E., Grossart, H. P., & Simon, M. (1994). Direct observation of phytoplankton, TEP and aggregates on polycarbonate filters using brightfield microscopy. *Journal of Plankton Research*, 16(12), 1811–1815. <https://doi.org/10.1093/plankt/16.12.1811>
- Long, R., & Azam, F. (1996). Abundant protein-containing particles in the sea. *Aquatic Microbial Ecology*, 10, 213–221. <https://doi.org/10.3354/ame010213>
- Longhurst, A. R., & Glen Harrison, W. (1989). The biological pump: Profiles of plankton production and consumption in the upper ocean. *Progress in Oceanography*, 22(1), 47–123. [https://doi.org/10.1016/0079-6611\(89\)90010-4](https://doi.org/10.1016/0079-6611(89)90010-4)
- Lunau, M., Lemke, A., Dellwig, O., & Simon, M. (2006). Physical and biogeochemical controls of microaggregate dynamics in a tidally affected coastal ecosystem. *Limnology and Oceanography*, 51(2), 847–859.

<https://doi.org/10.4319/lo.2006.51.2.0847>

- Lunau, M., Sommer, A., Lemke, A., Grossart, H. P., & Simon, M. (2004). A new sampling device for microaggregates in turbid aquatic systems. *Limnology and Oceanography: Methods*, 2(12), 387–397. <https://doi.org/10.4319/lom.2004.2.387>
- Lupa, B., Hendrickson, E. L., Leigh, J. A., & Whitman, W. B. (2008). Formate-Dependent H₂ Production by the Mesophilic Methanogen *Methanococcus maripaludis*. *Applied and Environmental Microbiology*, 74(21), 6584–6590. <https://doi.org/10.1128/AEM.01455-08>
- Lyons, M. M., & Dobbs, F. C. (2012). Differential utilization of carbon substrates by aggregate-associated and water-associated heterotrophic bacterial communities. *Hydrobiologia*, 686(1), 181–193. <https://doi.org/10.1007/s10750-012-1010-7>
- Macreadie, P. I., Anton, A., Raven, J. A., Beaumont, N., Connolly, R. M., Friess, D. A., Kelleway, J. J., Kennedy, H., Kuwae, T., Lavery, P. S., Lovelock, C. E., Smale, D. A., Apostolaki, E. T., Atwood, T. B., Baldock, J., Bianchi, T. S., Chmura, G. L., Eyre, B. D., Fourqurean, J. W., ... Duarte, C. M. (2019). The future of Blue Carbon science. *Nature Communications*, 10(1), 1–13. <https://doi.org/10.1038/s41467-019-11693-w>
- Madsen, T. V., & Sand-Jensen, K. (1991). Photosynthetic carbon assimilation in aquatic macrophytes. *Aquatic Botany*, 41(1), 5–40. [https://doi.org/10.1016/0304-3770\(91\)90037-6](https://doi.org/10.1016/0304-3770(91)90037-6)
- Mahlstedt, S. A., & Walsh, C. T. (2010). Investigation of Anticapsin Biosynthesis Reveals a Four-Enzyme Pathway to Tetrahydroxyproline in *Bacillus subtilis*. *Biochemistry*, 49(5), 912–923. <https://doi.org/10.1021/bi9021186>
- Mander, G. J., Pierik, A. J., Huber, H., & Hedderich, R. (2004). Two distinct heterodisulfide reductase-like enzymes in the sulfate-reducing archaeon *Archaeoglobus profundus*. *European Journal of Biochemistry*, 271(6), 1106–1116. <https://doi.org/10.1111/j.1432-1033.2004.04013.x>
- Mantoura, R. F. C., & Woodward, E. M. S. (1983). Conservative behaviour of riverine dissolved organic carbon in the Severn Estuary: Chemical and geochemical

implications. *Geochimica et Cosmochimica Acta*, 47(7), 1293–1309.

[https://doi.org/10.1016/0016-7037\(83\)90069-8](https://doi.org/10.1016/0016-7037(83)90069-8)

Mari, X., Beauvais, S., Lemée, R., & Pedrotti, M. L. (2001). Non-Redfield C:N ratio of

transparent exopolymeric particles in the northwestern Mediterranean Sea.

Limnology and Oceanography, 46(7), 1831–1836.

<https://doi.org/10.4319/lo.2001.46.7.1831>

Mari, X., Passow, U., Migon, C., Burd, A. B., & Legendre, L. (2017). Progress in

Oceanography Transparent exopolymer particles: Effects on carbon cycling in the ocean. *Progress in Oceanography*, 151, 13–37.

<https://doi.org/10.1016/j.pocean.2016.11.002>

Mari, X., Torréton, J. P., Bich-Thuy Trinh, C., Bouvier, T., Van Thuoc, C., Lefebvre, J. P., & Ouillon, S. (2012). Aggregation dynamics along a salinity gradient in the Bach Dang estuary, North Vietnam. *Estuarine, Coastal and Shelf Science*, 96(1), 151–158.

<https://doi.org/10.1016/j.ecss.2011.10.028>

Martens, N., Biederick, J., & Schaum, C.-E. (2024). Picophytoplankton prevail year-round in the Elbe estuary. *Plant-Environment Interactions*, 5(5), e70014.

<https://doi.org/10.1002/pei3.70014>

Martens, N., Russnak, V., Woodhouse, J., Grossart, H.-P., & Schaum, C.-E. (2024).

Metabarcoding reveals potentially mixotrophic flagellates and picophytoplankton as key groups of phytoplankton in the Elbe estuary. *Environmental Research*, 252, 119126. <https://doi.org/10.1016/j.envres.2024.119126>

Massicotte, P. (2019). *eemR: Tools for Pre-Processing Emission-Excitation-Matrix (EEM) Fluorescence Data* [Computer software]. <https://CRAN.R-project.org/package=eemR>

Matoušů, A., Rulík, M., Tušer, M., Bednářík, A., Šimek, K., & Bussmann, I. (2018). Methane dynamics in a large river: A case study of the Elbe River. *Aquatic Sciences*, 81(1), 12. <https://doi.org/10.1007/s00027-018-0609-9>

Mayrberger, Jenifer M. (2011). *Studies of genera cytophaga-flavobacterium in context of the soil carbon cycle* [Doctoral, Michigan State University].

<https://doi.org/10.25335/E00M-8N88>

McIlroy, S. J., & Nielsen, P. H. (2014). The Family Saprospiraceae. In E. Rosenberg, E. F. DeLong, S. Lory, E. Stackebrandt, & F. Thompson (Eds.), *The Prokaryotes: Other Major Lineages of Bacteria and The Archaea* (pp. 863–889). Springer.

https://doi.org/10.1007/978-3-642-38954-2_138

McKnight, D. M., Boyer, E. W., Westerhoff, P. K., Doran, P. T., Kulbe, T., & Andersen, D. T. (2001). Spectrofluorometric characterization of dissolved organic matter for indication of precursor organic material and aromaticity. *Limnology and Oceanography*, 46(1), 38–48. <https://doi.org/10.4319/lo.2001.46.1.0038>

Middelboe, M., Søndergaard, M., Letarte, Y., & Borch, N. H. (1995). Attached and free-living bacteria: Production and polymer hydrolysis during a diatom bloom. *Microbial Ecology*, 29(3), 231–248. <https://doi.org/10.1007/BF00164887>

Middelburg, J. J., & Herman, P. M. J. (2007). Organic matter processing in tidal estuaries. *Marine Chemistry*, 106(1), 127–147. <https://doi.org/10.1016/j.marchem.2006.02.007>

Mistry, J., Chuguransky, S., Williams, L., Qureshi, M., Salazar, G. A., Sonnhammer, E. L. L., Tosatto, S. C. E., Paladin, L., Raj, S., Richardson, L. J., Finn, R. D., & Bateman, A. (2021). Pfam: The protein families database in 2021. *Nucleic Acids Research*, 49(D1), D412–D419. <https://doi.org/10.1093/nar/gkaa913>

Mohapatra, B. R. (2024). Genome features and carbohydrate-active enzymes repertoire of a novel *Stenotrophomonas sepilia* Alg010 strain isolated from *Sargassum* seaweed waste. *Data in Brief*, 54, 110533. <https://doi.org/10.1016/j.dib.2024.110533>

Møller, E. F. (2007). Production of dissolved organic carbon by sloppy feeding in the copepods *Acartia tonsa*, *Centropages typicus*, and *Temora longicornis*. *Limnology and Oceanography*, 52(1), 79–84. <https://doi.org/10.4319/lo.2007.52.1.00079>

Møller, E., Thor, P., & Nielsen, T. (2003). Production of DOC by *Calanus finmarchicus*, *C. glacialis* and *C. hyperboreus* through sloppy feeding and leakage from fecal pellets. *Marine Ecology Progress Series*, 262, 185–191. <https://doi.org/10.3354/meps262185>

Moran, M. A., Ferrer-González, F. X., Fu, H., Nowinski, B., Olofsson, M., Powers, M. A.,

- Schreier, J. E., Schroer, W. F., Smith, C. B., & Uchimiya, M. (2022). The Ocean's labile DOC supply chain. *Limnology and Oceanography*, 67(5), 1007–1021.
<https://doi.org/10.1002/lno.12053>
- Morán, X. A. G., Ducklow, H. W., & Erickson, M. (2013). Carbon fluxes through estuarine bacteria reflect coupling with phytoplankton. *Marine Ecology Progress Series*, 489, 75–85. <https://doi.org/10.3354/meps10428>
- Murphy, K. R., Stedmon, C. A., Graeber, D., & Bro, R. (2013). Fluorescence spectroscopy and multi-way techniques. PARAFAC. *Analytical Methods*, 5(23), 6557–6566.
<https://doi.org/10.1039/C3AY41160E>
- Murray, R. H., Erler, D. V., & Eyre, B. D. (2015). Nitrous oxide fluxes in estuarine environments: Response to global change. *Global Change Biology*, 21(9), 3219–3245. <https://doi.org/10.1111/gcb.12923>
- Muthukrishnan, T., Govender, A., Dobretsov, S., & Abed, R. M. M. (2017). Evaluating the reliability of counting bacteria using epifluorescence microscopy. *Journal of Marine Science and Engineering*, 5(1), 4. <https://doi.org/10.3390/JMSE5010004>
- Nayfach, S., Camargo, A. P., Schulz, F., Eloë-Fadrosh, E., Roux, S., & Kyrpides, N. C. (2021). CheckV assesses the quality and completeness of metagenome-assembled viral genomes. *Nature Biotechnology*, 39(5), 578–585.
<https://doi.org/10.1038/s41587-020-00774-7>
- Nercessian, O., Noyes, E., Kalyuzhnaya, M. G., Lidstrom, M. E., & Chistoserdova, L. (2005). Bacterial Populations Active in Metabolism of C1 Compounds in the Sediment of Lake Washington, a Freshwater Lake. *Applied and Environmental Microbiology*, 71(11), 6885–6899. <https://doi.org/10.1128/AEM.71.11.6885-6899.2005>
- Nguyen, T. T. H., Zakem, E. J., Ebrahimi, A., Schwartzman, J., Caglar, T., Amarnath, K., Alcolombri, U., Peaudecerf, F. J., Hwa, T., Stocker, R., Cordero, O. X., & Levine, N. M. (2022). Microbes contribute to setting the ocean carbon flux by altering the fate of sinking particulates. *Nature Communications*, 13(1), 1657.
<https://doi.org/10.1038/s41467-022-29297-2>

- Norbisrath, M., Pätsch, J., Dähnke, K., Sanders, T., Schulz, G., van Beusekom, J. E. E., & Thomas, H. (2022). Metabolic alkalinity release from large port facilities (Hamburg, Germany) and impact on coastal carbon storage. *Biogeosciences*, 19(22), 5151–5165. <https://doi.org/10.5194/bg-19-5151-2022>
- Norland, S. (1993). The Relationship Between Biomass and Volume of Bacteria. In P. F. Kemp, B. F. Sherr, E. B. Sherr, & J. J. Cole (Eds.), *Handbook of Methods in Aquatic Microbial Ecology* (pp. 303–307). Taylor & Francis Group.
- Nurk, S., Meleshko, D., Korobeynikov, A., & Pevzner, P. A. (2017). metaSPAdes: A new versatile metagenomic assembler. *Genome Research*, 27(5), 824. <https://doi.org/10.1101/GR.213959.116>
- O'Boyle, S., & Silke, J. (2010). A review of phytoplankton ecology in estuarine and coastal waters around Ireland. *Journal of Plankton Research*, 32(1), 99–118. <https://doi.org/10.1093/plankt/fbp097>
- O'Connor, J. A., Erler, D. V., Ferguson, A., & Maher, D. T. (2022). The tidal freshwater river zone: Physical properties and biogeochemical contribution to estuarine hypoxia and acidification - The “hydrologic switch.” *Estuarine, Coastal and Shelf Science*, 268, 107786. <https://doi.org/10.1016/j.ecss.2022.107786>
- Olm, M. R., Brown, C. T., Brooks, B., & Banfield, J. F. (2017). dRep: A tool for fast and accurate genomic comparisons that enables improved genome recovery from metagenomes through de-replication. *The ISME Journal* 2017 11:12, 11(12), 2864–2868. <https://doi.org/10.1038/ismej.2017.126>
- Olofsson, M., Ferrer-González, F. X., Uchimiya, M., Schreier, J. E., Holderman, N. R., Smith, C. B., Edison, A. S., & Moran, M. A. (2022). Growth-stage-related shifts in diatom endometabolome composition set the stage for bacterial heterotrophy. *ISME Communications*, 2(1), 28. <https://doi.org/10.1038/s43705-022-00116-5>
- Paczkowska, J., Rowe, O. F., Figueroa, D., & Andersson, A. (2019). Drivers of phytoplankton production and community structure in nutrient-poor estuaries receiving terrestrial organic inflow. *Marine Environmental Research*, 151, 104778.

<https://doi.org/10.1016/j.marenvres.2019.104778>

Painchaud, J., Therriault, J., & Legendre, L. (1995). Assessment of Salinity-Related Mortality of Freshwater Bacteria in the Saint Lawrence Estuary. *Applied and Environmental Microbiology*, 61(1), 205–208.

Painter, S. C., Lapworth, D. J., Woodward, E. M. S., Kroeger, S., Evans, C. D., Mayor, D. J., & Sanders, R. J. (2018). Terrestrial dissolved organic matter distribution in the North Sea. *Science of The Total Environment*, 630, 630–647.

<https://doi.org/10.1016/j.scitotenv.2018.02.237>

Paoli, L., Ruscheweyh, H.-J., Forneris, C. C., Hubrich, F., Kautsar, S., Bhushan, A., Lotti, A., Clayssen, Q., Salazar, G., Milanese, A., Carlström, C. I., Papadopoulou, C., Gehrig, D., Karasikov, M., Mustafa, H., Larralde, M., Carroll, L. M., Sánchez, P., Zayed, A. A., ... Sunagawa, S. (2022). Biosynthetic potential of the global ocean microbiome. *Nature*, 607(7917), 111–118. <https://doi.org/10.1038/s41586-022-04862-3>

Papenmeier, S., Schrottke, K., & Bartholomä, A. (2014). Over time and space changing characteristics of estuarine suspended particles in the German Weser and Elbe estuaries. *Journal of Sea Research*, 85, 104–115.

<https://doi.org/10.1016/j.seares.2013.03.010>

Park, S., Park, J., Yoo, K.-C., Yoo, J., Kim, K., Jo, N., Jang, H.-K., Kim, J., Kim, J., Kim, J., & Lee, S.-H. (2021). Seasonal Variations in the Biochemical Compositions of Phytoplankton and Transparent Exopolymer Particles (TEPs) at Jang Bogo Station (Terra Nova Bay, Ross Sea), 2017–2018. *Water*, 13(16), Article 16.

<https://doi.org/10.3390/w13162173>

Parks, D. H., Chuvochina, M., Waite, D. W., Rinke, C., Skarshewski, A., Chaumeil, P.-A., & Hugenholtz, P. (2018). A standardized bacterial taxonomy based on genome phylogeny substantially revises the tree of life. *Nature Biotechnology*, 36(10), 996–1004. <https://doi.org/10.1038/nbt.4229>

Passow, U. (2002). Transparent exopolymer particles (TEP) in aquatic environments. *Progress in Oceanography*, 55(3–4), 287–333. <https://doi.org/10.1016/S0079->

6611(02)00138-6

- Passow, U., & De La Rocha, C. L. (2006). Accumulation of mineral ballast on organic aggregates: MINERAL BALLAST AND ORGANIC AGGREGATES. *Global Biogeochemical Cycles*, 20(1), n/a-n/a. <https://doi.org/10.1029/2005GB002579>
- Paysan-Lafosse, T., Andreeva, A., Blum, M., Chuguransky, S. R., Grego, T., Pinto, B. L., Salazar, G. A., Bileschi, M. L., Llinares-López, F., Meng-Papaxanthos, L., Colwell, L. J., Grishin, N. V., Schaeffer, R. D., Clementel, D., Tosatto, S. C. E., Sonnhammer, E., Wood, V., & Bateman, A. (2025). The Pfam protein families database: Embracing AI/ML. *Nucleic Acids Research*, 53(D1), D523–D534.
<https://doi.org/10.1093/nar/gkae997>
- Pein, J., Eisele, A., Sanders, T., Daewel, U., Stanev, E. V., van Beusekom, J. E. E., Staneva, J., & Schrum, C. (2021). Seasonal Stratification and Biogeochemical Turnover in the Freshwater Reach of a Partially Mixed Dredged Estuary. *Frontiers in Marine Science*, 8. <https://www.frontiersin.org/articles/10.3389/fmars.2021.623714>
- Petersen, W., Schroeder, F., & Bockelmann, F.-D. (2011). FerryBox—Application of continuous water quality observations along transects in the North Sea. *Ocean Dynamics*, 61(10), 1541–1554. <https://doi.org/10.1007/s10236-011-0445-0>
- Pierce, E., Becker, D. F., & Ragsdale, S. W. (2010). Identification and Characterization of Oxalate Oxidoreductase, a Novel Thiamine Pyrophosphate-dependent 2-Oxoacid Oxidoreductase That Enables Anaerobic Growth on Oxalate *. *Journal of Biological Chemistry*, 285(52), 40515–40524. <https://doi.org/10.1074/jbc.M110.155739>
- Pitt, A., Schmidt, J., Koll, U., & Hahn, M. W. (2019). Aquirufa antheringensis gen. Nov., sp. Nov. And Aquirufa nivalisilvae sp. Nov., representing a new genus of widespread freshwater bacteria. *International Journal of Systematic and Evolutionary Microbiology*, 69(9), 2739–2749. <https://doi.org/10.1099/ijsem.0.003554>
- Ploug, H., Zimmermann-Timm, H., & Schweitzer, B. (2002). Microbial communities and respiration on aggregates in the Elbe Estuary, Germany. *Aquatic Microbial Ecology*, 27(3), 241–248. <https://doi.org/10.3354/ame027241>

- Poffenbarger, H. J., Needelman, B. A., & Megonigal, J. P. (2011). Salinity Influence on Methane Emissions from Tidal Marshes. *Wetlands*, 31(5), 831–842.
<https://doi.org/10.1007/s13157-011-0197-0>
- Rackley, S. A. (2010). Ocean Storage. *Carbon Capture and Storage*, 267–286.
<https://doi.org/10.1016/b978-1-85617-636-1.00012-2>
- Ramond, P., Galand, P. E., & Logares, R. (2025). Microbial functional diversity and redundancy: Moving forward. *FEMS Microbiology Reviews*, 49, fuae031.
<https://doi.org/10.1093/femsre/fuae031>
- Ransom, B., Shea, K. F., Burkett, P. J., Bennett, R. H., & Baerwald, R. (1998). Comparison of pelagic and nepheloid layer marine snow: Implications for carbon cycling. *Marine Geology*, 150(1–4), 39–50. [https://doi.org/10.1016/S0025-3227\(98\)00052-8](https://doi.org/10.1016/S0025-3227(98)00052-8)
- Raymond, J., Siefert, J. L., Staples, C. R., & Blankenship, R. E. (2004). The Natural History of Nitrogen Fixation. *Molecular Biology and Evolution*, 21(3), 541–554.
<https://doi.org/10.1093/molbev/msh047>
- Ren, L., Jensen, K., Porada, P., & Mueller, P. (2022). Biota-mediated carbon cycling—A synthesis of biotic-interaction controls on blue carbon. *Ecology Letters*, 25(2), 521–540. <https://doi.org/10.1111/ele.13940>
- Rewrie, L. C. V., Voynova, Y. G., van Beusekom, J. E. E., Sanders, T., Körtzinger, A., Brix, H., Ollesch, G., & Baschek, B. (2023). Significant shifts in inorganic carbon and ecosystem state in a temperate estuary (1985–2018). *Limnology and Oceanography*, n/a(n/a). <https://doi.org/10.1002/lo.12395>
- Reynolds, C. S., & Descy, J.-P. (1996). The production, biomass and structure of phytoplankton in large rivers. *Large Rivers*, 10(1–4), 161–187.
<https://doi.org/10.1127/lr/10/1996/161>
- Rieck, A., Herlemann, D. P. R., Jürgens, K., & Grossart, H. P. (2015). Particle-associated differ from free-living bacteria in surface waters of the baltic sea. *Frontiers in Microbiology*, 6(DEC). <https://doi.org/10.3389/fmicb.2015.01297>
- Riemann, L., Rahav, E., Passow, U., Grossart, H.-P., de Beer, D., Klawonn, I., Eichner, M.,

- Benavides, M., & Bar-Zeev, E. (2022). Planktonic Aggregates as Hotspots for Heterotrophic Diazotrophy: The Plot Thickens. *Frontiers in Microbiology*, 13. <https://doi.org/10.3389/fmicb.2022.875050>
- Rolinski, S. (1999). On the dynamics of suspended matter transport in the tidal river Elbe: Description and results of a Lagrangian model. *Journal of Geophysical Research: Oceans*, 104(C11), 26043–26057. <https://doi.org/10.1029/1999JC900230>
- Rösel, S., Allgaier, M., & Grossart, H.-P. (2012). Long-Term Characterization of Free-Living and Particle-Associated Bacterial Communities in Lake Tiefwaren Reveals Distinct Seasonal Patterns. *Microbial Ecology*, 64(3), 571–583. <https://doi.org/10.1007/s00248-012-0049-3>
- Rösel, S., & Grossart, H.-P. (2012). Contrasting dynamics in activity and community composition of free-living and particle-associated bacteria in spring. *Aquatic Microbial Ecology*, 66(2), 169–181. <https://doi.org/10.3354/ame01568>
- Roux, P., Siano, R., Collin, K., Bilien, G., Sinquin, C., Marchand, L., Zykwinska, A., Delbarre-Ladrat, C., & Schapira, M. (2021). Bacteria enhance the production of extracellular polymeric substances by the green dinoflagellate *Lepidodinium chlorophorum*. *Scientific Reports*, 11(1), 4795. <https://doi.org/10.1038/s41598-021-84253-2>
- Ruscheweyh, H.-J., Milanese, A., Paoli, L., Karcher, N., Clayssen, Q., Keller, M. I., Wirbel, J., Bork, P., Mende, D. R., Zeller, G., & Sunagawa, S. (2022). Cultivation-independent genomes greatly expand taxonomic-profiling capabilities of mOTUs across various environments. *Microbiome*, 10(1), 212. <https://doi.org/10.1186/s40168-022-01410-z>
- Sá, A. K. D. S., Feitosa, F. A. N., Cutrim, M. V. J., Flores-Montes, M. J., dos S. Costa, D., & Cavalcanti, L. F. (2023). Phytoplankton community dynamics in response to seawater intrusion in a tropical macrotidal river-estuary continuum. *Hydrobiologia*, 850(20), 4351–4383. <https://doi.org/10.1007/s10750-022-04851-7>
- Sanders, T., Heineke, M., Götz, F., Russnak, V., Husmann, E., Dähnke, K., Schöl, A., Große, F., & Voynova, Y. G. (2023). Increasing of oxygen minimum events in a

temperate estuary caused by warming and reduced discharge (EGU23-13978).

EGU23. Copernicus Meetings. <https://doi.org/10.5194/egusphere-egu23-13978>

Sanders, T., Schöl, A., & Dähnke, K. (2018). Hot Spots of Nitrification in the Elbe Estuary and Their Impact on Nitrate Regeneration. *Estuaries and Coasts*, 41(1), 128–138. <https://doi.org/10.1007/s12237-017-0264-8>

Santoro, A. (2010). Microbial nitrogen cycling at the saltwater–freshwater interface. *Hydrogeology Journal*, 18, 187–202. <https://doi.org/10.1007/s10040-009-0526-z>

Santos, A. L., Oliveira, V., Baptista, I., Henriques, I., Gomes, N. C. M., Almeida, A., Correia, A., & Cunha, A. (2012). Effects of UV-B Radiation on the Structural and Physiological Diversity of Bacterioneuston and Bacterioplankton. *Applied and Environmental Microbiology*, 78(6), 2066–2069. <https://doi.org/10.1128/AEM.06344-11>

Santos Correa, S., Schultz, J., Lauersen, K. J., & Soares Rosado, A. (2022). Natural carbon fixation and advances in synthetic engineering for redesigning and creating new fixation pathways. *Journal of Advanced Research*, 47, 75–92. <https://doi.org/10.1016/j.jare.2022.07.011>

Sanyal, P., Ray, R., Paul, M., Gupta, V. K., Acharya, A., Bakshi, S., Jana, T. K., & Mukhopadhyay, S. K. (2020). Assessing the Dynamics of Dissolved Organic Matter (DOM) in the Coastal Environments Dominated by Mangroves, Indian Sundarbans. *Frontiers in Earth Science*, 8.

<https://www.frontiersin.org/articles/10.3389/feart.2020.00218>

Savenije, H. H. G. (2005). *Salinity and Tides in Alluvial Estuaries* (1st ed.). Elsevier. <https://shop.elsevier.com/books/salinity-and-tides-in-alluvial-estuaries/savenije/978-0-444-52107-1>

Sawana, A., Adeolu, M., & Gupta, R. S. (2014). Molecular signatures and phylogenomic analysis of the genus Burkholderia: Proposal for division of this genus into the emended genus Burkholderia containing pathogenic organisms and a new genus Paraburkholderia gen. nov. harboring environmental species. *Frontiers in Genetics*, 5. <https://doi.org/10.3389/fgene.2014.00429>

- Schoer, J. H. (1990). Determination of the origin of suspended matter and sediments in the Elbe estuary using natural tracers. *Estuaries*, 13(2), 161–172.
<https://doi.org/10.2307/1351585>
- Schöneich-Argent, R. I., Dau, K., & Freund, H. (2020). Wasting the North Sea? – A field-based assessment of anthropogenic macrolitter loads and emission rates of three German tributaries. *Environmental Pollution*, 263, 114367.
<https://doi.org/10.1016/j.envpol.2020.114367>
- Schröder, M., & Siedler, G. (1989). Turbulent momentum and salt transport in the mixing zone of the Elbe estuary. *Estuarine, Coastal and Shelf Science*, 28(6), 615–638.
[https://doi.org/10.1016/0272-7714\(89\)90050-4](https://doi.org/10.1016/0272-7714(89)90050-4)
- Seemann, T. (2013). *barrnap 0.9: Rapid ribosomal RNA prediction* [Perl].
<https://github.com/tseemann/barrnap> (Original work published 2013)
- Serra Moncadas, L., Hofer, C., Bulzu, P.-A., Pernthaler, J., & Andrei, A.-S. (2024). Freshwater genome-reduced bacteria exhibit pervasive episodes of adaptive stasis. *Nature Communications*, 15(1), 3421. <https://doi.org/10.1038/s41467-024-47767-7>
- Shi, X., Su, Z., Tao, X., Zhou, X., Zhao, J., Wang, R., & Qin, J. (2023). Fe controls the reproduction of zoogloea and sludge bulking in oil-in-iron wastewater. *Frontiers in Water*, 5. <https://doi.org/10.3389/frwa.2023.1289276>
- Shutova, Y., Baker, A., Bridgeman, J., & Henderson, R. K. (2014). Spectroscopic characterisation of dissolved organic matter changes in drinking water treatment: From PARAFAC analysis to online monitoring wavelengths. *Water Research*, 54, 159–169. <https://doi.org/10.1016/j.watres.2014.01.053>
- Silva, L., Calleja, M. L., Huete-Stauffer, T. M., Ivetic, S., Ansari, M. I., Viegas, M., & Morán, X. A. G. (2019). Low Abundances but High Growth Rates of Coastal Heterotrophic Bacteria in the Red Sea. *Frontiers in Microbiology*, 9, 3244.
<https://doi.org/10.3389/fmicb.2018.03244>
- Silva, R. N., Steindorff, A. S., & Monteiro, V. N. (2014). Metabolic Diversity of *Trichoderma*. In V. K. Gupta, M. Schmoll, A. Herrera-Estrella, R. S. Upadhyay, I. Druzhinina, & M.

G. Tuohy (Eds.), *Biotechnology and Biology of Trichoderma* (pp. 363–376). Elsevier.

<https://doi.org/10.1016/B978-0-444-59576-8.00027-8>

Simon, M., Grossart, H. P., Schweitzer, B., & Ploug, H. (2002). Microbial ecology of organic aggregates in aquatic ecosystems. *Aquatic Microbial Ecology*, 28(2), 175–211.

<https://doi.org/10.3354/ame028175>

Simon, M., Scheuner, C., Meier-Kolthoff, J. P., Brinkhoff, T., Wagner-Döbler, I., Ulrich, M., Klenk, H.-P., Schomburg, D., Petersen, J., & Göker, M. (2017). Phylogenomics of Rhodobacteraceae reveals evolutionary adaptation to marine and non-marine habitats. *The ISME Journal*, 11(6), 1483–1499.

<https://doi.org/10.1038/ismej.2016.198>

Sohn, J. H., Kwon, K. K., Kang, J.-H., Jung, H.-B., & Kim, S.-J. (2004). Novosphingobium pentaromativorans sp. Nov., a high-molecular-mass polycyclic aromatic hydrocarbon-degrading bacterium isolated from estuarine sediment. *International Journal of Systematic and Evolutionary Microbiology*, 54(5), 1483–1487.

<https://doi.org/10.1099/ij.s.0.02945-0>

Soued, C., Bogard, M. J., Finlay, K., Bortolotti, L. E., Leavitt, P. R., Badiou, P., Knox, S. H., Jensen, S., Mueller, P., Lee, S. C., Ng, D., Wissel, B., Chan, C. N., Page, B., & Kowal, P. (2024). Salinity causes widespread restriction of methane emissions from small inland waters. *Nature Communications*, 15(1), 717.

<https://doi.org/10.1038/s41467-024-44715-3>

Spencer, R. G. M., Ahad, J. M. E., Baker, A., Cowie, G. L., Ganeshram, R., Upstill-Goddard, R. C., & Uher, G. (2007). The estuarine mixing behaviour of peatland derived dissolved organic carbon and its relationship to chromophoric dissolved organic matter in two North Sea estuaries (U.K.). *Estuarine, Coastal and Shelf Science*, 74(1), 131–144. <https://doi.org/10.1016/j.ecss.2007.03.032>

Stanev, E. V., Brink-Spalink, G., & Wolff, J.-O. (2007). Sediment dynamics in tidally dominated environments controlled by transport and turbulence: A case study for the East Frisian Wadden Sea. *Journal of Geophysical Research: Oceans*, 112(C4).

<https://doi.org/10.1029/2005JC003045>

Statham, P. J. (2012). Nutrients in estuaries—An overview and the potential impacts of climate change. *Science of The Total Environment*, 434, 213–227.

<https://doi.org/10.1016/j.scitotenv.2011.09.088>

Stedmon, C. A., & Bro, R. (2008). Characterizing dissolved organic matter fluorescence with parallel factor analysis: A tutorial. *Limnology and Oceanography: Methods*, 6(11), 572–579. <https://doi.org/10.4319/lom.2008.6.572>

Steinsdóttir, H. G. R., Schauberger, C., Mhatre, S., Thamdrup, B., & Bristow, L. A. (2022). Aerobic and anaerobic methane oxidation in a seasonally anoxic basin. *Limnology and Oceanography*, 67(6), 1257–1273. <https://doi.org/10.1002/limo.12074>

Stoderegger, K., & Herndl, G. J. (1998). Production and release of bacterial capsular material and its subsequent utilization by marine bacterioplankton. *Limnology and Oceanography*, 43(5), 877–884. <https://doi.org/10.4319/lo.1998.43.5.0877>

Street, J. H., & Paytan, A. (2005). Iron, phytoplankton growth, and the carbon cycle. *Metal Ions in Biological Systems*, 43, 153–193. <https://doi.org/10.1201/9780824751999.ch7>

Sugie, K., Fujiwara, A., Nishino, S., Kameyama, S., & Harada, N. (2020). Impacts of Temperature, CO₂, and Salinity on Phytoplankton Community Composition in the Western Arctic Ocean. *Frontiers in Marine Science*, 6, 821.

<https://doi.org/10.3389/fmars.2019.00821>

Sun, X., Li, Z., Ding, X., Ji, G., Wang, L., Gao, X., Chang, Q., & Zhu, L. (2022). Effects of Algal Blooms on Phytoplankton Composition and Hypoxia in Coastal Waters of the Northern Yellow Sea, China. *Frontiers in Marine Science*, 9.

<https://doi.org/10.3389/fmars.2022.897418>

Suttle, D. P., Bugg, B. Y., Winkler, J. K., & Kanalas, J. J. (1988). Molecular cloning and nucleotide sequence for the complete coding region of human UMP synthase. *Proceedings of the National Academy of Sciences*, 85(6), 1754–1758.

<https://doi.org/10.1073/pnas.85.6.1754>

Tanaka, K., Kuma, K., Hamasaki, K., & Yamashita, Y. (2014). Accumulation of humic-like

fluorescent dissolved organic matter in the Japan Sea. *Scientific Reports*, 4(1), 5292.

<https://doi.org/10.1038/srep05292>

Taubert, M., Grob, C., Crombie, A., Howat, A. M., Burns, O. J., Weber, M., Lott, C., Kaster,

A.-K., Vollmers, J., Jehmlich, N., von Bergen, M., Chen, Y., & Murrell, J. C. (2019).

Communal metabolism by Methylococcaceae and Methylophilaceae is driving rapid aerobic methane oxidation in sediments of a shallow seep near Elba, Italy.

Environmental Microbiology, 21(10), 3780–3795. <https://doi.org/10.1111/1462-2920.14728>

Tee, H. S., Waite, D., Lear, G., & Handley, K. M. (2021). Microbial river-to-sea continuum:

Gradients in benthic and planktonic diversity, osmoregulation and nutrient cycling.

Microbiome, 9(1), 190. <https://doi.org/10.1186/s40168-021-01145-3>

Teikari, J. E., Fewer, D. P., Shrestha, R., Hou, S., Leikoski, N., Mäkelä, M., Simojoki, A.,

Hess, W. R., & Sivonen, K. (2018). Strains of the toxic and bloom-forming Nodularia spumigena (cyanobacteria) can degrade methylphosphonate and release methane.

The ISME Journal, 12(6), 1619–1630. <https://doi.org/10.1038/s41396-018-0056-6>

Telesh, I. V., & Khlebovich, V. V. (2010). Principal processes within the estuarine salinity

gradient: A review. *Marine Pollution Bulletin*, 61(4), 149–155.

<https://doi.org/10.1016/j.marpolbul.2010.02.008>

Tersteegen, A., Linder, D., Thauer, R. K., & Hedderich, R. (1997). Structures and Functions

of Four Anabolic 2-Oxoacid Oxidoreductases in *Methanobacterium*

Thermoautotrophicum. *European Journal of Biochemistry*, 244(3), 862–868.

<https://doi.org/10.1111/j.1432-1033.1997.00862.x>

Thornton, D. C. O. (2014). Dissolved organic matter (DOM) release by phytoplankton in the

contemporary and future ocean. *European Journal of Phycology*, 49(1), 20–46.

<https://doi.org/10.1080/09670262.2013.875596>

Thornton, D. C. O. (2018). Coomassie Stainable Particles (CSP): Protein containing

exopolymer particles in the ocean. *Frontiers in Marine Science*, 5(JUN), 206.

<https://doi.org/10.3389/fmars.2018.00206>

- Tobias-Hünefeldt, S. P., van Beusekom, J. E. E., Russnak, V., Dähnke, K., Streit, W. R., & Grossart, H.-P. (2024). Seasonality, rather than estuarine gradient or particle suspension/sinking dynamics, determines estuarine carbon distributions. *Science of The Total Environment*, 926, 171962. <https://doi.org/10.1016/j.scitotenv.2024.171962>
- Tobias-Hünefeldt, S. P., Wenley, J., Baltar, F., & Morales, S. E. (2020). Ecological drivers switch from bottom-up to top-down during model microbial community successions. *ISME Journal*, 1–13. <https://doi.org/10.1038/s41396-020-00833-6>
- Tobias-Hünefeldt, S. P., Wing, S. R., Espinel-Velasco, N., Baltar, F., & Morales, S. E. (2019). Depth and location influence prokaryotic and eukaryotic microbial community structure in New Zealand fjords. *Science of The Total Environment*, 693, 133507. <https://doi.org/10.1016/j.scitotenv.2019.07.313>
- Tranvik, L. J., Downing, J. A., Cotner, J. B., Loiselle, S. A., Striegl, R. G., Ballatore, T. J., Dillon, P., Finlay, K., Fortino, K., Knoll, L. B., Kortelainen, P. L., Kutser, T., Larsen, S., Laurion, I., Leech, D. M., Leigh McCallister, S., McKnight, D. M., Melack, J. M., Overholt, E., ... Weyhenmeyer, G. A. (2009). Lakes and reservoirs as regulators of carbon cycling and climate. *Limnology and Oceanography*, 54(6 PART 2), 2298–2314. https://doi.org/10.4319/lo.2009.54.6_part_2.2298
- Trevathan-Tackett, S. M., Sherman, C. D. H., Huggett, M. J., Campbell, A. H., Laverock, B., Hurtado-McCormick, V., Seymour, J. R., Firl, A., Messer, L. F., Ainsworth, T. D., Negandhi, K. L., Daffonchio, D., Egan, S., Engelen, A. H., Fusi, M., Thomas, T., Vann, L., Hernandez-Agreda, A., Gan, H. M., ... Macreadie, P. I. (2019). A horizon scan of priorities for coastal marine microbiome research. *Nature Ecology and Evolution*, 3(11), 1509–1520. <https://doi.org/10.1038/s41559-019-0999-7>
- Trgovec-Greif, L., Hellinger, H.-J., Mainguy, J., Pfundner, A., Frishman, D., Kiening, M., Webster, N. S., Laffy, P. W., Feichtinger, M., & Rattei, T. (2024). VOGDB—Database of Virus Orthologous Groups. *Viruses*, 16(8), 1191. <https://doi.org/10.3390/v16081191>
- Urvoy, M., Gourmelon, M., Serghine, J., Rabiller, E., L'Helguen, S., & Labry, C. (2022). Free-

living and particle-attached bacterial community composition, assembly processes and determinants across spatiotemporal scales in a macrotidal temperate estuary.

Scientific Reports, 12(1), 13897. <https://doi.org/10.1038/s41598-022-18274-w>

van Beusekom, J., Fehling, D., & Bold, S. (2021). *Pelagic oxygen consumption rates in the Elbe estuary: Proxies and spatial patterns*.

van Hoek, W. J., Wang, J., Vilmin, L., Beusen, A. H. W., Mogollón, J. M., Müller, G., Pika, P. A., Liu, X., Langeveld, J. J., Bouwman, A. F., & Middelburg, J. J. (2021). Exploring Spatially Explicit Changes in Carbon Budgets of Global River Basins during the 20th Century. *Environmental Science & Technology*, 55(24), 16757–16769.
<https://doi.org/10.1021/acs.est.1c04605>

Vance, J. M., Currie, K., Suanda, S. H., & Law, C. S. (2024). Drivers of seasonal to decadal mixed layer carbon cycle variability in subantarctic water in the Munida Time Series. *Frontiers in Marine Science*, 11. <https://doi.org/10.3389/fmars.2024.1309560>

Vorholt, J. A., Vaupel, M., & Thauer, R. K. (1996). A Polyferredoxin with Eight [4Fe–4S] Clusters as a Subunit of Molybdenum Formylmethanofuran Dehydrogenase from Methanosaarcina barkeri. *European Journal of Biochemistry*, 236(1), 309–317.
<https://doi.org/10.1111/j.1432-1033.1996.t01-1-00309.x>

Walker, S. A., Amon, R. M. W., & Stedmon, C. A. (2013). Variations in high-latitude riverine fluorescent dissolved organic matter: A comparison of large Arctic rivers. *Journal of Geophysical Research: Biogeosciences*, 118(4), 1689–1702.
<https://doi.org/10.1002/2013JG002320>

Wan, W., Grossart, H.-P., He, D., Liu, W., Wang, S., & Yang, Y. (2023). Differentiation strategies for planktonic bacteria and eukaryotes in response to aggravated algal blooms in urban lakes. *iMeta*, 2(1), e84. <https://doi.org/10.1002/imt2.84>

Wang, F.-Q., Bartosik, D., Sidhu, C., Siebers, R., Lu, D.-C., Trautwein-Schult, A., Becher, D., Huettel, B., Rick, J., Kirstein, I. V., Wiltshire, K. H., Schweder, T., Fuchs, B. M., Bengtsson, M. M., Teeling, H., & Amann, R. I. (2024). Particle-attached bacteria act as gatekeepers in the decomposition of complex phytoplankton polysaccharides.

Microbiome, 12(1), 32. <https://doi.org/10.1186/s40168-024-01757-5>

Wang, X., & Andutta, F. (2013). *Sediment Transport Dynamics in Ports, Estuaries and Other Coastal Environments* (pp. 3–35). <https://doi.org/10.5772/51022>

Weishaar, J. L., Aiken, G. R., Bergamaschi, B. A., Fram, M. S., Fujii, R., & Mopper, K. (2003). Evaluation of specific ultraviolet absorbance as an indicator of the chemical composition and reactivity of dissolved organic carbon. *Environmental Science and Technology*, 37(20), 4702–4708. <https://doi.org/10.1021/es030360x>

Wells, J. T. (1995). Chapter 6 Tide-Dominated Estuaries and Tidal Rivers. In G. M. E. Perillo (Ed.), *Developments in Sedimentology* (Vol. 53, pp. 179–205). Elsevier.
[https://doi.org/10.1016/S0070-4571\(05\)80026-3](https://doi.org/10.1016/S0070-4571(05)80026-3)

Wells, N. S., Chen, J.-J., Maher, D. T., Huang, P., Erler, D. V., Hipsey, M., & Eyre, B. D. (2020). Changing sediment and surface water processes increase CH₄ emissions from human-impacted estuaries. *Geochimica et Cosmochimica Acta*, 280, 130–147.
<https://doi.org/10.1016/j.gca.2020.04.020>

Whitman, W. (2015). Emticicia. In *Bergey's Manual of Systematics of Archaea and Bacteria* (pp. 1–2). John Wiley & Sons, Ltd.
<https://doi.org/10.1002/9781118960608.gbm00264>

Wickham, H. (2016). *ggplot2: Elegant Graphics for Data Analysis*. Springer-Verlag New York. <http://ggplot2.org>

Williams, J. R., & Giering, S. L. C. (2022). In Situ Particle Measurements Deemphasize the Role of Size in Governing the Sinking Velocity of Marine Particles. *Geophysical Research Letters*, 49(21), e2022GL099563. <https://doi.org/10.1029/2022GL099563>

Winterscheid, A., Reiss, M., & Shaikh, S. (2019). *About the analysis of sedimentation dynamics in an estuarine waterway and its implications on sediment management concepts*. 681–690. <https://doi.org/10.3850/38WC092019-0902>

Wörner, U., Zimmermann-Timm, H., & Kausch, H. (2002). Aggregate-Associated Bacteria and Heterotrophic Flagellates in the River Elbe—Their Relative Significance along the Longitudinal Profile from km 46 to km 583. *International Review of Hydrobiology*,

87(2–3), 255–266. [https://doi.org/10.1002/1522-2632\(200205\)87:2/3<255::AID-IROH255>3.0.CO;2-R](https://doi.org/10.1002/1522-2632(200205)87:2/3<255::AID-IROH255>3.0.CO;2-R)

Xie, H., & Zafiriou, O. C. (2009). Evidence for significant photochemical production of carbon monoxide by particles in coastal and oligotrophic marine waters. *Geophysical Research Letters*, 36(23). <https://doi.org/10.1029/2009GL041158>

Xiong, Y. J., & Liu, J. F. (2018). Can Saltwater Intrusion Affect a Phytoplankton Community and Its Net Primary Production? A Study Based on Satellite and Field Observations. *Estuaries and Coasts*, 41(8), 2317–2330.

Yamada, Y., Tomaru, Y., Fukuda, H., & Nagata, T. (2018). Aggregate Formation During the Viral Lysis of a Marine Diatom. *Frontiers in Marine Science*, 5. <https://doi.org/10.3389/fmars.2018.00167>

Yan, C., Sheng, Y., Ju, M., Ding, C., Li, Q., Luo, Z., Ding, M., & Nie, M. (2020). Relationship between the characterization of natural colloids and metal elements in surface waters. *Environmental Science and Pollution Research*, 27(25), 31872–31883. <https://doi.org/10.1007/s11356-020-09500-x>

Yao, J., Chen, Z., Ge, J., & Zhang, W. (2024). Source-to-sink pathways of dissolved organic carbon in the river–estuary–ocean continuum: A modeling investigation. *Biogeosciences*, 21(23), 5435–5455. <https://doi.org/10.5194/bg-21-5435-2024>

Yuan, Y., Barrett, D., Zhang, Y., Kahne, D., Sliz, P., & Walker, S. (2007). Crystal structure of a peptidoglycan glycosyltransferase suggests a model for processive glycan chain synthesis. *Proceedings of the National Academy of Sciences*, 104(13), 5348–5353. <https://doi.org/10.1073/pnas.0701160104>

Yuan, Y., Li, X., Xie, Z., Xue, L., Yang, B., Zhao, W., & Craft, C. B. (2022). Annual Lateral Organic Carbon Exchange Between Salt Marsh and Adjacent Water: A Case Study of East Headland Marshes at the Yangtze Estuary. *Frontiers in Marine Science*, 8. <https://www.frontiersin.org/articles/10.3389/fmars.2021.809618>

Zander, F., Comans, R. N. J., & Gebert, J. (2023). Linking patterns of physical and chemical organic matter fractions to its lability in sediments of the tidal Elbe river. *Applied*

Geochemistry, 156, 105760. <https://doi.org/10.1016/j.apgeochem.2023.105760>

Zander, F., Heimovaara, T., & Gebert, J. (2020). Spatial variability of organic matter degradability in tidal Elbe sediments. *Journal of Soils and Sediments*, 20(6), 2573–2587. <https://doi.org/10.1007/s11368-020-02569-4>

Zeder, M., Kohler, E., & Pernthaler, J. (2010). Automated quality assessment of autonomously acquired microscopic images of fluorescently stained bacteria. *Cytometry Part A*, 77A(1), 76–85. <https://doi.org/10.1002/CYTO.A.20810>

Zhang, Y., Ren, J., & Zhang, W. (2020). Flocculation under the control of shear, concentration and stratification during tidal cycles. *Journal of Hydrology*, 586, 124908. <https://doi.org/10.1016/j.jhydrol.2020.124908>

Zhao, Y., Liu, P., Rui, J., Cheng, L., Wang, Q., Liu, X., & Yuan, Q. (2020). Dark carbon fixation and chemolithotrophic microbial community in surface sediments of the cascade reservoirs, Southwest China. *Science of The Total Environment*, 698, 134316. <https://doi.org/10.1016/j.scitotenv.2019.134316>

Zhou, J., Theroux, S. M., Bueno de Mesquita, C. P., Hartman, W. H., Tian, Y., & Tringe, S. G. (2022). Microbial drivers of methane emissions from unrestored industrial salt ponds. *The ISME Journal*, 16(1), 284–295. <https://doi.org/10.1038/s41396-021-01067-w>

Zhou, Z., Martin, C., Kosmopoulos, J. C., & Anantharaman, K. (2023). ViWrap: A modular pipeline to identify, bin, classify, and predict viral–host relationships for viruses from metagenomes. *iMeta*, 2(3), e118. <https://doi.org/10.1002/imt2.118>

Zimmermann, H. (1997). The microbial community on aggregates in the Elbe Estuary, Germany. *Aquatic Microbial Ecology*, 13(1), 37–46. <https://doi.org/10.3354/ame013037>

Zimmermann, H., & Kausch, H. (1996). Microaggregates in the Elbe Estuary: Structure and colonization during spring. *Advances in Limnology*, 48(Special Issue), 85–92.

Zimmermann-Timm, H. (2002). Characteristics, dynamics and importance of aggregates in rivers—An invited review. *International Review of Hydrobiology*, 87(2–3), 197–240.

[https://doi.org/10.1002/1522-2632\(200205\)87:2/3<197::AID-IROH197>3.0.CO;2-7](https://doi.org/10.1002/1522-2632(200205)87:2/3<197::AID-IROH197>3.0.CO;2-7)

Zimmermann-Timm, H., Hoberg, M., Holst Henry, & Müller, S. (2002). Estuarine aggregates in the longitudinal profile of the River Elbe: Seasonal changes in occurrence, characteristics and colonization. *Large Rivers*, 263–283.

<https://doi.org/10.1127/lr/13/2002/263>

Zoccarato, L., & Grossart, H. P. (2019). *Relationship Between Lifestyle and Structure of Bacterial Communities and Their Functionality in Aquatic Systems* (pp. 13–52). Springer, Cham. https://doi.org/10.1007/978-3-030-16775-2_2

Zoccarato, L., Sher, D., Miki, T., Segrè, D., & Grossart, H.-P. (2022). A comparative whole-genome approach identifies bacterial traits for marine microbial interactions.

Communications Biology, 5(1), 1–13. <https://doi.org/10.1038/s42003-022-03184-4>

Appendices

Appendix A: Chapter 2

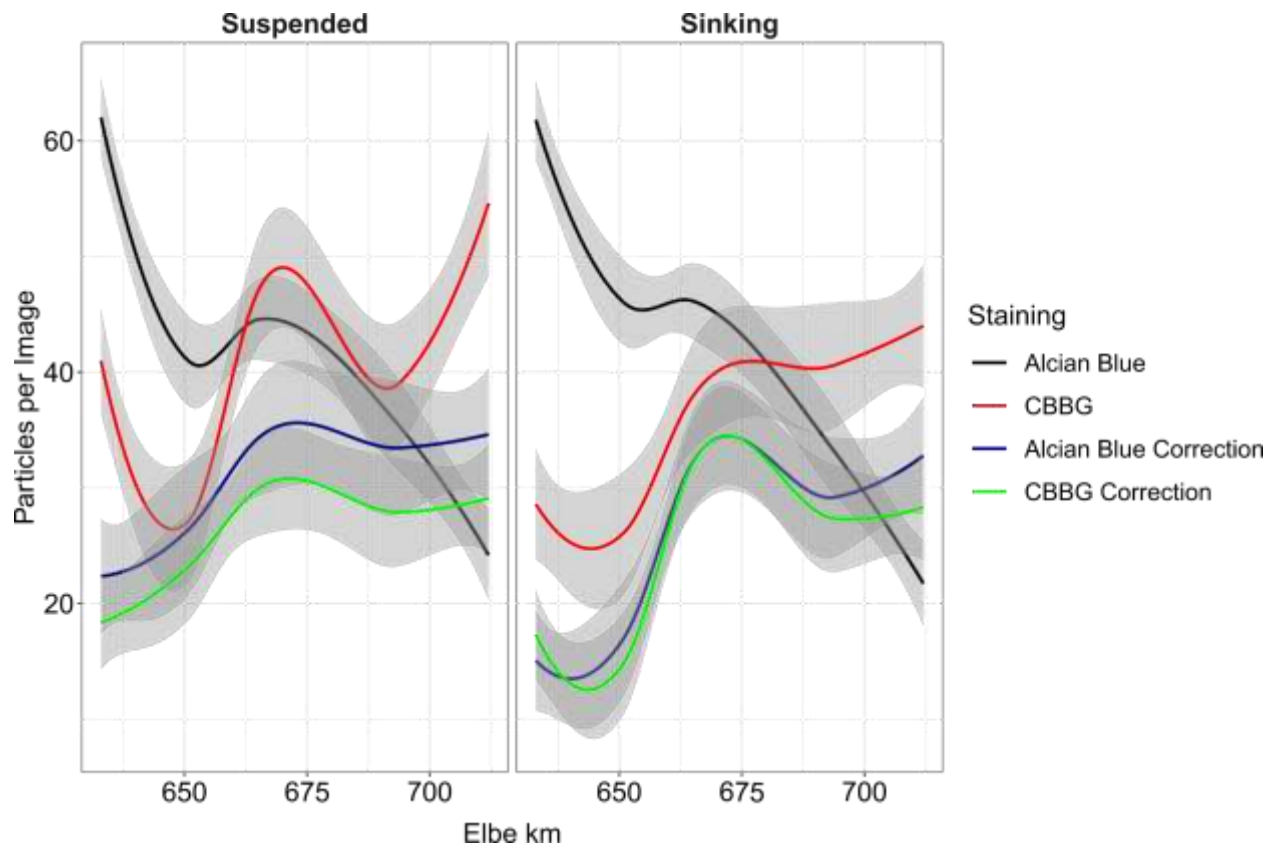


Figure S2.1. Particles per microscope image. Colours represent the different conditions, with Alcian Blue (black) and Coomassie Brilliant Blue (red) stained filters, and the unstained filters that passed through the same macro to correct for Alcian Blue (blue) and Coomassie Brilliant Blue (green) false positives. All seasons and fractions are shown together here, with the coloured lines representing the mean, and the grey areas their respective 95% confidence interval.

Available at: https://github.com/SvenTobias-Hunefeldt/ElbeParticlesDOM/blob/50456fa1c82f8a760b30f59d232a8bf5233739f9/Figure_S2_2_EEMPARAFAC_ComponentsResiduals.pdf

Figure S2.2. EEM PARAFAC sample components and residuals. The sample, individual component, and residual fluorescence displayed on an excitation and emission matrix.

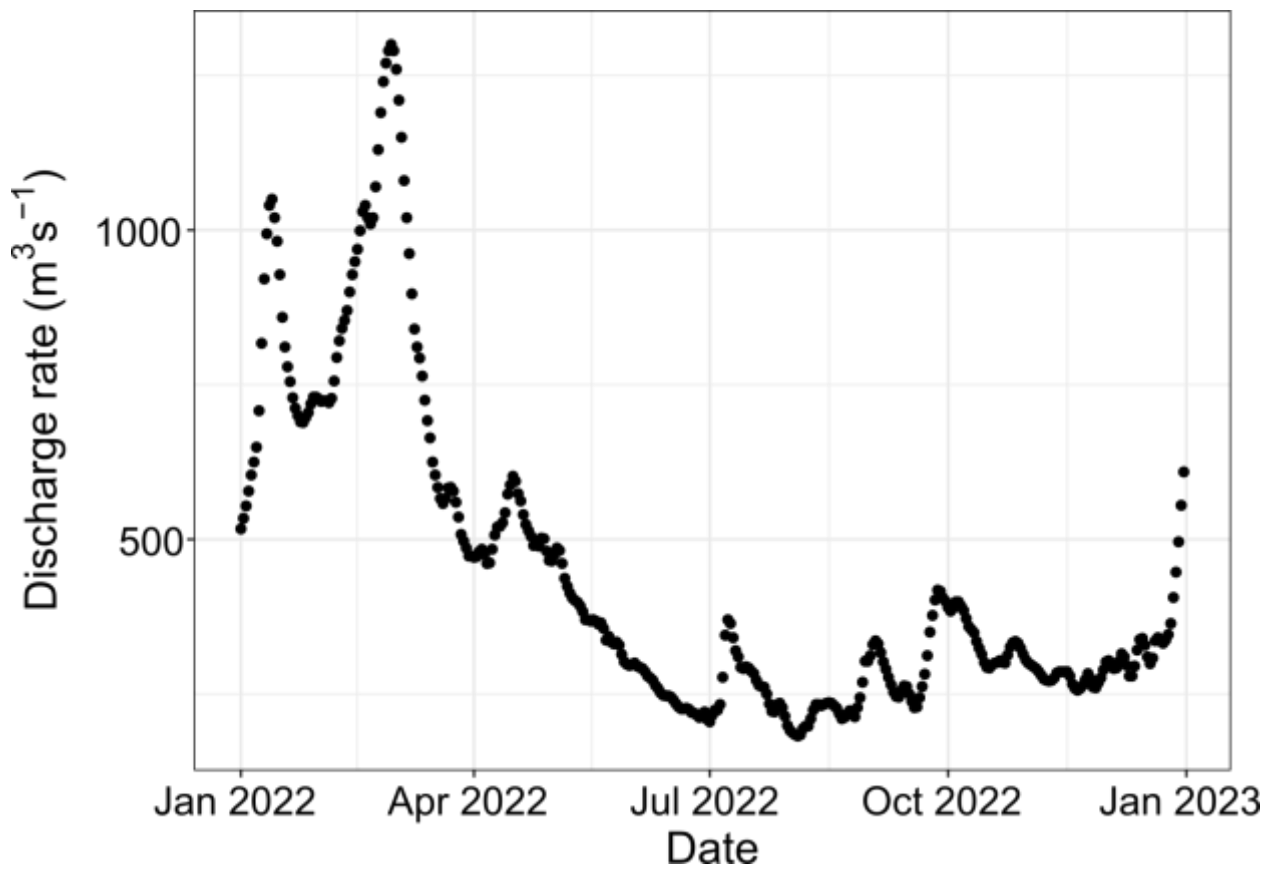


Figure S2.3. Elbe Estuary Discharge 2022 at Neu Darchau, data extracted from the FGG-Elbe Datenportal (FGG-Elbe, 2021).

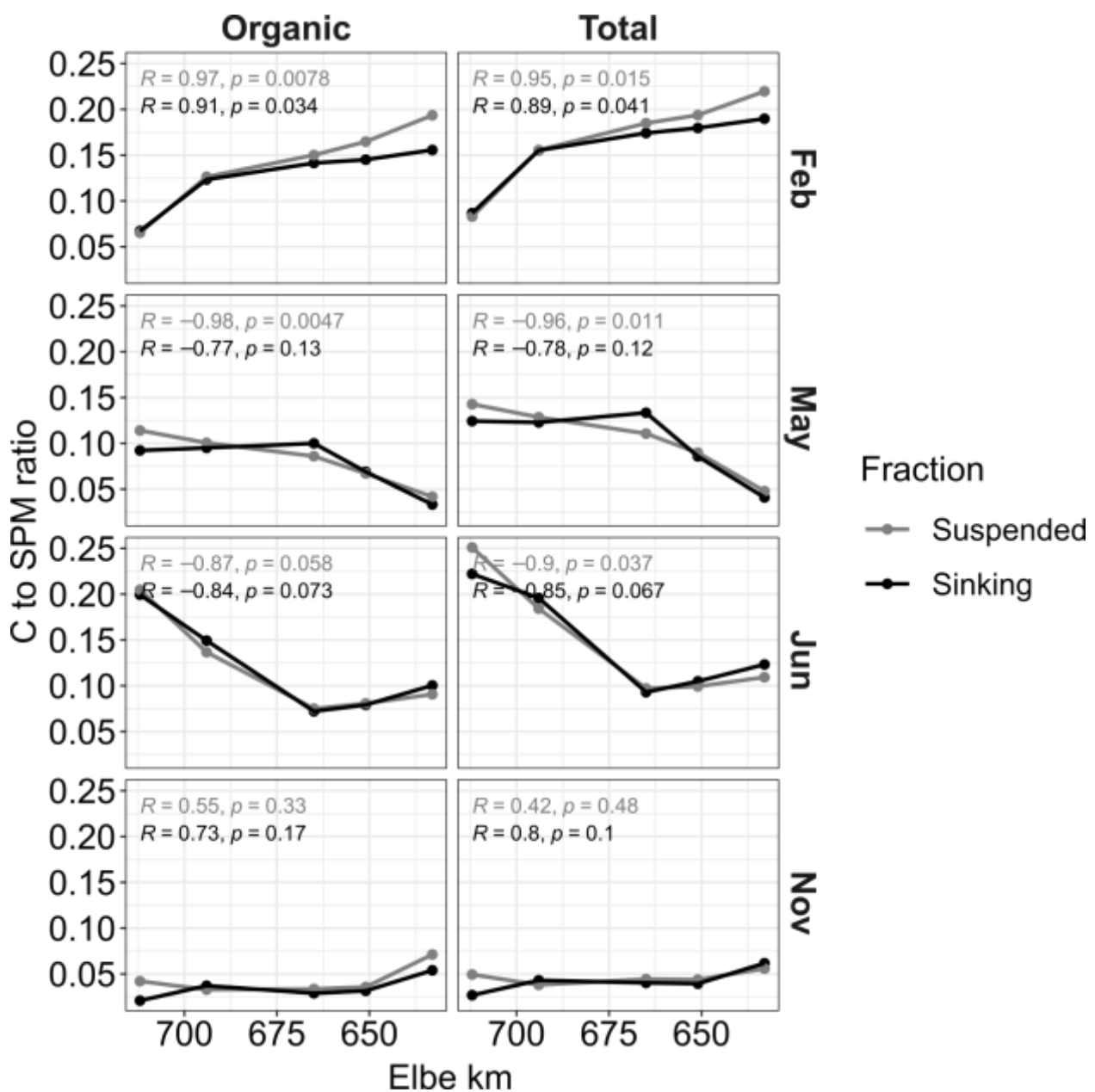


Figure S2.4. Particle Carbon content to dry-weight ratio of particles. Colours denote the suspended (grey) and sinking (black) fraction. The average of parallel measurements is displayed.

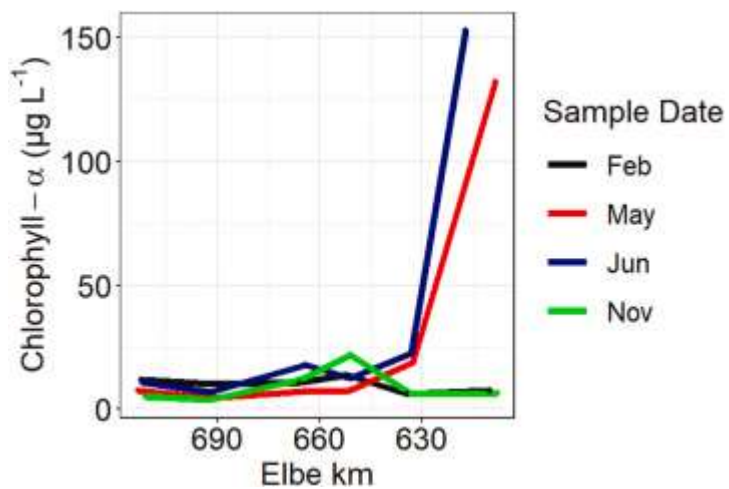


Figure S2.5. Chlorophyll- α over the Elbe during 2022. Colours represent sampling times. The average of parallel measurements is displayed.

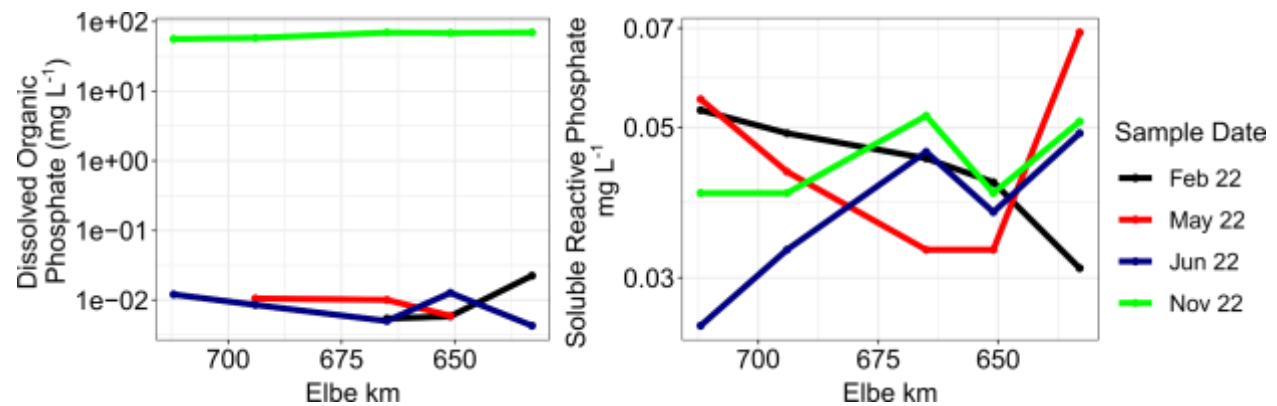


Figure S2.6. Total dissolved organic phosphate and soluble reactive phosphate. Colours denote sample times. The average of parallel measurements is displayed.

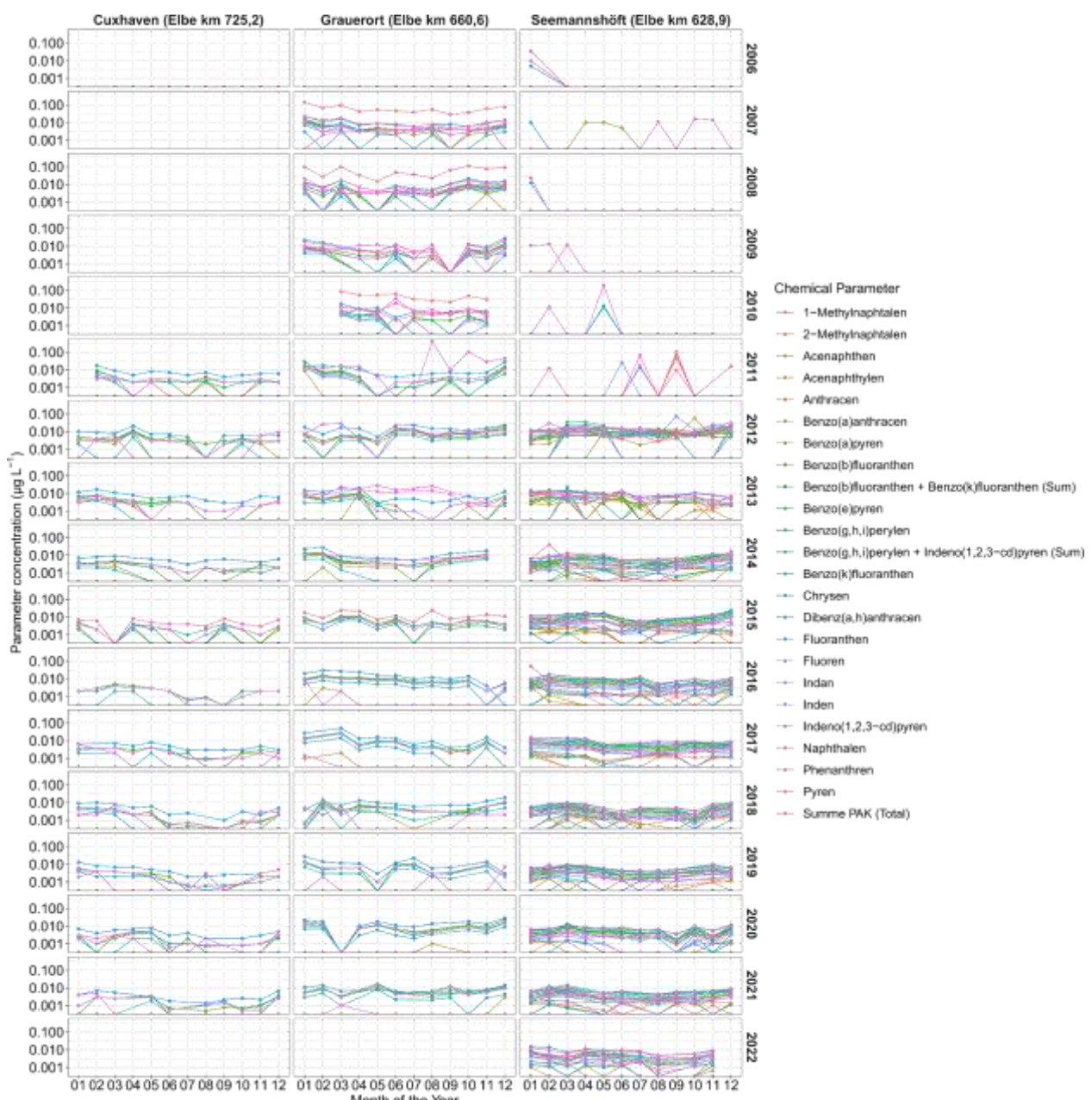


Figure S2.7. PAHs (Polycyclic aromatic hydrocarbons) in the Elbe Estuary. Colours denote different measured chemicals, separated by year and month of sampling. The average of parallel measurements is displayed. Months start in January (01) to December (12). Data was extracted from the ‘Daten Portal der FGG Elbe’ (FGG-Elbe, 2021)

Appendix B: Chapter 3

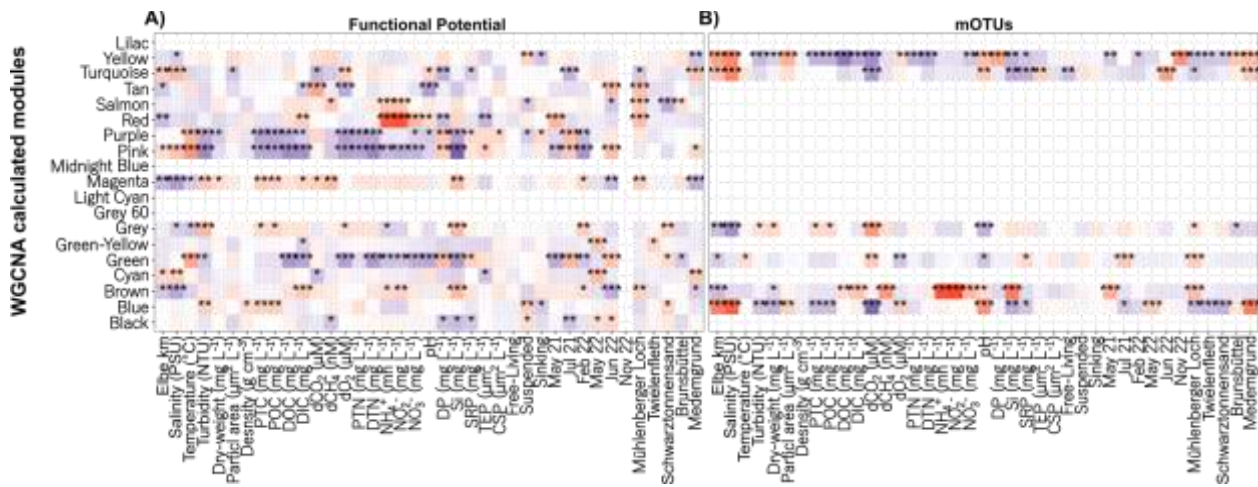


Figure S3.1. WGcNA network module correlations to physicochemical gradients. mOTU and functional potential underwent Weighted Correlation Network Analysis (WGcNA), clustering genes (**A**) and mOTUs (**B**) into modules based on co-occurrence. Colours represent the direction and strength of the Mantel Pearson correlation (red is positive and blue is negative), while p-value is denoted as stars (" ": non-significant, * < 0.05, ** < 0.01, *** < 0.001). WGcNA modules independently calculated for each community aspect.

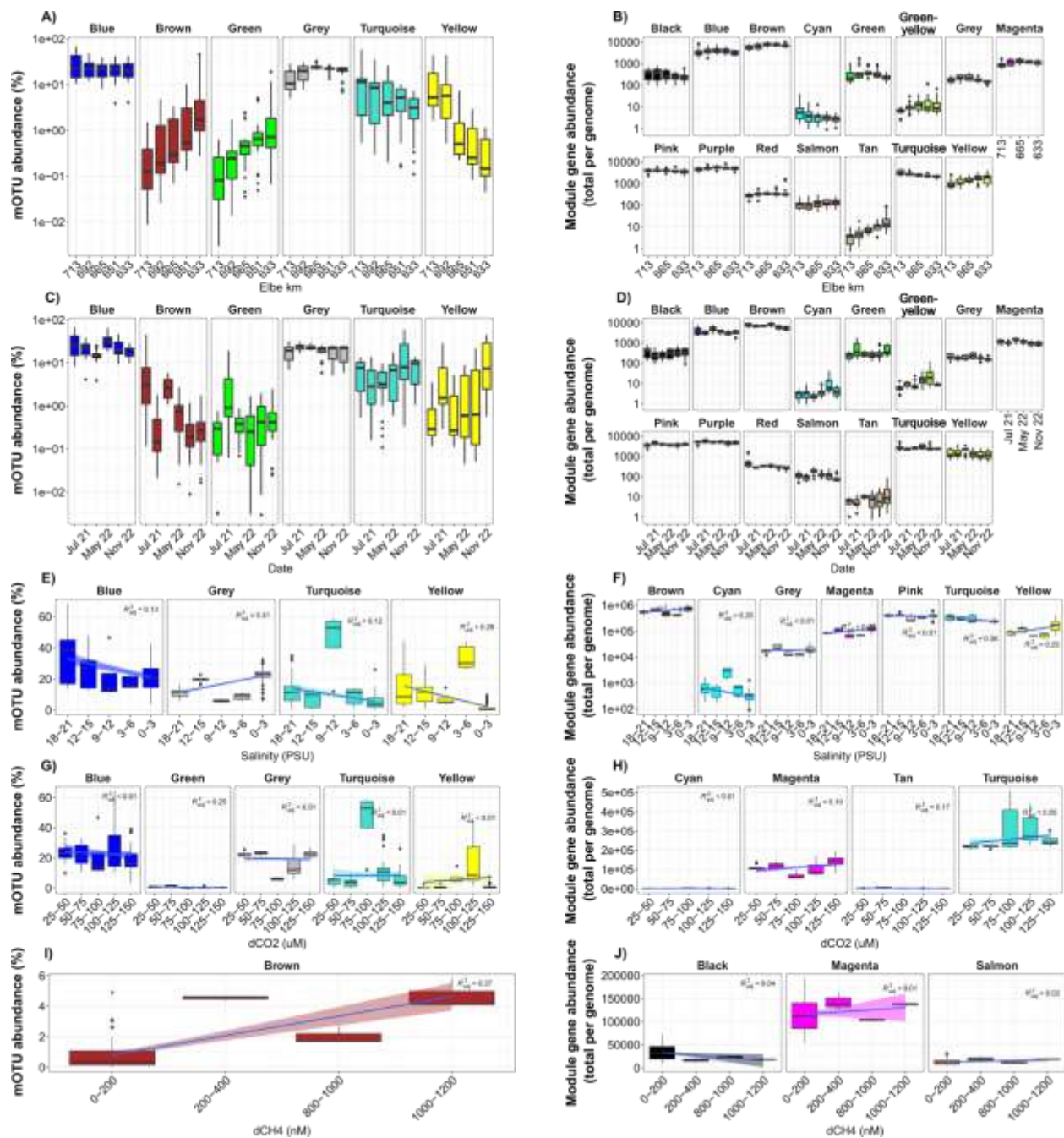


Figure S3.2. WGCNA module abundance in relation to spatiotemporal and correlated factors. Total module mOTU (**A, C**) and genes per genome (**B, D**) abundance is shown in relation to Elbe km (**A, B**) and sample dates (**C, D**). Additionally, mOTU (**E, G, I**) and functional potential (**F, H, J**) module abundances are shown against salinity (**E, F**), dCO₂ (**G, H**), and dCH₄ (**I, J**) concentrations with a line of best fit adjusted R² value.

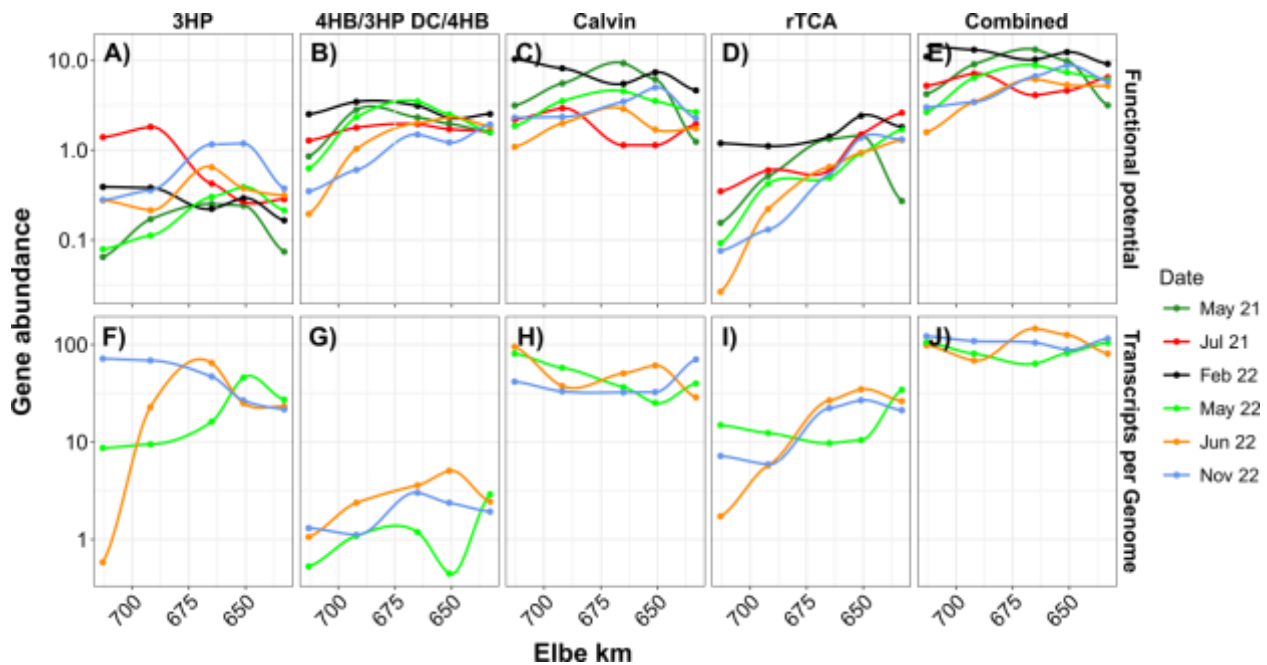


Figure S3.3. Carbon fixation pathway functional potential and transcription in the Elbe Estuary. The mean of two samples is depicted using different colours for sample dates, for both genes per genome (**A-E**) and transcripts per gene (**F-J**). Depicted carbon fixation pathways are (**A, F**) the 3-hydroxypropionate (3HP) bi-cycle, (**B, G**) the combined 4-hydroxybutyrate/3-hydroxypropionate (4HB/3HP) cycle and dicarboxylate/4-hydroxybutyrate (DC/4HB) cycle, (**C, H**) the Calvin cycle, (**D, I**) the reverse tricarboxylic acid (rTCA) cycle, and (**E, J**) the sum of the pathways. Since Wood–Ljungdahl pathway—WLP) and reductive glycine pathways operate in both oxidative and reductive directions with identical enzymes (e.g., in methane or acetate oxidation), we are unable to predict the direction and cannot proceed with further analysis.

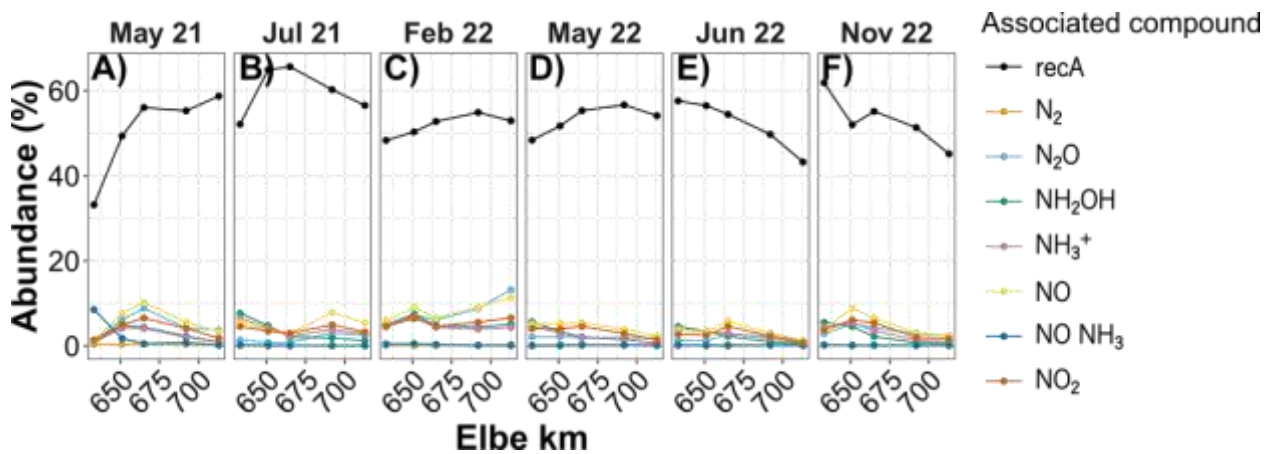


Figure S3.4. Nitrogen cycling associated gene abundance. The mean of two samples abundance (genome normalised) of genes associated with the processing of the colour dependent compounds.

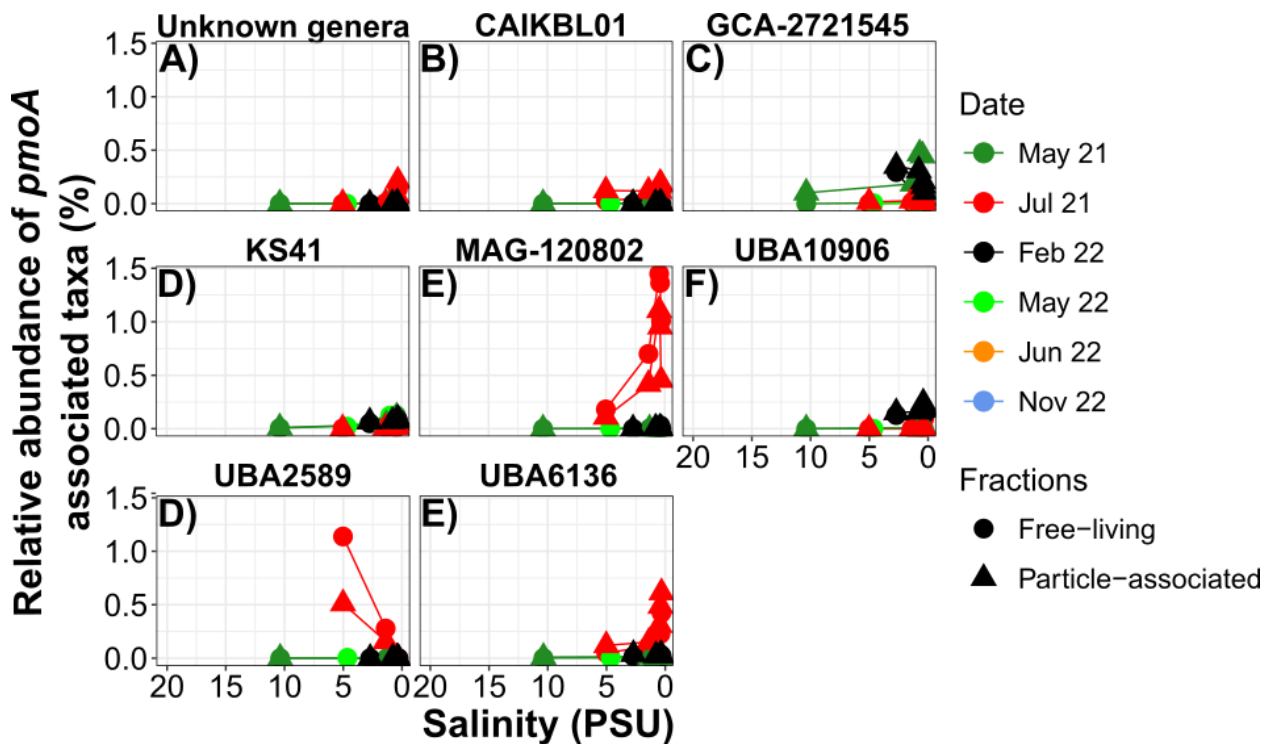


Figure S3.5. Abundance of *pmoA* correlated taxa. The mean of two samples of *pmoA* correlated taxa are depicted across the Elbe Estuary with colours indicating sample dates. Taxa names are shown above the plot, with taxa abundance shown against salinity as PSU.



Figure S3.6. Abundance of TEP correlated taxa. The mean of two samples of TEP correlated taxa are depicted across the Elbe Estuary with colours indicating sample dates. Taxa names are shown above the plot, with taxa abundance shown against salinity as PSU.

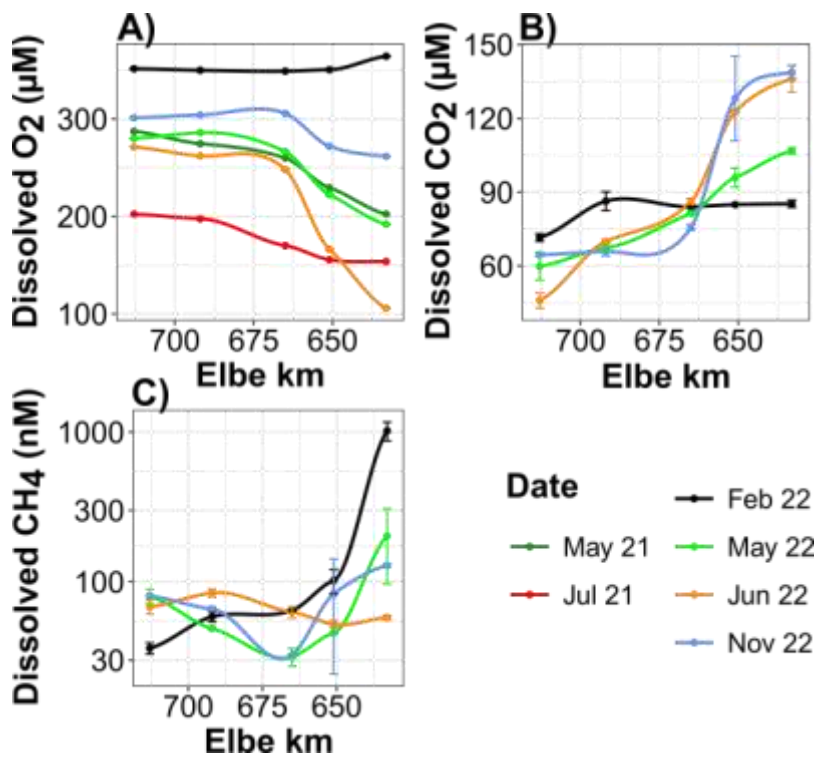


Figure S3.7. Dissolved gases in the Elbe Estuary. Dissolved (A) O₂, (B) CO₂, and (C) CH₄ are shown across the Elbe Estuary, with colour noting sampling dates. Shaded areas represent the 95% confidence interval.

Available at: https://github.com/SvenTobias-Hunefeldt/ElbeMicrobiome/blob/0096471bbccb9f44628c4d9bcc344d0249b30c8/TableS1_or_S3.1_IndicatorAnalysis.xlsx

Table S3.1. Indicator mOTUs, genes, and transcripts across particle fractions. Differences include free-living vs. particle-associated and suspended vs. sinking particles. Either mOTU taxonomies or gene names and KEGG IDs are included, in addition to test statistics, gene function (if relevant), and relevant citations.